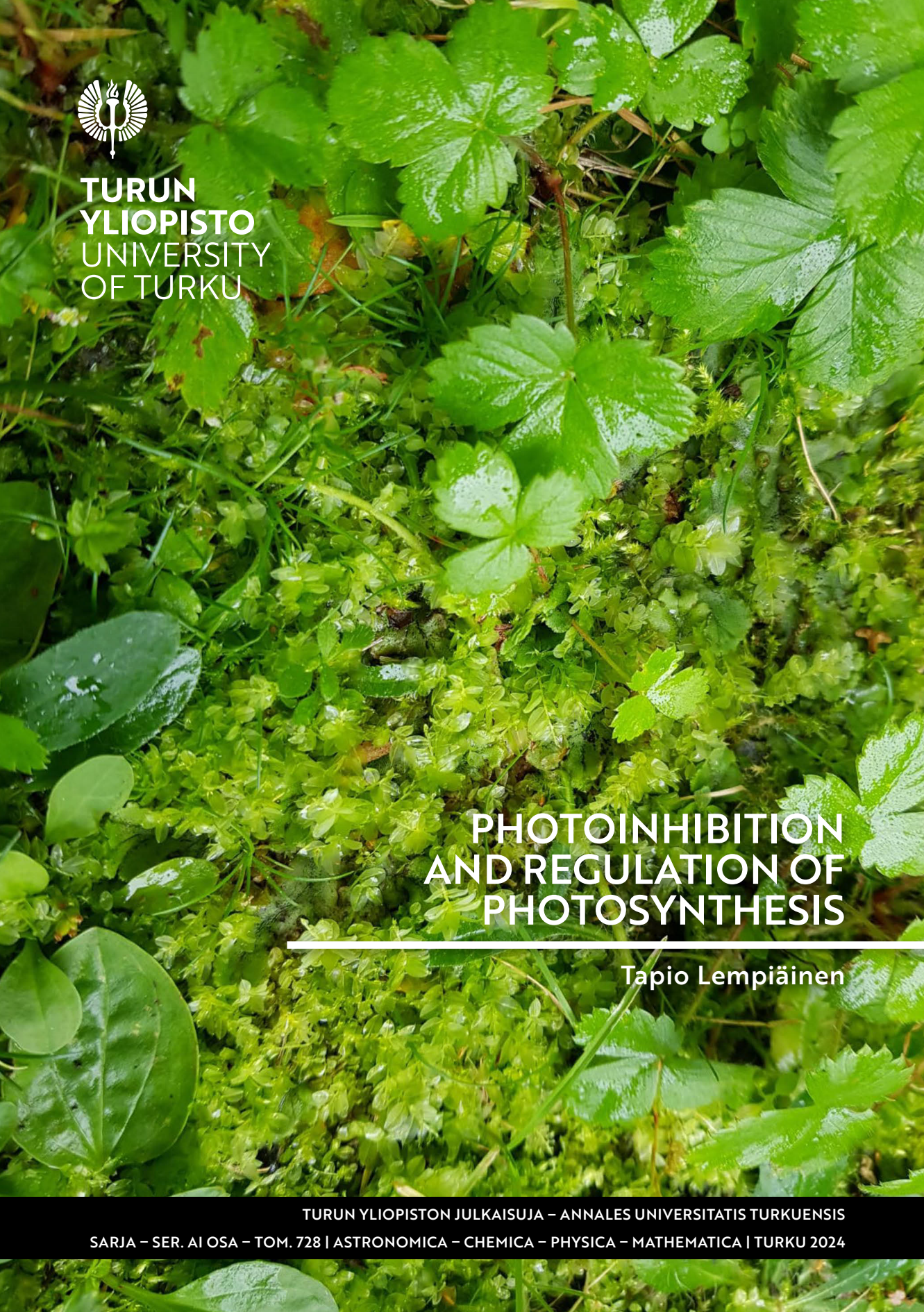

TURUN YLIOPISTO
UNIVERSITY OF TURKU

PHOTOINHIBITION AND REGULATION OF PHOTOSYNTHESIS

Tapio Lempiäinen

TURUN YLIOPISTON JULKAISUJA – ANNALES UNIVERSITATIS TURKUENSIS
SARJA – SER. AI OSA – TOM. 728 | ASTRONOMICA – CHEMICA – PHYSICA – MATHEMATICA | TURKU 2024

TURUN
YLIOPISTO
UNIVERSITY
OF TURKU

PHOTOINHIBITION AND REGULATION OF PHOTOSYNTHESIS

Tapio Lempiäinen

TURUN YLIOPISTON JULKAISUJA – ANNALES UNIVERSITATIS TURKUENSIS
SARJA – SER. AI OSA – TOM. 728 | ASTRONOMICA – CHEMICA – PHYSICA – MATHEMATICA | TURKU 2024

University of Turku

Faculty of Technology
Department of Life Technologies
Molecular Plant Biology unit
Doctoral programme in Technology

Supervised by

Prof. Eva-Mari Aro
Department of Life Technologies
University of Turku

Prof. Eevi Rintamäki
Department of Life Technologies
University of Turku

Associate Prof. Mikko Tikkanen
Department of Life Technologies
University of Turku

Dr. Dorota Muth-Pawlak
Department of Life Technologies
University of Turku

Reviewed by

Prof. Roman Sobotka
Institute of Microbiology
CAS Centre Algatech
Czech Republic

Prof. Anjana Jajoo
School of Life Sciences
Devi Ahilya University
India

Opponent

Prof. Giles Johnson
Department of Earth and Environmental Sciences
University of Manchester
United Kingdom

The originality of this publication has been checked in accordance with the University of Turku quality assurance system using the Turnitin OriginalityCheck service.

Cover Image: Tapio Lempiäinen

ISBN 978-951-29-9992-7 (PRINT)
ISBN 978-951-29-9993-4 (PDF)
ISSN 0082-7002 (Print)
ISSN 2343-3175 (Online)
Painosamala, Turku, Finland 2024

“only those with their feet on rock can build castles in the air”

Terry Pratchett

UNIVERSITY OF TURKU
Faculty of Technology
Department of Life Technology
Molecular Plant Biology
TAPIO LEMPIÄINEN: Photoinhibition and regulation of photosynthesis
Doctoral Dissertation, 158 pp.
Doctoral programme in Technology
November 2024

ABSTRACT

Plants are photosynthetic organisms that use light to reduce carbon dioxide, nitrate and sulfate to synthesise the organic molecules that are the building blocks of all life. The reductants are produced in the photosynthetic linear electron transfer chain in which two photosystems, PSII and PSI, operate in series. Excitation of PSII extracts electrons from water and the electrons are transferred to PSI for a second excitation, after which the electrons are potent reductants for anabolic reactions. Both photosystems require light to function, but they can also be damaged by light. This phenomenon is called photoinhibition. Plants have several overlapping mechanisms to prevent photoinhibition, but too large or rapid changes in environmental conditions can overwhelm the capacity of these protective mechanisms.

The first two papers included in the thesis, investigated the effects of photoinhibition of either PSI or PSII on the regulation of photosynthesis in Arabidopsis (*Arabidopsis thaliana*), a common model organism. The observed changes occurred in the phosphorylation of light-harvesting antenna proteins, which regulate the allocation of light to PSI and PSII. The detected changes, previously associated with acclimation to fluctuations in light intensity and quality, are able to restore the functional balance between the photosystems after photoinhibition. PSI photoinhibition also induces the accumulation of ATP synthase and cytochrome b_6f complex in the thylakoid membrane. Chronic PSI photoinhibition also alters the redox regulation of enzymes involved in light reactions and carbon metabolism. These mechanisms have previously been linked to acclimation to changes in environmental conditions. My results show that the same mechanisms are also important in minimising the adverse effects of photoinhibition.

The third paper included in the thesis, examined how a 10°C drop in temperature alters high light acclimation in lettuce (*Lactuca sativa*). Under these conditions, lettuce is extremely efficient at quenching excitation energy to heat and protecting the PSII photoinhibition repair cycle from photodamage. This is proposed to occur through the concerted function of phosphorylation of the minor antenna protein, LHCB4, and accumulation of the light-harvesting-like protein, SEP2. Further analysis also revealed that PSII repair is regulated at the maturation stage of the reaction centre protein D1 under these conditions. The distinct regulatory mechanisms identified in lettuce show that plants have diverse mechanisms to protect photosynthesis, depending on the plant species and the environmental stresses to which they are exposed. The molecular characterisation of these different mechanisms paves the way for improving the stress tolerance and productivity of crop species.

KEYWORDS: light-harvesting, photoinhibition, photosynthesis, protein phosphorylation

TURUN YLIOPISTO
Teknillinen tiedekunta
Bioteknologian laitos
Molekulaarinen kasvibiologia
TAPIO LEMPIÄINEN: Fotoinhibitio ja fotosynteesin säätely
Väitöskirja, 158 s.
Teknologian tohtoriohjelman
Marraskuu 2024

TIIVISTELMÄ

Kasvit muodostavat elämälle välttämättömiä orgaanisia molekyylejä pelkistämällä hiilidioksidia, nitraattia ja sulfaattia. Tähän tarvittavat pelkistimet tuotetaan fotosynteesin lineaarisessa elektroninsiirtoketjussa, jossa kaksi fotosysteemiä, PSII ja PSI, toimivat sarjassa. PSII:n viritys irrottaa elektronit vedestä, jotka siirretään edelleen PSI:een uudelleen viritettäviksi, jonka jälkeen ne kykenevät toimimaan tehokkaina pelkistiminä metaboliareaktioissa. Molemmat fotosysteemit tarvitsevat valoa toimiakseen, mutta ne myös vaurioituvat herkästi valon vaikutuksesta. Tätä ilmiötä kutsutaan fotoinhibitioksi. Kasveilla on useita päällekkäisiä mekanismeja, joilla ne pyrkivät estämään fotoinhibitiota, mutta ympäristöolosuhteiden liian suuret ja nopeat muutokset voivat ylittää näiden suojamekanismien kapasiteetin. Tämä aiheuttaa toiminnallisten fotosysteemien määrän vähenemisen viherhiukkasissa.

Väitöskirjan kahdessa ensimmäisessä osajulkaisussa tutkittiin, miten PSI:n tai PSII:n fotoinhibitio vaikuttaa fotosynteesin säätelyyn lituruohossa (*Arabidopsis thaliana*), kasvibiologian malliorganismissa. Suurin muutos säätelyssä tapahtuu fotosysteemeille valoa keräävien antenniproteiinien fosforylaatiossa, mikä säätelee valon jakaantumista PSI:lle ja PSII:lle. Havaitut muutokset, jotka on aiemmin liitetty sopeutumiseen valon määrän ja laadun vaihtelussa, pystyvät myös palauttamaan fotosysteemien välisen tasapainon fotoinhibition jälkeen. Lisäksi PSI:n fotoinhibitio muuttaa ATP-syntaasin ja sytokromi b_6f -kompleksin määriä tylakoidi-membraanissa. PSI:n krooninen fotoinhibitio aiheuttaa myös muutoksia viher-hiukkasten valoreaktioihin ja hiilimetaboliaan liittyvien entsyymien pelkistystilassa sekä tähän perustuvassa säätelyssä. Aikaisemmin edellä mainittuja mekanismeja on tutkittu sopeutumisessa ympäristöolosuhteiden muutoksiin. Tulokseni kuitenkin osoittavat, että samoilla mekanismeilla on tärkeä merkitys fotoinhibition haittavaikutusten lieventämisessä.

Väitöskirjan kolmannessa osajulkaisussa selvitettiin, miten 10 °C:n lasku lämpötilassa vaikuttaa salaatin (*Lactuca sativa*) sopeutumiseen kirkkaaseen valoon. Salaatti pystyy tehokkaasti muuntamaan liiallisen viritysenergian lämmöksi sekä suojaamaan PSII:n fotoinhibition korjauskiertoa ylimääräisiltä valovaurioilta näissä olosuhteissa. Tämä näyttäisi johtuvan pienen antenniproteiinin, LHCB4:n, spesifisestä fosforylaatiosta sekä stressin indusoiman proteiinin, SEP2:n, määrän noususta. Tarkempi analyysi myös paljasti reaktiokeskusproteiini D1:n C-terminaalisen prosessoinnin säätelevän PSII:n korjauskierron tehokkuutta alemmassa lämpötilassa. Salaatissa havaitut erityiset säätelymekanismit osoittavat, että kasvien välillä on suurta vaihtelua fotosynteesin suojamismekanismeissa. Nämä mekanismit riippuvat sekä kasvilajista että ympäristöstressistä. Kasvilajien välisten erojen tunteminen on keskeistä, jotta esimerkiksi viljelykasvien stressinsietokykyä voitaisiin parantamaa muokkaamalla niihin parhaiksi havaitut säätelymekanismit.

ASIASANAT: fotoinhibitio, fotosynteesi, proteiinien fosforylaatio, valonkeräys

Table of Contents

Abbreviations

1,3-BPGA	1,3-bisphosphoglyrecate
$^1O_2$	singlet oxygen
2-CysPrx	2-Cysteine peroxiredoxin
2OG	2-oxoglutarate
2-PG	2-phosphoglycolate
^{3}Chl	triplet chlorophyll
3-PGA	3-phosphoglycerate
ACN	acetonitrile
ADP	adenosine diphosphate
AGC	automatic gain control
AMP	adenosine monophosphate
AOX	alternative oxidase
APS	adenosine 5'-phosphosulfate
ATP	adenosine triphosphate
ATPS	ATP sulfurylase
BSA	bovine serum albumin
C_2	PSII dimer
C_2S	PSII dimer with one LHCII trimer
C_2S_2	PSII dimer with two LHCII trimers
C_2S_2M	PSII dimer with three LHCII trimers
$C_2S_2M_2$	PSII dimer with four LHCII trimers
$CaCl_2$	calcium chloride
CAO	chlorophyllide a oxygenase
CBB	Calvin-Benson-Bassham
CBSX1	cystathionine-b-synthase domain containing protein in heterotrophic plastids
CBSX2	cystathionine-b-synthase domain containing protein in leaf chloroplasts
CET	cyclic electron transfer
CHL	Chloroplastic lipocalin
Chl a	chlorophyll a
Chl b	chlorophyll b
Chl_0	Chlorophyll in PSI reaction centre
Chl_{0A}	Chlroophyll in PSI reaction centre
Chl_A	Chlroophyll in PSI reaction centre
Chl_{D1}	chlorophyll in PSII reaction centre
Chl_{D2}	chlorophyll in PSII reaction centre
CO_2	carbon dioxide
CP43	PSII internal light-harvesting protein
CP47	PSII internal light-harvesting protein
CP47-D2	intermediate in PSII repair cycle
CV	compensation voltage
Cyt b_6f	Cytochrome b_6f complex
D1	PSII reaction centre protein
D2	PSII reaction centre protein
DCBQ	2,6-dichloro-1,4-benzoquinone, artificial electron acceptor
DCIP	2,6-Dichlorophenolindophenol, artificial electron acceptor
DEG	protease involved in PSII repair
DHA	dehydroascorbate
DHAR	dehydroascorbate reductase
DMBQ	2,6-dimethoxy-1,4-benzoquinone, artificial electron acceptor
DMF	dimethylformamide
DNA	deoxyribonucleic acid
DTT	dithiothreitol
ECL	enhanced chemiluminescence
ECS	electrochromic shift

EDTA	ethylenediaminetetraacetic acid
ELIP1.2	early light induced protein 1.2
E_m	midpoint potential
F_0	minimal fluorescence
F_A	iron sulfur cluster in PSI
FAIMS	high-field asymmetric-waveform ion-mobility mass spectrometry
F_B	iron sulfur cluster in PSI
FBPase	fructose 1,6-bisphosphatase
Fd	ferredoxin
Fd-GOGAT	Fd-dependent glutamate synthase
FDR	false discovery rate
Fe^{2+}	ferrous iron
Fe_2S_2	iron sulfur cluster
Fe_4S_4	iron sulfur cluster
Flv	flavodiiron
F_M	maximal fluorescence
F_M'	maximal fluorescence in light
F_M'^{ref}	reference maximal fluorescence
FNR	ferredoxin NADPH reductase
FRET	Förster resonance energy transfer
FTR	Fd-dependent thioredoxin reductase
FTSH	ATP-dependent protease involved in PSII repair
F_V/F_M	PSII maximal quantum yield
Fx	iron sulfur cluster in PSI
GA3P	glyceraldehyde 3-phosphate
GADPH	NADP-glyceraldehyde-3-phosphate dehydrogenase
g_{H+}	thylakoid proton conductivity
Gpx	glutathione peroxidase
GR	glutathione reductase
GS	glutamine synthetase
H_2O_2	hydrogen peroxide
H_2S	hydrogen sulfide
HCD	higher-energy collisional dissociation
HCO_3^-	bicarbonate
Hlip	high-light-induced protein
$HO^\bullet$	hydroxyl radical
HPLC	high performance liquid chromatography
IAA	iodoacetamide
iRT	indexed retention time
KEA3	thylakoid proton/potassium antiporter
LED	light emitting diode
LET	linear electron transfer
LHCA	PSI light-harvesting complex
LHCA1	PSI light-harvesting antenna protein
LHCA2	PSI light-harvesting antenna protein
LHCA3	PSI light-harvesting antenna protein
LHCA4	PSI light-harvesting antenna protein
LHCA5	PSI light-harvesting antenna specific for the complex with NDH1
LHCA6	PSI light-harvesting antenna specific for the complex with NDH1
LHCB1	PSII major light-harvesting antenna protein
LHCB2	PSII major light-harvesting antenna protein
LHCB3	PSII major light-harvesting antenna protein
LHCB4	PSII minor light-harvesting protein
LHCB4.1	isoform of PSII minor light-harvesting antenna protein
LHCB4.2	isoform of PSII minor light-harvesting antenna protein
LHCB4.3	isoform of PSII minor light-harvesting antenna protein
LHCB5	PSII minor light-harvesting protein
LHCB6	PSII minor light-harvesting protein
LHCB8	other name for LHCB4.3 isoform of PSII minor light-harvesting antenna protein
LHCII	PSII light-harvesting complex
LHCII	PSII light-harvesting complex
LHCSR	stress-related light-harvesting protein in eukaryotic algae and lower plants
LIL	light-harvesting-like
L-trimer	loosely bound LHCII trimer
MAL-PEG	pegylated maleimide
MDA	monodehydroascorbate
MDAR	monodehydroascorbate reductase
MDH	malate dehydrogenase
MET	mitochondrial electron transfer chain

$MnCl_2$	manganese chloride
MS/MS	tandem mass spectrometry
M-trimer	moderately bound LHCII trimer
NAD^+	nicotinamide adenine dinucleotide
NADH	dihydro-nicotinamide adenine dinucleotide
NADP+	nicotinamide adenine dinucleotide phosphate
NADPH	dihydro-nicotinamide adenine dinucleotide phosphate
NADPH-MDH	NADPH-dependent malate dehydrogenase
NDH1	type 1 NADPH dehydrogenase
NEM	N-ethylmaleimide
NH_4^+	ammonium
nLC-ESI-FAIMS-MS/MS	nanoflow liquid chromatography electrospray ionisation high-field asymmetric-waveform ion-mobility mass spectrometry tandem mass spectrometry
NO_2^-	nitrite
NO_3^{2-}	nitrate
NPQ	non-photochemical quenching
NTRC	NADPH-dependent thioredoxin reductase
O_2	molecular oxygen
$O_2^{\bullet}$	superoxide
OEC	oxygen-evolving complex
OHP	one-helix protein
P680	PSII reaction centre chlorophyll pair
$P680^{+\bullet}$	PSII oxidised reaction centre chlorophyll pair
P700	PSI reaction centre chlorophyll pair
$P700^{+\bullet}$	PSI oxidised reaction centre chlorophyll pair
PAPS	3'-phosphoadenosine 5'-phosphosulfate
PBCP	PSII core phosphatase
PC	plastocyanin
P_{D1}	chlorophyll in PSII reaction centre
P_{D2}	chlorophyll in PSII reaction centre
PGK	3-phosphoglycerate kinase
PGR5	protein associated with cyclic electron transfer
PGR5-PGRL1	proteins complex associated with cyclic electron transfer
Pheo a	pheophytin a
$Pheo_{D1}$	pheophytin in PSII reaction centre
$Pheo_{D2}$	pheophytin in PSII reaction centre
PhQ	phylloquinone
P_M	maximal P700 oxidation
pmf	proton motive force
PO_4^{3-}	phosphate
PORA	protochlorophyllide oxidoreductase A
ppm	parts per million
PQ	plastoquinone
pre-D1	unprocessed PSII reaction centre protein
PRK	phosphoribulokinase
PrxIIE	type II peroxiredoxin
PrxQ	peroxiredoxin Q
PsaA	PSI reaction centre protein
PsaB	PSI reaction centre protein
PSAC	PSI core complex stromal protein
PSAD	PSI core complex stromal protein
PSAF	PSI core complex minor protein, connecting LHCA to core
PSAG	PSI core complex minor protein, connecting LHCA to core
PSAH	PSI core complex minor protein, connecting LHCII to core
PsaJ	PSI core complex minor protein, connecting LHCA to core
PSAL	PSI core complex minor protein, connecting LHCII to core
PSAN	PSI core complex minor protein, connecting LHCA to core
PSAO	PSI core complex minor protein, connecting LHCII to core
PSBH	PSII core complex minor protein
PSBS	light-harvesting-like protein functioning in qE
PSI	photosystem I
PSII	photosystem II
PSI-LHCI-LHCII	PSI complex with additional antenna
PSI-NDH1	PSI complex for cyclic electron transfer
PSI-PSII	complex with PSI and PSII
PTOX	plastid terminal oxidase
PVDF	polyvinylidene difluoride
Q_A	PSII tightly bound plastoquinone

$Q_A^{-\bullet}$	PSII reduced tightly bound quinone radical
Q_B	PSII exchangeable plastoquinone
$Q_B^{-\bullet}$	PSII reduced loosely bound quinone radical
qE	energy-dependent quenching
qH	lipocalin-dependent quenching
qL_T	fraction of open and functional PSII reaction centres
Q_O	plastoquinol binding site at cytochrome b_6f complex
qZ	zeaxanthin-dependent quenching
RC	reaction centre
RES	reactive electrophilic species
RNA	ribonucleic acid
ROQH1	relaxation of qH1
ROS	reactive oxygen species
Rubisco	ribulose 1,5-bisphosphate carboxylase/oxygenase
RuBP	ribulose 1,5-bisphosphate
sAPX	stromal ascorbate peroxidase
SBPase	sedoheptulose 1,7-bisphosphatases
SDS-PAGE	sodium dodecyl sulfate polyacrylamide gel electrophoresis
SEP2	stress enhanced protein 2
SO_3^{2-}	sulfite
SO_4^{2-}	sulfate
SOD	superoxide dismutase
SOQ1	suppressor of quenching
STN7	kinase involved in state transitions
STN8	kinase phosphorylating PSII core proteins and LHCB4
S-trimer	strongly bound LHCII trimer
TAP38	phosphatase involved in state transitions
tAPX	thylakoid ascorbate peroxidase
TCA	tricarboxylic acid
TPI	triose phosphate isomerase
Trx-f1	thioredoxin regulating carbon fixation
Trx-m1	thioredoxin regulating malate valve
Trx-m2	thioredoxin regulating malate valve
Trx-m4	thioredoxin regulating cyclic electron transfer
Trx-x	thioredoxin reducing antioxidant system

List of Original Publications

This dissertation is based on the following original publications, which are referred to in the text by their Roman numerals:

I Tapio Lempiäinen, Eevi Rintamäki, Eva-Mari Aro, Mikko Tikkanen. Plants acclimate to Photosystem I photoinhibition by readjusting the photosynthetic machinery. *Plant, Cell & Environment*, 2022, *45*(10), 2954–2971

II Sanna Gunell, Tapio Lempiäinen, Eevi Rintamäki, Eva-Mari Aro, Mikko Tikkanen. Enhanced function of non-photoinhibited photosystem II complexes upon PSII photoinhibition. *Biochimica et Biophysica Acta – Bioenergetics*, 2023; *1864*(3), 148978.

III Tapio Lempiäinen, Dorota Muth-Pawlak, Julia Vainonen, Eevi Rintamäki, Mikko Tikkanen, Eva-Mari Aro. Sustained non-photochemical quenching and regulation of PSII repair cycle during combined high light and low temperature stress in lettuce. *Manuscript*

1 Introduction

As light-dependent autotrophic organisms, vascular plants are the main primary producers in terrestrial ecosystems by synthesising organic molecules: carbohydrates, amino acids, lipids, and nucleotides from common inorganic substances: carbon dioxide (CO_2), nitrate (NO_3^{2-}) and sulfate (SO_4^{2-}). The photosynthetic light reactions that drive these anabolic reactions take place in the green parts of plants, mainly in the specialised organs: the leaves. Leaves have evolved to maximise the surface area for light interception and carbon dioxide exchange from the air through stomata to provide the substrates for light reactions and carbon fixation, while minimising water loss. Autotrophic leaves are supported by heterotrophic organs, roots and stems, which take up water and inorganic nutrients from the soil and transport them to the leaves. Reproductive parts are a third type of heterotrophic organ, forming seeds for plant propagation. All these heterotrophic tissues depend on the organic compounds produced in the leaves. Plants must optimise the allocation of resources between these different organs as well as the protective secondary metabolites according to the abiotic and biotic environmental conditions to maximise the survival, growth and reproduction of the plant.

Cultivation techniques, providing optimal growth conditions, and plant breeding have dramatically changed the allocation of resource to seed production in major crop species, which has led to a dramatic increase in agricultural production during the Green Revolution. To my knowledge, these advances have not altered the basic functions of photosynthetic light reactions that are ultimately responsible for plant productivity, which would make them a logical next step for improving plant productivity. However, although we have a relatively good understanding of the function of light reactions, we still have a limited understanding of the regulation of light reactions under adverse environmental conditions, and of the diversity of such regulation in different plant species. This could hamper the rational improvement of plant productivity through the genetic engineering of light reactions, as there may be unexpected negative consequences of the modifications, especially under field conditions where multiple stresses co-occur. More research is therefore needed on the effects of multiple stresses in different plant species to identify the most robust, flexible and efficient mechanisms for improving environmental acclimation.

1.1 Endosymbiont theory – origins of energy metabolism

Plant energy metabolism is carried out by two specific organelles: the heterotrophic mitochondria, which generate adenosine triphosphate (ATP) by oxidation of organic molecules in the tricarboxylic acid (TCA) cycle followed by oxidative phosphorylation, and the autotrophic chloroplasts, which generate ATP and reducing power by light-dependent oxidation of water which is coupled to photophosphorylation. The endosymbiont theory states that the bioenergetic organelles of eukaryotes, mitochondria and chloroplasts, are descended from free-living alphaproteobacteria and cyanobacteria. The first eukaryote was formed when an Asgard archaeon engulfed heterotrophic alphaproteobacteria, which evaded digestion and over time became an endosymbiont, mitochondria. The second endosymbiont was formed when a eukaryote cell engulfed autotrophic cyanobacteria, leading to the evolution of chloroplasts.

During evolution, both endosymbionts have lost genes to the nucleus to the point where most organellar proteins are nuclear encoded. Still, both endosymbionts have small circular genomes that encode proteins and RNA for replication and for transcription and translation of endosymbiont-encoded proteins, in particular the components of the electron transfer reactions. It has been proposed that the retention of these genes is due to the hydrophobicity of the proteins involved in the electron transfer reactions, but also to the need for tight regulation of the translation and assembly of proteins in the electron transfer reactions to avoid the formation of harmful reactive oxygen species (ROS) (1.6.1) (Allen, 2015; Giannakis et al., 2022).

1.2 Chloroplasts – photoautotrophic organelles of plants

The function of chloroplasts has diversified after the endosymbiosis and chloroplasts can differentiate into, or develop from, several classes of plastids that are not photosynthetically active (Sierra et al., 2023). Plastids, particularly the chloroplasts, are the main anabolic organelles in plant cells, synthesising carbohydrates, amino acids, nucleotides, lipids and protein cofactors in their soluble compartment, the stroma. However, many of the enzymes in these biosynthetic pathways are not of cyanobacterial origin (Reyes-Prieto and Moustafa, 2012), highlighting that plastid/chloroplast metabolism has changed after endosymbiosis.

All plastids have a porous outer membrane and a continuous inner membrane enclosing the soluble stroma, but the chloroplasts have an additional inner thylakoid membrane system. The thylakoid membrane houses the protein complexes for photosynthetic light reactions and forms the confined inner space, the lumen. Thylakoid membranes in vascular plants have two distinct domains: the appressed

grana stacks, which contain most of the photosystem II (PSII) and light-harvesting complexes (LHCII), and the non-appressed stroma-exposed thylakoids, which connect the grana stacks and contain photosystem I (PSI) and ATP synthase, while cytochrome b_6f complex (Cyt b_6f) is found in both structural domains (Rantala et al., 2020). Grana and stroma thylakoids are connected by grana margin slits that allow lumenal and thylakoid soluble electron carriers to diffuse between the domains, while the edges of grana and stroma thylakoids apparently form the curvature domain, which seems to have mainly a structural function, but the structural changes in curvature may also have regulatory aspects.

The thylakoid-embedded protein complexes: PSII, Cyt b_6f and PSI form linear electron transfer chain (LET) that oxidises water to molecular oxygen (O_2) and transfer the electrons to the stromal electron acceptor ferredoxin (Fd) (Figure 1). PSII and Cyt b_6f are connected by lipophilic two-electron carrier plastoquinone (PQ), while Cyt b_6f and PSI are connected by lumenal one-electron carrier plastocyanin (PC). Electron transfer at PSII and Cyt b_6f is coupled to proton translocation into the lumen, forming a proton gradient which is used by ATP synthase to drive the endothermic coupling of adenosine diphosphate (ADP) and phosphate (PO_4^{3-}) to ATP. Most of the reduced Fd is used to reduce nicotinamide adenine dinucleotide phosphate ($NADP^+$) to dihydro-nicotinamide adenine dinucleotide phosphate (NADPH) by ferredoxin NADPH reductase (FNR).

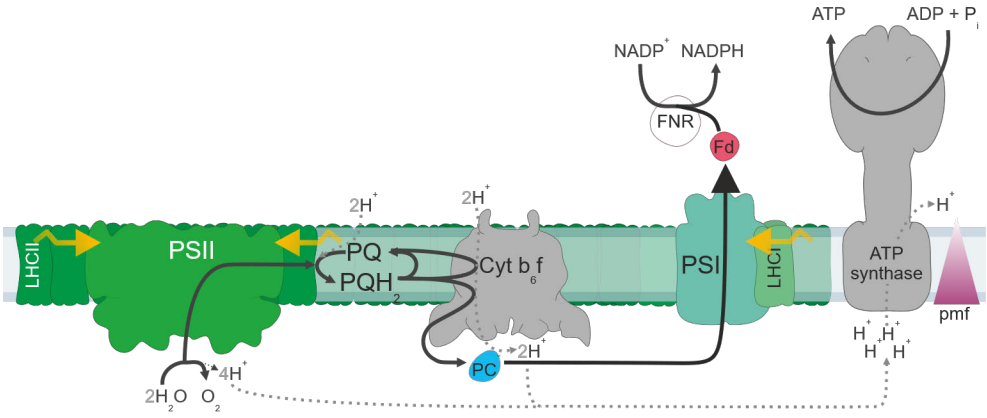

Figure 1. Simplified figure of linear electron transfer and ATP and NADPH synthesis in the thylakoid membrane and stroma. Chapter 1.31 describes the LET and generation of ATP and NADPH in more detail. The figure is a modified version of a figure made by Sanna Gunell.

1.3 Biochemistry of photosynthesis in a nutshell: basics reactions, components and metabolic interactions

In the following, I will give a brief introduction to the photosynthetic carbon assimilation reactions, interactions and metabolic shuttles (chapters 1.3.1 - 1.3.4), which use the energy fixed in photosynthetic light reactions to produce the carbon-based metabolites essential for our life. I will then introduce the thylakoid-bound photosynthetic pigments and protein complexes (chapters 1.3.5 - 1.3.11), which can convert solar energy via the LET into chemical energy, ATP and NADPH, the basic requirement for sustaining life on Earth. Finally, I will introduce the external light harvesting system that collects light for the photosystems (Chapters 1.3.12-14).

1.3.1 Carbon assimilation and photorespiration

Most of the NADPH produced in LET, is used in the chloroplast stroma in the reductive pentose phosphate pathway, called the Calvin-Benson-Bassham (CBB) cycle, to reduce CO_2 to carbohydrates (Figure 2). The CBB cycle starts with the ribulose 1,5-bisphosphate carboxylase/oxygenase (Rubisco) catalysed carboxylation of five-carbon ribulose 1,5-bisphosphate (RuBP) with CO_2 and its conversion to two three-carbon 3-phosphoglycerates (3-PGA). 3-phosphoglycerate kinase (PGK) phosphorylates 3-PGA to 1,3-bisphosphoglyrecate (1,3-BPGA) which is then reduced to glyceraldehyde 3-phosphate (GA3P) by NADP-glyceraldehyde-3-phosphate dehydrogenase (GADPH). One-sixth of the formed GA3P can be taken out from the CBB cycle, while the rest is required for the regeneration of RuBP through six-carbon fructose 1,6-bisphosphate, four-carbon erythrose 4-phosphate and seven-carbon sedoheptulose 1,7-bisphosphate to ribulose 5-phosphate by several enzymes, of which fructose 1,6-bisphosphatase (FBPase) and sedoheptulose 1,7-bisphosphatases (SBPase) catalyse unidirectional reactions that drive the regeneration phase forward. Finally, ribulose 5-phosphate is phosphorylated to RuBP by phosphoribulokinase (PRK) to complete the cycle. After three cycles of CO_2 fixation, GA3P can be redirected from the cycle for downstream metabolism of which the sucrose synthesis in the cytoplasm and starch synthesis in the chloroplast are the main sinks. Sucrose is transported to heterotrophic tissues or growing leaves while starch is stored in the chloroplast.

In addition to the carboxylation reaction, Rubisco also catalyses the oxygenation of RuBP as a major side reaction, which is enhanced at low intracellular CO_2 concentrations (Bathellier et al., 2020). This oxygenation leads to the formation of 3-PGA and two-carbon 2-phosphoglycolate (2-PG), which is an inhibitor of triose phosphate isomerase (TPI) in the downstream processing of GA3P. This means that the accumulation of 2-PG leads to a feedback loop that downregulates RuBP

regeneration, which then leads to lower RuBP oxygenation, while simultaneously preventing the draining of GA3P from the CBB to downstream sinks (Timm et al., 2016). However, this type of regulation, which may be important for sensing intracellular CO_2 concentration, would quickly lead to the halting of the CBB cycle unless 2-PG is removed.

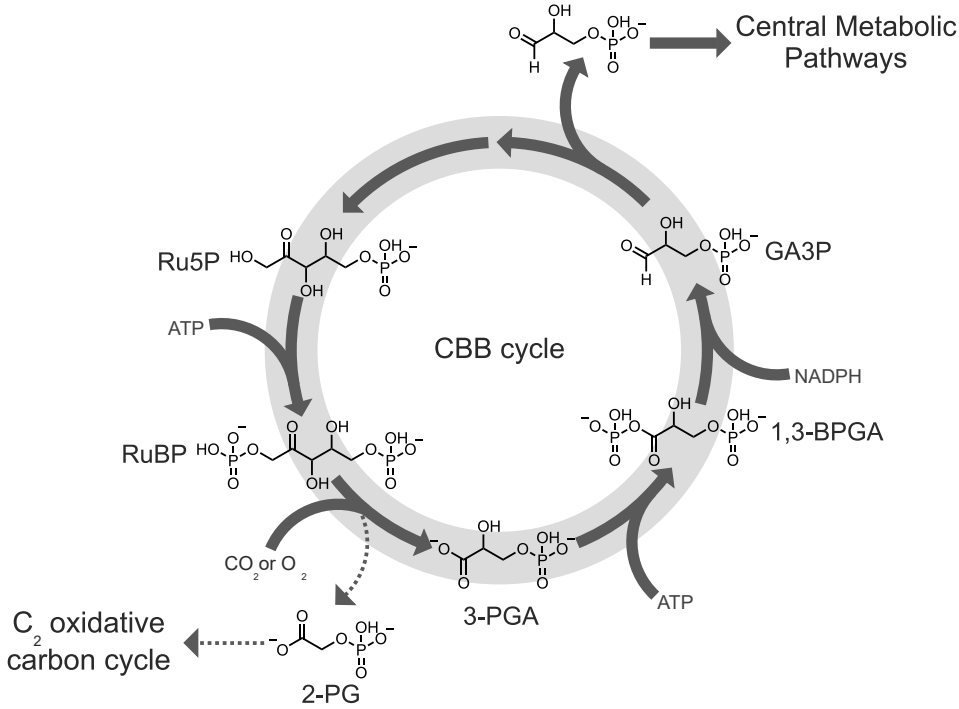

Figure 2. Simplified figure of CBB cycle in chloroplast stroma. Chapter 1.31 describes the function of the CBB cycle in more detail.

2-PG is salvaged by the C_2 oxidative carbon cycle which converts two molecules of 2-PG to GA3P via a complex metabolic pathway that occurs in chloroplasts, mitochondria and peroxisomes. In the first step, 2-PG is dephosphorylated by phosphoglycolate phosphatase to glycolate, which is then transported to the peroxisomes. Glycolate is then oxidised in the peroxisomes by glycolate oxidase to glyoxylate, which produces hydrogen peroxide (H_2O_2), which is detoxified by catalase. Glyoxylate is aminated by glutamate-glyoxylate aminotransferase to form 2-oxoglutarate (2OG) and glycine. The latter is then transported to the mitochondria where two glycines are converted to serine by the glycine decarboxylase complex and serine hydroxymethyltransferase, releasing CO_2 and ammonium (NH_4^+) and reducing nicotinamide adenine dinucleotide (NAD^+) to dihydro-nicotinamide

adenine dinucleotide (NADH). Serine is transported back to the peroxisome where it is deaminated to hydroxypyruvate by serine-2-oxoglutarate aminotransferase, which regenerates half of the glutamines needed to aminate glyoxylate in the previous peroxisomal step. Hydroxypyruvate reductase then uses NADH to reduce hydroxypyruvate to glycerate, which is transported to the chloroplasts and phosphorylated to 3-PGA by glycerate kinase. 3-PGA is then phosphorylated and reduced to GA3P before being used to regenerate RuBP. To complete the cycle, NH_4^+ released in the mitochondria is used to regenerate the 2OG produced in the peroxisomes by transporting both of these molecules to the chloroplasts where NH_4^+ is first fixed to glutamine by glutamine synthetase (GS) and then 2OG is aminated to glutamate by Fd-dependent glutamate synthase (Fd-GOGAT), which is transported back to the peroxisomes.

1.3.2 Photoassimilation of nitrate and sulfate

Like carbon, also inorganic nitrogen and sulfur are mostly available as oxides, mainly NO_3^{2-} and SO_4^{2-}, which need to be reduced for the synthesis of organic molecules. As, NO_3^{2-} and SO_4^{2-} are highly oxidised, their reduction in most plant species is linked to photosynthetic light reactions, where reducing power is directly available.

NO_3^{2-}, taken up by roots, is transported to leaves where it is reduced to nitrite (NO_2^-) by cytosolic NADH-dependent nitrate reductase. NO_2^- is then transported to the chloroplasts, reduced to NH_4^+ by Fd-dependent nitrite reductase, and then used for glutamine synthesis from 2OG by GS and Fd-GOGAT enzymes, which are also involved in the refixation of NH_4^+ in photorespiratory metabolism (chapter 1.2.1). Glutamine is then further used in transamination reactions to form other amino acids.

SO_4^{2-} reduction occurs in plastids where SO_4^{2-} is first activated to adenosine 5'-phosphosulfate (APS) by ATP sulfurylase (ATPS). The sulfate group in APS is reduced to sulfite (SO_3^{2-}) by glutathione-dependent APS reductase, but it can also be used for sulfonation reactions after phosphorylation to 3'-phosphoadenosine 5'-phosphosulfate (PAPS) by APS kinase. Released SO_3^{2-} is reduced by Fd to hydrogen sulfide (H_2S) by sulfite reductase. H_2S reacts with *O*-acetylated-serine in a reaction catalysed by *O*-acetyl-serine (thiol) lyase to form cysteine, which is then used to synthesise other organic and inorganic compounds containing reduced sulfur, such as iron-sulfur (FeS) clusters. Enzymes for cysteine synthesis have three different isoforms in plastids, mitochondria and cytosol, but cysteine synthesis appears to occur mainly in the cytosol with *O*-acetyl-serine being transported from the mitochondria (Takahashi et al., 2011).

1.3.3 The ins and outs of metabolite shuttles

Due to their central role in anabolism, chloroplasts export several metabolites to the cytosol, but chloroplasts are also able to export excess reducing power through malate shuttles, which consist of the malate-oxaloacetate metabolite pair, malate/oxaloacetate transporter and malate dehydrogenase enzymes (MDH) in the chloroplasts, mitochondria, peroxisomes and cytosol (Kinoshita et al., 2011; Selinski and Scheibe, 2018). The malate shuttle allows chloroplastic NADPH or NADH to reduce cytosolic NAD^+, which can be further transported to the mitochondria by several metabolite shuttles (Höhner et al., 2021; Zheng et al., 2021). The malate shuttle can also provide the NADH required for hydroxypyruvate reduction in peroxisomes during photorespiration, while NADH generated during glycine decarboxylation is used for oxidative phosphorylation (Shameer et al., 2019). This allows chloroplastic NADPH to be used for ATP production or dissipation of excess reductants by alternative dehydrogenases and oxidases or uncoupling proteins in mitochondria (see 1.3.4).

Chloroplasts are also able to export ATP and NADPH via the GA3P shuttle, which exports GA3P to the cytosol where it is oxidised and phosphorylated by glyceraldehyde 3-phosphate dehydrogenase to form 1,3-bisphosphoglycerate (1,3-BPG), which is coupled to the reduction of NAD^+ to NADH. 1,3-BPG is then dephosphorylated to 3-PGA by phosphoglycerate kinase, which generates ATP from ADP, and the formed 3-PGA is transported back to the chloroplast where it is regenerated to GA3P in the CBB cycle (Heineke et al., 1991). GA3P can also be oxidised by the non-phosphorylating glyceraldehyde 3-phosphate kinase to reduce $NADP^+$ to NADPH.

These metabolite shuttles can also function between different cell types, for example in C_4 photosynthesis in maize, the GA3P shuttle provides additional NADPH and ATP for the fixation of CO_2 released from malic enzyme-catalysed malate decarboxylation (Arrivault et al., 2017).

1.3.4 Mitochondria – working together with the chloroplasts

As with chloroplasts, also the function of mitochondria has diversified after eukaryotes became autotrophic, and the mitochondrial metabolism is closely linked to chloroplast metabolism in the light (Haferkamp and Schmitz-Esser, 2012; Møller et al., 2021; Igamberdiev and Bykova, 2022), but still, the main function of mitochondria is to produce ATP for metabolism in the cytosol and nucleus (Shameer et al., 2019; Vera-Vives et al., 2024).

Mitochondria have two membrane systems, consisting of an outer membrane and an inner membrane, which is folded to form cristae structures to increase the surface area of the inner membrane. The space enclosed by the inner membrane is called the

mitochondrial matrix and it contains enzymes for the TCA cycle and other metabolic pathways as well as mitochondrial DNA and ribosomes. The inner membrane houses the membrane complexes for the mitochondrial electron transfer chain (MET): NADH dehydrogenase, succinate dehydrogenase, cytochrome bc_1 complex and cytochrome c oxidase, which together with mitochondrial ATP synthase carry out oxidative phosphorylation. NADH dehydrogenase reduces ubiquinone (UQ) to ubiquinol (UQH_2) and simultaneously translocates protons to the intermembrane space, whereas succinate dehydrogenase only reduces UQ. Next, in cytochrome bc_1 complex, the UQH_2-dependent reduction of cytochrome c is coupled to proton translocation. Finally, electrons from reduced cytochrome c are used to reduce oxygen to water and transfer additional protons to the intermembrane space at cytochrome c oxidase. The transferred protons are used for ATP synthesis, as in chloroplasts, and ATP is transported across the membranes to the cytosol by adenine nucleotide transporters.

In the dark, oxidative phosphorylation is mainly driven by reductants generated from the catabolism of starch and sucrose in glycolysis and the TCA cycle. In the light, the TCA cycle switches to non-cyclic mode and is mainly used to acylate malate to citrate, which is oxidised to 2OG in the cytosol from where it can be transported to the chloroplasts for nitrogen assimilation (1.2.2.) or used for other anabolic reactions, such as 2OG-dependent dioxygenases in secondary metabolism (Sweetlove et al., 2010; Toleco et al., 2020; Lee et al., 2021; Igamberdiev and Bykova, 2022). Therefore, in the light oxidative phosphorylation is mainly driven by NADH generated during photorespiratory glycine decarboxylation (Shameer et al., 2019) or by the aforementioned metabolite shuttles from chloroplasts and cytosol. However, under high photorespiratory flux, the NADH production in glycine decarboxylation can saturate oxidative phosphorylation and mitochondria switch to alternative electron transfer pathways. The alternative electron transfer pathway consists of type II NAD(P)H hydrogenases, which can reduce UQ without proton pumping, and alternative oxidase (AOX), which can oxidise UQ without proton transfer across the membrane. These proteins thus consume excess reducing power without forming a proton gradient. These alternative pathways can also operate under high illumination to allow increased fluxes for citrate synthesis and consume excess reducing power without forming excess ATP (Florez-Sarasa et al., 2016). Mitochondria also have uncoupling proteins that can discharge the proton gradient formed, allowing the cytochrome pathway to dissipate excess reducing power (Toleco et al., 2020; Møller et al., 2021).

1.3.5 Photosynthetic pigments - interacting with light

The green colour of leaves is generally an indication of photosynthetic light reactions, as the chlorophyll pigments are essential for photochemistry at the photosystems, which absorb violet, blue and red light strongly, while green light is less absorbed. Land plants have two different chlorophylls, chlorophyll a (Chl a) and chlorophyll b (Chl b), which are macrocyclic tetrapyrroles that chelate a magnesium ion to the secondary amines and ester-linked diterpene phytol at the periphery of the macrocycle (Figure 3). The macrocycle forms a conjugated double bond system that allows chlorophylls to interact with visible light and the spectral differences between Chl a and Chl b are due to oxidation of the C7 methyl group in Chl a to formyl in Chl b by the enzyme chlorophyllide a oxygenase (CAO). The photosystem core complexes contain only Chl a, but the external light-harvesting antenna of both photosystems contain both Chl a and Chl b. The reaction centre of PSII also contain pheophytin a (Pheo a), which is Chl a without the chelated magnesium ion. Chlorophylls in the light-harvesting antenna rapidly transfer excitation energy to the reaction centres because Chl a has a lower first excited state than Chl b. The spectral properties of chlorophylls are further modified by the protein matrix in the reaction centres and antenna complexes (Sirohiwal and Pantazis, 2021), which promotes controlled photochemistry and enhances the directionality of excitation energy transfer.

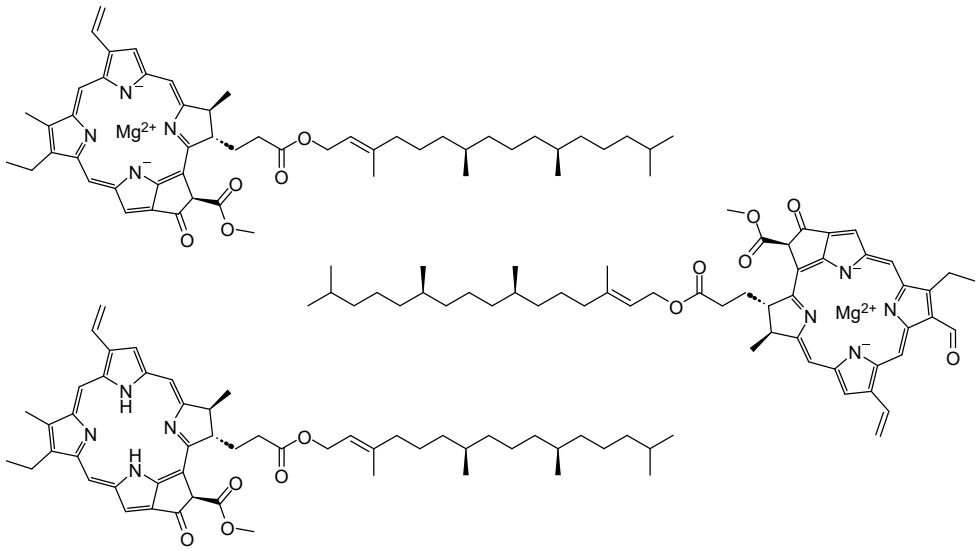

Figure 3. Structures of chlorophyll a, chlorophyll b and pheophytin a from top to bottom.

The photosystems also contain β-carotene which is a tetraterpenoid molecule with methylated cyclohexenyl rings at each end linked by a linear conjugated double bond system that allows the absorption of blue light (Figure 4). The light-harvesting antenna proteins bind xanthophylls, which are oxidised carotenoids. Lutein is doubly hydroxylated α-carotene, which is a regioisomer of β-carotene with different positions of the double bond in one of the cyclohexenyl rings. In comparison, zeaxanthin is doubly hydroxylated β-carotene that can be further derivatised by epoxidation of a cyclohexenyl double bond to antheraxanthin or by two epoxidations to violaxanthin. Violaxanthin is also isomerised to neoxanthin by opening one epoxy groups to form an allene structure with the adjacent double bond. Carotenoids have a dual function in photosynthesis, being able to transfer excitation energy to chlorophylls, but also to safely quench the chlorophylls during excess illumination. The quenching of chlorophyll excitation by carotenoids is possible due to their rapid vibrational relaxation, which is faster in linear carotenoids than in macrocyclic chlorophylls.

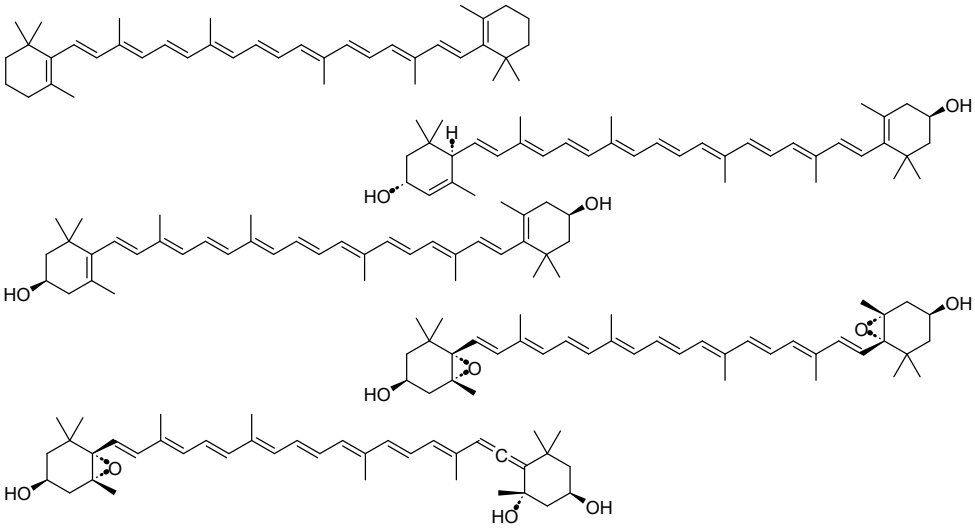

Figure 4. Structures of β-carotene, lutein, zeaxanthin, violaxanthin and all-trans neoxanthin from top to bottom.

Vascular plants also have other ubiquitous pigments, phenylalanine-derived hydroxycinnamic acid derivatives and flavonoids, which are not required for photosynthesis (Figure 5). However, they protect plants from ultraviolet (UV) light, shield them from excessive visible light and act as potent antioxidants (Hakala-Yatkin et al., 2010; Fernández-Marín et al., 2020; Leonardelli et al., 2024). Hydroxycinnamic acids and flavonoid glycosides are mostly stored in the vacuole, while flavonoid aglycones are embedded in the epicuticular wax layer. Hydroxycinnamic acid derivates are composed of a six-carbon aromatic ring which

is conjugated to an α,β-unsaturated carbonyl. The aromatic ring in hydroxycinnamic acid derivates can be oxidised and the carboxylic acid moiety is often esterified to polyols. The flavonoid structure consists of two aromatic rings connected by a third oxygen-containing ring, which can be either aromatic or aliphatic depending on the oxidation state. In addition to these oxidations in the connecting ring, the basic flavonoid structure can be heavily modified, tuning the chemical and spectroscopic properties of these pigments.

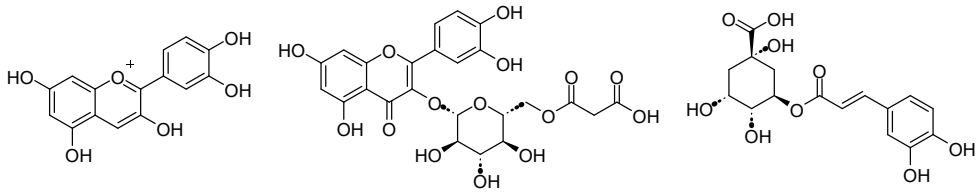

Figure 5. Structures of cyanidin, quercetin 3-*O*-(6''-*O*-malonyl)-β-D-glucoside (examples of flavonoids) and chlorogenic acid (example of hydroxycinnamic acid derivatives) from left to right.

1.3.6 Photochemical reactions and major thylakoid multisubunit protein complexes

The basic function of the major thylakoid-embedded protein complexes of photosynthetic light reactions has remained almost unchanged during the evolution of land plants. However, the addition of several small subunits to the protein complexes during evolution has modified the assembly of the complexes and, in particular, the regulation of these complexes. For example, the disappearance of the type 1 NADPH-dehydrogenase (NDH1) from certain lineages would be expected to require a different type of regulation. To understand how the changes in environmental conditions or metabolic requirements affect the function of thylakoid reactions, it is important to understand the photochemical, electron transfer and proton transfer reactions catalysed by these complexes.

1.3.7 Photosystem II

PSII is a dimeric core protein complex consisting of the reaction centre proteins D1 and D2 and the inner light-harvesting proteins CP43 and CP47 together with an additional 16 small subunits, which are mostly bound to the sides of the monomeric complex or at the lumenal side of CP43 and CP47 (Su et al., 2017). The PSII reaction centre couples water oxidation to plastoquinone reduction through a photochemical reaction. Water oxidation occurs on the lumenal side of the complex, where the oxygen-evolving complex (OEC) harbours a Mn_4O_5Ca cluster that undergoes four

consecutive oxidations to generate O_2 from two water molecules, simultaneously releasing four protons into the lumen. The influx of water and the efflux of protons occur through specific channels on the lumenal side of PSII. OEC is oxidised by photochemically oxidised reaction centre chlorophyll pair ($P680^{+\bullet}$) via redox active tyrosine residue (Tyr_Z) in the D1 protein. The PSII reaction centre complex has four Chl a molecules (P_{D1}, P_{D2}, Chl_{D1} and Chl_{D2}) and two Pheo a molecules ($Pheo_{D1}$ and $Pheo_{D2}$) bound to the D1 and D2 proteins (Figure 6). P_{D1} and P_{D2} are stacked along their planes to form an excitonic dimer (P680) surrounded on both sides by Chl_{D1} and Chl_{D2}, while the pheophytins are located on the top of these chlorophylls. Excitation of the reaction centre chlorophylls leads to charge separation at P_{D1} and the excited electron is initially transferred to $Pheo_{D1}$, while the positive charge is rapidly localised to the P_{D1} and P_{D2} pair forming $P680^{+\bullet}$ (Sirohiwal and Pantazis, 2023). The electron is transferred from $Pheo_{D1}$ to a tightly bound plastoquinone (Q_A) in the D2 protein and then, via a histidine and bicarbonate (HCO_3^-) chelated ferrous iron (Fe^{2+}), to a loosely bound plastoquinone (Q_B) in the D1 protein forming semiquinone ($Q_B^{-\bullet}$). $Q_B^{-\bullet}$ is further reduced to Q_B^{2-}, which is then protonated by iron-chelating histidine (His215) and by hydrogen-bonded serine (Ser264) and histidine (His252) pair, forming plastoquinol (PQH_2) (Saito et al., 2013). The formed PQH_2 is released from the Q_B binding pocket to the thylakoid membrane, allowing the binding of a new PQ.

1.3.8 Cytochrome b_6f complex

PQH_2 released from PSII is oxidised by the Cyt b_6f complex in a bifurcation reaction in which one of the electrons from PQH_2 is used to reduce PC in the high potential chain via histidine- and cysteine-bound Rieske Fe_2S_2 cluster and cytochrome f-bound heme-chelated iron, while the second electron is recycled to reduce PQ in the low potential chain via b_p, b_c and possibly c_n heme-chelated irons. The oxidation of PQH_2 results in the release of the bound protons to the lumen and the recycling of half of the electrons back to PQ, meaning that the transfer of one electron to PC is coupled to the transfer of two protons to the lumen (Sarewicz et al., 2021).

1.3.9 Photosystem I

PC is oxidised by oxidised PSI reaction centre chlorophyll pair ($P700^{+\bullet}$). The reaction centre chlorophylls are bound to the PsaA and PsaB proteins, both of which also bind a large internal chlorophyll antenna with a function similar to that of the CP43 and CP47 internal antenna bound to the PSII reaction centre (RC) complex (Figure 6). Excitation of the PSI reaction centre chlorophylls leads to charge separation and the electron is first transferred to Chl_0 and then to phylloquinone (PhQ), from where it is transferred to cysteine-bound four-iron-four-sulfur cluster (Fe_4S_4) F_X. In contrast to

PSII, electron transfer to F_x can occur in both branches, A and B, of the reaction centre complex. From F_X, the electrons are transferred the PsaC-bound Fe_4S_4 clusters F_A and F_B. and finally, to the Fe_2S_2 cluster of Fd (Caffarri et al., 2014).

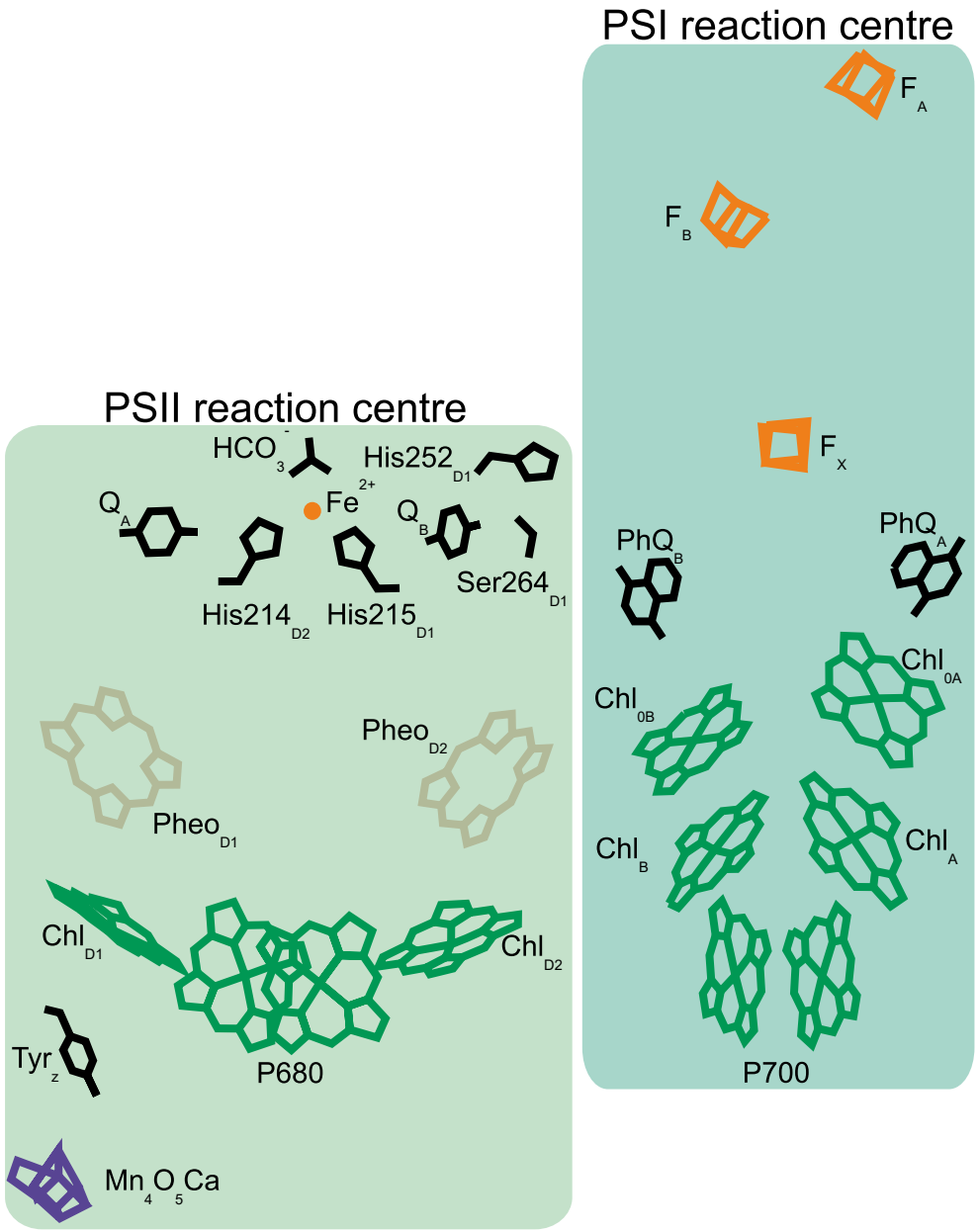

Figure 6. Simplified structures of PSII and PSI reaction centres. The figure is based on structures of PSII-LHCII and PC-PSI-Fd resolved by cryo-electron microscopy (Su et al., 2017; Caspy et al., 2020). Chapters 1.3.7 and 1.3.9 describe the function of the reaction centres in more detail.

1.3.10 ATP synthase

ATP synthase is a molecular machine that uses the proton motive force across the thylakoid membrane, generated by LET and cyclic electron transfer (CET) (chapter 1.5.2), to couple the efflux of protons to ATP synthesis. Lumenal protons enter a channel in the F_O part to the a-subunit where they protonate glutamate in one of the proteins in the c_{14} ring and after rotation of 12 c-subunits, the protons exit the ring to the stromal side through another channel in the a-subunit. Rotation of the c_{14} ring is coupled to rotation of the central stalk, composed of γ and ε subunits, which alters the structure of the adenosine nucleotide-binding domain F_1, composed of three dimers of α and β subunits, which catalyses ATP synthesis from ADP and PO_4^{3-}. F_O and F_1 are held in place by the peripheral arm, composed of b and b' subunits and a cap made of δ subunit. A full rotation of the central stalk generates three ATP molecules, and based on the number of subunits in F_O, the ATP/H^+ ratio has been estimated to be 4.7, but experimental data gives the lower value of 3.9 (Petersen et al., 2012). The discrepancy between these values affects the interpretation of the ratio between reductants and ATP produced in the light reactions, which has implications for the theoretical background of the regulation of photosynthesis (chapter 1.5).

1.3.11 Type 1 NADPH dehydrogenase

Contrary to its name, type 1 NADPH dehydrogenase (NDH1) is an Fd:PQ oxidoreductase that couples the oxidation of two Fd to the reduction of PQ to PQH_2, while simultaneously pumping four protons from the stroma to the lumen. The mechanism of proton pumping is still not yet fully understood, but the enzyme can function in both directions depending on the pH of the lumen and the redox state of the PQ and Fd pools (Strand et al., 2017; Richardson et al., 2021).

1.3.12 Eukaryotic external light-harvesting antenna

Since the first endosymbiosis event the evolution of photosynthetic light reactions has been only minor (Oliver et al., 2023), but major changes have occurred in the external light-harvesting system and its regulation leading to a higher quantum efficiency of light harvesting and adaptation of plants to more dynamic terrestrial environments (Cao et al., 2020; Croce and van Amerongen, 2020). Eukaryotic light-harvesting proteins have evolved from cyanobacterial high-light-induced proteins (Hlip), which are critical for PSII biogenesis, repair and photoprotection (Komenda and Sobotka, 2016). Presumably, the different Hlip genes fused to form different families of light-harvesting-like (LIL) proteins to function in photoprotection (Montané and Kloppstech, 2000; Lee et al., 2020; Psencik et al., 2020; Levin et al., 2023) before their evolution led to light harvesting (Engelken et al., 2010). Light-

harvesting and light-harvesting-like proteins have evolved together because they have complementary roles in harvesting light under low light conditions and dissipating excess light as heat under high light conditions. LHCB4 is thought to be the evolutionary oldest light-harvesting protein, and its appearance coincides with the loss of cyanobacterial-like soluble antenna, the phycobilisomes. Light-harvesting proteins expanded rapidly into a large family before the diversification of green algae. LHCSR, PSBS and the xanthophyll cycle evolved at the same time as light-harvesting antenna, highlighting the importance of photoprotection under fluctuating environmental conditions (Koziol et al., 2007; Neilson and Durnford, 2010).

1.3.13 Photosystem II external antenna

PSII has a modular external light-harvesting antenna (LHCII) which is composed of three minor antenna, LHCB4, LHCB5 and LHCB6 and major antenna composed of trimers of LHCB1, LHCB2 and LHCB3, which are named according to their binding strength to strongly (S), moderately (M) and loosely (L) bound trimers. The minor antenna LHCB4 is bound to CP47 and LHCB5 to CP43, while LHCB6 is bound to LHCB4, together with the M-trimer formed by LHCB3 and two LHCB1. The S-trimer is bound to the interface between CP43 and LHCB5 (Su et al., 2017). PSII supercomplexes are named according to the number of LHCII trimers (S and M) attached to the PSII core dimer (C_2). $C_2S_2M_2$ is the largest complex isolated from land plants (Figure 7), and the antenna size is first reduced by detaching M-trimers with LHCB4 and LHCB6, forming C_2S_2M and C_2S_2 complexes, until the S-trimers are also detached with LHCB5 forming, C_2S and C_2 complexes. Complexes containing L-trimers have not yet been isolated but spectroscopic studies have shown that the functional antenna size is larger than $C_2S_2M_2$, suggesting that a larger number of antenna complexes are connected to PSII (Croce and van Amerongen, 2020).

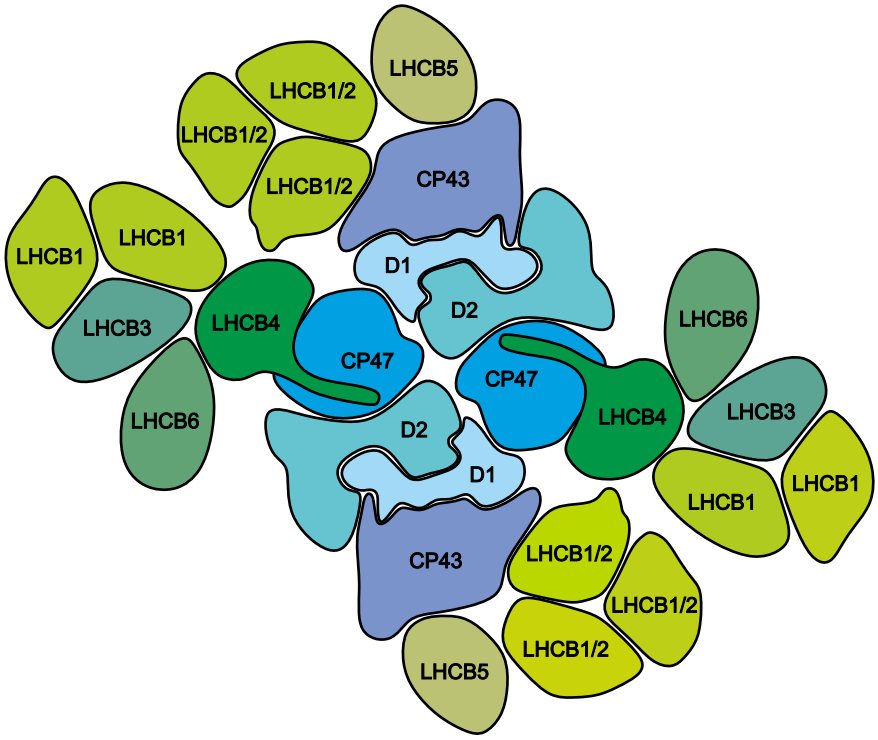

Figure 7. Simplified structure of $C_2S_2M_2$ PSII-LHCII supercomplex. Minor subunits of PSII core complex are omitted for clarity. The figure is based on structure resolved by cryo-electron microscopy (Su et al., 2017). More detailed description of the complexes in chapter 1.3.13.

1.3.14 Photosystem I external antenna

The PSI antenna system (LHCA) has two dimers composed of LHCA1, LHCA4, LHCA2 and LHCA3 and it forms a belt of antenna connected to PsaA and PsaB, with PSAG, PSAF, PsaJ and PSAN in the interphase mediating the excitation energy transfer from the antenna to the PSI core (Mazor et al., 2015; Pan et al., 2018). Compared to LHCII, the LHCA system has distinct spectral differences, as some of the Chl a have shifted absorption maxima, increasing the far-red absorption of the PSI antenna system, which is advantageous under canopy shading, that enriches far-red light (Croce and Van Amerongen, 2013). PSI can also receive light from the L-trimers, either through the formation of a specific PSI-LHCI-LHCII supercomplex, which is mediated by phosphorylated LHCB2 interacting with PSAH, PSAL and PSAO (Figure 8) (Pan et al., 2018), or indirectly via the LHCA belt (Yadav et al., 2017; Schiphorst et al., 2021). These interactions allow the L-LHCII trimers to act as a shared antenna lake for both photosystems (Grieco et al., 2015). PSI can also form supercomplexes with PSII (Järvi et al., 2011), which could

increase the size of PSI antenna as excitation energy is efficiently transferred from PSII to PSI, which has lower-energy chlorophylls. In the isolated complex, the core antenna of PSI and PSII are in direct contact on the PsaB side of PSI, which means that the formation of the PSI-LHCI-LHCII complex does not compete with the formation of the PSI-PSII complex (Yokono et al., 2019). However, it has been suggested that the PSI-PSII complex functions in photoprotection of PSII rather than in increasing the size of PSI antenna (Yokono et al., 2015).

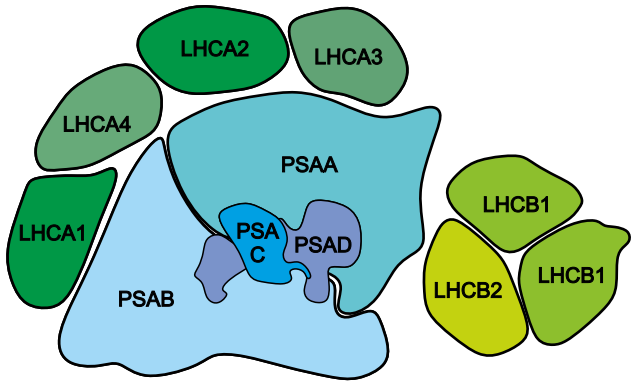

Figure 8. Simplified structure of PSI-LHCI-LHCII supercomplex. Minor subunits of PSI core complex are omitted for clarity. The figure is based on structure resolved by cryo-electron microscopy (Pan et al., 2018). More detailed description of the complexes in chapter 1.3.14.

Some land plants also have a third type of PSI supercomplex optimised for CET (PSI-NDH1), in which two PSIs are bound to NDH1, and this interaction is mediated by the specific antenna proteins LHCA5 and LHCA6, which replace LHCA4 and LHCA2 in two different PSI complexes (Figure 9) (Shen et al., 2022).

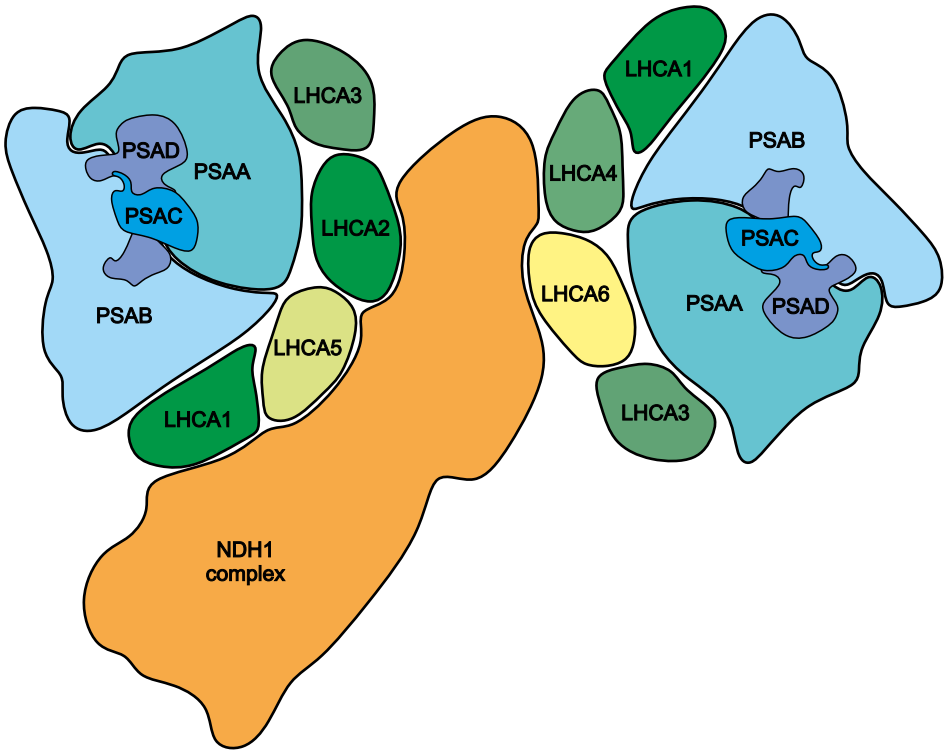

Figure 9. Simplified structures of PSI-NDH1 supercomplex. Minor subunits of PSI core complex and different subunits of NDH1 are omitted for clarity. The figure is based on structure resolved by cryo-electron microscopy (Shen et al., 2022). More detailed description of the complexes in chapter 1.3.14.

1.4 Dangers of light reactions – photodamage to reaction centres

Both photosystems perform extreme redox reactions for biochemical systems, as the oxidised PSII reaction centre $P680^{+\bullet}$ is one of the strongest biological oxidants, while PSI is one of the strongest biological reductants. While other excited chlorophylls are also reactive, the rapid downhill excitation energy transfer means that excited chlorophylls are short-lived in the antenna system when photosystems can use the excitation energy for photochemistry or dissipate it as heat (Caffarri et al., 2014). These reactive intermediates can induce chemical modifications in the cofactors or polypeptides that damage the photosystems directly or through secondary reactions, mainly by activating O_2 to reactive singlet oxygen ($^1O_2$) or superoxide ($O_2^{\bullet}$). $O_2^{\bullet}$ is rapidly decomposed to hydrogen peroxide (H_2O_2), either non-enzymatically or enzymatically by superoxide dismutases (SOD). H_2O_2 is less reactive than $O_2^{\bullet}$, but it can react with free transition metal ions to form the extremely reactive hydroxyl

radical ($HO^{\bullet}$), which can initiate radical reactions with organic molecules (Asada, 2006; Khorobrykh et al., 2020).

Photosynthesis is intricately regulated to prevent the accumulation of these reactive intermediates and the formation of ROS, but under some conditions, the damage cannot be completely prevented, and plants must have efficient mechanisms to repair the damaged reaction centres. ROS can also damage other cellular components, so suppression of ROS formation and removal of ROS is important for reasons other than prevention of damage to photosystems (Juan et al., 2021).

Photodamage is part of photoinhibition, which means that the activity of light reactions is reduced by light, but photoinhibition can also be caused by down-regulation of light-harvesting or inhibition of repair. Therefore, photodamage is used here exclusively to describe chemical modifications in photosystems that prevent them from functioning in LET.

1.4.1 Photosystem II photodamage and repair

PSII photodamage has been extensively studied, but there is still no consensus on the exact mechanism(s) or the primary site of damage. It is likely that several mechanisms operate in parallel, and the relative contribution of these mechanisms depends on the prevailing environmental and metabolic conditions (Murata et al., 2007; Oguchi et al., 2009; Vass, 2012). Furthermore, regardless of the primary site of photodamage, secondary reactions may also damage other sites, making it difficult to identify the primary site of photodamage. Regardless of the mechanism and site of primary photodamage, the endpoint appears to be the same. The damaged reaction centre protein D1 is degraded, and a new copy is synthesised to replace the damaged one during the PSII repair cycle, allowing PSII to function efficiently as long as the rate of repair keeps pace with the rate of damage.

The mechanisms of PSII photodamage have been broadly divided into donor- and acceptor-side mechanisms. In donor-side mechanisms, the initial site of damage occurs near the OEC or directly at the OEC, where excitation of the metal cluster by UV or blue light destabilises the complex, leading to detachment of manganese ion, which in turn prevents the water splitting and hence electron donation to oxidised $P680^{+\bullet}$ (Hakala et al., 2005; Hakala-Yatkin et al., 2010). OEC is also prone to misses and, for some unknown reason, the catalytic cycle does not always proceed normally, preventing electron donation to oxidised $P680^{+\bullet}$. As a strong oxidant, the long-lived $P680^{+\bullet}$ can extract electrons from the surrounding organic molecules, leading to the generation of putatively harmful oxidative modifications. $P680^{+\bullet}$ can also be re-reduced by charge recombination from downstream electron acceptors, and these recombination reactions can lead to the formation of triplet chlorophyll (^3Chl), which, due to its long-lived excited state, can react with O_2 to form $^1O_2$ (Mattila et

al., 2023). Unlike the ground-state triplet O_2, excited $^1O_2$ is extremely reactive with organic molecules, particularly with double bonds of aromatic amino acids, chlorophylls and carotenoids present near the reaction centre (Takegawa et al., 2019). Again, these secondary oxidative modifications are thought to be the cause of photodamage to PSII, but the exact sites have not been conclusively elucidated.

$^1O_2$ is also involved in the acceptor-side mechanism, where the forward electron transfer is prevented by electron acceptors saturation, increasing the probability of charge recombination and intersystem crossing directly to ^{3}Chl. Acceptor side limitation can also lead to a double reduction of Q_A, which is then released from the reaction centre D2 protein. The lack of Q_A prevents normal PSII function, which in turn increases the rate of $^1O_2$ production and secondary oxidative damage, which may be beneficial under these conditions since Q_A cannot be replaced without D1 resynthesis (Hayase et al., 2023). Charge recombination can also be enhanced by a strong electric field generated the by accumulation of protons in the lumen during the light reactions and electron transfer (Davis et al., 2016).

In the PSII repair cycle, the external outer antenna is detached from the photodamaged PSII complexes and the damaged PSII core complex is transferred from the appressed grana membrane to the grana margins for repair (Järvi et al., 2015). After dimer monomerisation, CP43 is detached from the complex, allowing DEG-proteases to access the damaged D1 protein to cleave the protein into shorter peptides, which are then progressively degraded by ATP-dependent FTSH-proteases. At the same time, the OEC is disassembled and pigments released from the RC complex are transferred to one-helix proteins (OHPs) and either reused or targeted for degradation (Wang and Grimm, 2021). After removal of damaged D1, the CP47-D2 complex interacts with D1-translating polysomes and new D1 is synthesised directly into the complex with co-insertion of the pigments and other cofactors. The C-terminus of the newly synthesised pre-D1 is then cleaved before the complex can be reassembled completely (Che et al., 2013). OEC is then assembled on the lumenal side and photoactivated by the reaction centre. The repaired PSII cores are then dimerized and reassembled with the external antenna proteins to form the PSII-LHCII supercomplex.

1.4.2 Photosystem I photodamage and repair

The mechanism of PSI photodamage has been less controversial than PSII photodamage and the consensus is that the F_X, F_A and F_B Fe_4S_4 clusters are damaged in an O_2-dependent manner when the PSI electron acceptors are saturated, presumably by formation of $O_2^{\bullet}$ and secondary oxidation of Fe_4S_4 by $O_2^{\bullet}$ (Erling Tjus et al., 1999; Scheller, Henrik and Haldrup, 2005; Sonoike, 2007). Destruction of Fe_4S_4 clusters prevents electron transfer from P700 to stromal electron acceptors and

is often detected as a decrease in maximal P700 oxidation. The sequence of the damage to F_X, F_A and F_B Fe_4S_4 clusters during PSI photoinhibition starts with F_A and F_B, but a decrease in maximal P700 oxidation is only apparent after the damage to F_X clusters as well (Tiwari et al., 2016; Tiwari et al., 2024). PSI photodamage was first described in chilling-sensitive cucumber (*Cucumis sativus*) under moderate illumination at low temperature (Terashima et al., 1994; Sonoike et al., 1995). Later, it was also detected in more cold-tolerant Arabidopsis, barley (*Hordeum vulgare*) and potato (*Solanum tuberosum*) under similar conditions, but the degree of inhibition was much lower in these species (Havaux and Davaud, 1994; Tjus et al., 1998; Zhang and Scheller, 2004). PSI photodamage was therefore initially thought to be specific to low temperature, but the detection of PSI photodamage in the *pgr5* mutant and in plants treated with fluctuating light showed that it may be a more general phenomenon (Suorsa et al., 2012).

PSI photodamage leads to a decrease in the amount of the reaction centre proteins PsaA and PsaB, but on a very slow time scale (Scheller, Henrik and Haldrup, 2005; Sonoike, 2007). Damaged PSI reaction centres are therefore degraded in a similar way to PSII repair, with the exception that in PSI, where the reaction centre and the internal antenna are all bound to PsaA and PsaB, the entire PSI complex must to be re-synthesised, and not just the damaged reaction centre proteins as in PSII (Zhang and Scheller, 2004). Instead, the PSII core antenna CP43 and CP47 remain largely intact, during the repair cycle of PSII, like the external light-harvesting complexes. Compared to PSII repair, PSI repair is considerably slower, but the reason for this has not been extensively studied (Zhang and Scheller, 2004). Nevertheless, both PSII and PSI repair appear to be affected by environmental conditions (Murata et al., 2007; Zhang et al., 2011), suggesting that both are controlled processes.

1.5 Regulation of light reactions and stromal metabolism

Abiotic environmental conditions can change rapidly, and large changes in light intensity can occur in less than a second due to cloud movement or wind-induced changes in leaf angle or canopy shading (Burgess et al., 2021). The magnitude of temperature changes is not as large as in light intensity, but in temperate regions it can change by more than 15°C degrees during the day, and the daily averages can be greater than 10°C (Zhou et al., 2020; Sharma et al., 2023). The third dynamic abiotic factor is water availability, which affects the gas exchange, as plants must regulate evaporation through stomata to prevent excessive water loss during drought. This also reduces the evapotranspiration-driven transport of inorganic nutrients from roots to leaves. In addition to affecting leaf movement, wind also increases

evaporation by reducing the boundary layer, leading to increased evaporation, which then reduces leaf temperature and leads to impaired water use efficiency.

It is noteworthy that the changes in abiotic conditions affect light reactions and stromal metabolism differently. Light has a direct effect on the rate of light reactions. In contrast, temperature changes have a more direct effect on gas exchange and stromal metabolism, in particular on the rates of enzyme-catalysed reactions and by changing the ratio between carboxylation and oxygenation at Rubisco (Fernández-Marín et al., 2020; Hüner et al., 2022). Thus, plants have several dynamic short-term mechanisms that regulate the rate and output of both systems to maintain a balance between light reactions and stromal metabolism, thereby reducing the likelihood and consequences of harmful side reactions. At the same time, however, long-term regulatory mechanisms are also initiated to acclimate the plant to more stable changes in environmental conditions (Athanasiou et al., 2010; Karim and Johnson, 2021).

The output of chloroplast metabolism is also strongly influenced by metabolic needs of different cell types (Daloso et al., 2023). For example, young leaves have higher concentrations of phenylpropanoids and phenylalanine which require higher fluxes through the shikimate pathway in chloroplasts (Dethloff et al., 2017), whereas glandular trichomes use the ATP and NADPH generated in light reactions mainly to drive secondary metabolite production from imported sucrose (Balcke et al., 2017). Another extreme example is the mesophyll and bundle sheath cell chloroplasts of C_4 plants, such as maize, where mesophyll cells generate ATP and NADPH in LET, whereas bundle sheath cells mainly generate ATP with NDH1-dependent CET (chapter 1.5.2). This is regulated by lower expression of PSII assembly factors in the bundle sheath cells through altered light signalling (Meierhoff and Westhoff, 1993; Hendron and Kelly, 2020). A more moderate example of cell-type-specific regulation of light reactions has been observed in Arabidopsis, which has a higher accumulation of the PSI-NDH1 supercomplex in stems than in leaves (Laihonen et al., 2024). Indeed, the light reactions are also regulated at the developmental level and not only by the need to acclimate according to environmental cues.

1.5.1 Chloroplast antioxidant system

Under rapidly changing conditions, the chloroplast antioxidant system is in the first line of defence against ROS, and consist of several enzymatic and non-enzymatic antioxidants (Maruta et al., 2024). The antioxidant system must suppress not only the accumulation of several types of ROS, but also the secondary products of ROS generated by reactions with biomolecules, loosely classified as reactive electrophilic species (RES). RES are reactive with nucleophilic groups in biomolecules to form further adducts (Farmer and Mueller, 2013; Juan et al., 2021; Maruta et al., 2024).

Secondary reactions with ROS can also form organic radicals, which can initiate radical chain reactions, particularly in lipid membranes, therefore amplifying the deleterious effects of ROS.

The majority of $O_2^{\bullet}$ is generated at the acceptor side of PSI, most likely by stromal monodehydroascorbate reductase (MDAR), which has a dual function in ROS generation and scavenging (Asada, 1999; Khorobrykh et al., 2020). Generated $O_2^{\bullet}$ is rapidly converted by SOD to H_2O_2, which is then reduced to water by thylakoid or stromal ascorbate peroxidases (tAPX and sAPX) by oxidation of two ascorbates to monodehydroascorbate (MDA) radicals. The formed MDA radicals are reduced by monodehydroascorbate reductase (MDAR) to ascorbate with Fd or NADPH-derived electrons or disproportionated to dehydroascorbate (DHA) and ascorbate. DHA is reduced back to ascorbate by glutathione-dependent dehydroascorbate reductase (DHAR), while oxidised glutathione is reduced by NADPH-dependent glutathione reductase (GR). This chain reaction results in the reduction of O_2 to H_2O by PSII-derived electrons, and has been termed the water-water cycle, which allows relatively safe scavenging of excess reducing power. Ascorbate can also scavenge $^1O_2$, making it an effective antioxidant against the ROS derived from light reactions (Kramarenko et al., 2006; Khorobrykh et al., 2020).

The thylakoid membrane is protected from ROS by α-tocopherol and carotenoids. α-tocopherol scavenges peroxides and $^1O_2$, but it can also physically quench $^1O_2$ (Munné-Bosch, 2005), while oxidised α-tocopherol is regenerated by ascorbate (Asada, 1999). Carotenoids can also physically quench $^1O_2$ and scavenge it by forming apocarotenoids, but more importantly, carotenoids can quench ^{3}Chl and prevent the formation of $^1O_2$ (Khorobrykh et al., 2020).

Chloroplasts also have an overlapping system for H_2O_2 and lipid peroxide detoxification based on peroxidases and glutathione peroxidases. 2-Cysteine peroxiredoxin (2-CysPrx), peroxiredoxin Q (PrxQ) and type II peroxiredoxin (PrxIIE) are more specific for H_2O_2, whereas glutathione peroxidases (Gpx) are more efficient against lipid peroxides (Dietz, 2016). 2-CysPrx appears to be more important than APX in detoxifying H_2O_2 during excess illumination (Awad et al., 2015), demonstrating that these two systems are complementary. Glutathione also plays a role in scavenging RES by forming adducts in a reaction catalysed by glutathione transferase (Mueller and Berger, 2009; Mano et al., 2019). Glutathionylated adducts are transported to the vacuole, where glutathione can be released from the adduct by glutaredoxins.

1.5.2 Alternative electron transfer pathways

Alternative electron transfer pathways can be divided into cyclic pathways and O_2-reducing pathways. These pathways are thought to balance the production of

ATP and NADPH according to metabolic needs or to remove excess reductants with minimal accumulation of ROS. The PSI CET pathways pump electrons from PSI acceptors back into the electron transfer chain, thereby increasing the production of ATP at the expense of reductants, while the O_2-reducing pathways consume excess reductants, thereby increasing the relative production of ATP over NADPH in the chloroplast.

Two of the O_2-reducing pathways, the malate valve (chapter 1.3.3 and 1.3.4) and the water-water cycle (chapter 1.5.1), have been discussed above and these pathways operate at the PSI acceptor side. Another O_2 reduction pathway operating at the PSI acceptor side is catalysed by flavodiiron (Flv) proteins in cyanobacteria, green algae and lower plants (Zhang et al., 2009; Ilik et al., 2017). However, these proteins have been lost during the evolution of angiosperms. One reason for this may be the increased capacity of the water-water cycle in angiosperms (Maruta et al., 2024), which may have a similar function to Flv proteins in consuming the excess electrons. It is conceivable that the generation of ROS in the water-water cycle of angiosperms may play a role in signalling. This signalling may be important for plants to acclimate to changing environmental conditions (Foyer and Kunert, 2024), such as a constant increase in light intensity (chapter 1.5.8), and may explain the loss of the Flv proteins in angiosperms.

Photorespiration is also an O_2-reducing pathway, as Rubisco catalyses the oxidation of RuBP, but the salvage of 2-PG has a higher ATP/NADPH ratio than CO_2 fixation (Smith et al., 2023). This means that maintaining a high photorespiratory flux requires the activation of other alternative pathways to restore the ATP/NADPH balance, but the outputs of the photorespiratory metabolism can also change, making the effect highly dependent on the metabolic state of the cell (Walker et al., 2024).

Unlike the other O_2 reduction pathways, the plastid terminal oxidase (PTOX) acts between PSII and PSI by oxidising PQH_2. PTOX is also involved in carotenoid biosynthesis during chloroplast biogenesis and therefore its function has been difficult to study using deletion mutants. A recent study using the Arabidopsis *ptox* mutant, which expresses a bacterial carotenoid desaturase, showed that PTOX is important under high light illumination to oxidise the intersystem chain that protects PSI from photoinhibition (Messant et al., 2024). The mutant also has reduced PSII inhibition, suggesting that PTOX-generated ROS are likely to have regulatory functions by down-regulating PSII under excessive illumination.

CET around PSI has been known for decades, but the molecular mechanisms are still partly unresolved. One reason for this is that several pathways have been proposed to carry out CET in plants, namely NDH1, PGR5-PGRL1 and Cyt b_6f (Yamori and Shikanai, 2016). In the case of NDH1, it is clear that NDH1 can accept electrons from Fd to reduce PQ to PQH_2 while pumping protons into the lumen, but

the exact mechanisms, such as electron carriers and site of PQ reduction, remain elusive in the other pathways (Nawrocki et al., 2019).

1.5.3 Quenching of excess excitation energy

Under conditions that saturate the stromal metabolism and light reactions, the lifetime of excited chlorophylls in the antenna increases because the downward transfer of excitation energy is hindered. The accumulation of chlorophyll excited states could lead to the formation of $^1O_2$ in the antenna, so the rate of non-radiative relaxation of excited states must be increased to protect the antenna system from photodamage and to down-regulate the light reactions by limiting light harvesting. Collectively, this is referred to as non-photochemical quenching (NPQ), which consists of several mechanisms that quench the excitation energy at the external light-harvesting antenna and the reaction centres (Ivanov et al., 2008; Holzwarth et al., 2009; Belgio et al., 2014; Dall'Osto et al., 2017).

Energy-dependent quenching (qE) is rapidly induced when the output of light reactions exceeds the capacity of downstream metabolism, as occurs with a sudden increase in light intensity. This is due to acidification of the lumen, which protonates glutamate residues in the PSBS protein, changing its conformation. Activated PSBS is thought to act as a chaperone, modifying the structure of LHCII trimers from a light-harvesting state to a dissipative state by altering the interactions between the chlorophylls and carotenoids bound to the LHCII antenna (Saccon et al., 2020; Son et al., 2020a; Nicol and Croce, 2021; Ruban and Saccon, 2022). As qE depends on the conformational switch in the antenna proteins, it is rapidly relaxed within seconds when pH of the lumen increases and PSBS is deactivated.

Zeaxanthin-dependent quenching (qZ) is another mechanism activated by lumen acidification, which changes the pigment composition of the thylakoid membrane and the external light-harvesting antenna. Lumen acidification activates violaxanthin-deepoxidase (VDE), which converts violaxanthin via antheraxanthin to zeaxanthin. The formed zeaxanthin then replaces violaxanthin in the external light-harvesting antenna, thereby increasing the qE sensitivity of the LHCII trimers and directly promoting quenching at the minor light-harvesting antenna by changing their conformation (Dall'Osto et al., 2017; Kress and Jahns, 2017; Son et al., 2020b). qZ is relaxed when zeaxanthin is converted back to violaxanthin by zeaxanthin epoxidase (ZEP). qZ is induced and relaxed more slowly than qE because qZ relies on modification of thylakoid pigment pools, which are then equilibrated with the antenna-bound pigment pools.

The third mechanism for quenching external light-harvesting antenna is lipocalin-dependent quenching (qH), which again modifies the structure of LHCII trimers to a quenched state, but the exact mechanisms are still unclear (Bru et al.,

2022). However, the proteins required for qH formation and relaxation have been identified by mutant studies. Chloroplastic lipocalin (CHL) is required for the induction of qH, while redox-regulated suppressor of quenching (SOQ1) inhibits lipocalin (Brooks et al., 2013; Malnoë et al., 2017), and finally, the relaxation of qH1 (ROQH1) is required to return the antenna to the light-harvesting state (Amstutz et al., 2020). qH appears to relax more slowly than qE and qZ on the time scale of hours, but the analysis intervals were quite long, making it difficult to assess how persistent qH is in the wild-type plants (Amstutz et al., 2020).

The fourth quenching mechanism is reaction centre quenching at PSII, which is again quite poorly understood. Reaction centre quenching occurs in damaged and functional reaction centres. Damaged reaction centres quench by an unknown mechanism (Nawrocki et al., 2021), but in functional reaction centres it has been shown to occur through charge recombination reactions in reaction centres where the $Q_A/Q_A^{-\bullet}$ and/or $Q_B/Q_B^{-\bullet}$ midpoint potentials (E_m) are altered (Ivanov et al., 2008), and in closed reaction centres by still unresolved mechanism (Farooq et al., 2018).

1.5.4 Photosynthetic control at Cytochrome b_6f complex

PQH_2 oxidation at Cyt b_6f is the rate-limiting step in linear electron transfer and therefore the modulation of its activity is an efficient way to regulate electron transfer. Cyt b_6f is regulated according to light intensity, and under excess illumination, PQH_2 oxidation is slowed down, resulting in the oxidation of PC and P700. This regulation of electron transfer is called photosynthetic control and it is activated by acidification of the lumen (Joliot and Johnson, 2011). Lowering the lumenal pH is thought to increase the protonation of histidine bound to the Rieske Fe_2S_2 cluster. Protonation of this chelating histidine prevents the concerted proton and electron transfer reactions of PQH_2 oxidation (Ustynyuk and Tikhonov, 2018). The redox regulation of Cyt b_6f has also been suggested (Johnson, 2003), although the exact mechanism still remains unclear (Degen and Johnson, 2024). In addition, the recent structure of Cyt b_6f suggest that the phosphoprotein TSP9 may regulate its activity, possibly in a phosphorylation-dependent manner (Fristedt et al., 2009; Sarewicz et al., 2023).

1.5.5 Regulation of lumenal pH

As emphasised in previous chapters, the lumen acidification is critical for the regulation of photosynthetic light reactions. Lumen pH is mainly influenced by the balance between proton generation in OEC and proton influx at Cyt b_6f and NDH1, as well as by other possible CET pathways, which are counteracted by proton efflux through ATP synthase and thylakoid ion channels. ATP synthase uses the proton

motive force (pmf), which is composed of an electric field component (ΔΨ) and a proton gradient component (ΔpH). Since the lumen pH plays the main regulatory role in NPQ and photosynthetic control, adjusting the pmf partitioning to ΔpH and ΔΨ has the potential to fine-tune the regulation of light reactions. However, high ΔΨ increases the rate of recombination reactions at PSII, and thereby promotes $^1O_2$ production and PSII photoinhibition (Davis et al., 2016), implying that also ΔΨ must be tightly regulated.

The composition and magnitude of pmf is adjusted by ion channels, which can dissipate ΔΨ by influx of anions, mainly chloride, or by efflux of cations. On the other hand, the exchange of protons for cations converts between ΔΨ and ΔpH. Thylakoids have several ion channels, but only two of them, the chloride channel VCCN1 and the proton/potassium antiporter KEA3, have been extensively studied, and they appear to function under different conditions (Kunz et al., 2024). VCCN1 is important under sudden increases in light intensity, where it allows chloride to enter the lumen, dissipating ΔΨ and thereby protecting PSII from photoinhibition. VCCN1 was thought to be voltage-gated, and therefore activated when ΔΨ is too high (Herdean et al., 2016), but a recent report has questioned the regulatory mechanism of VCCN1 (Hagino et al., 2022). KEA3 is important under sudden decreases in light intensity, when ΔpH needs to be rapidly dissipated to relax qE and photosynthetic control from limiting the light reactions. KEA3 is regulated by the stromal ATP and NADPH levels and by stromal pH, allowing it to synchronise lumen pH-dependent regulation of light reactions with stromal metabolism (Uflewski et al., 2024). As VCCN1 and KEA3 ion channels function under different conditions, both of them are important for light acclimation, and dysregulation leads to photodamage (Uflewski et al., 2021; von Bismarck et al., 2023).

Proton efflux from the lumen is mainly regulated by the conductivity of ATP synthase, but the regulation of ATP synthase is poorly understood (Shikanai, 2023). The conductivity of ATP synthase decreases under high light intensity compared to low light or growth light (Kanazawa et al., 2017). This has been proposed to be due to PO_4^{3-} limitation of ATP synthase (Takizawa et al., 2008), and PO_4^{3-} concentration is in turn thought to be controlled by triose phosphate utilisation (McClain and Sharkey, 2019), which is dependent on the rate of metabolism beyond the CBB cycle. However, measurements with a FRET-based ATP sensor indicate that the stromal ATP concentration remains relatively stable with increasing light intensity (Uflewski et al., 2024). Metabolite analyses of isolated chloroplasts also show that the ATP/ADP ratio remains relatively stable in the light, even in the absence of known major ATP-consuming reactions (Kobayashi et al., 1979). It is therefore conceivable that some mechanism, other than PO_4^{3-} limitation, regulates the ATP synthase, especially since the use of triose phosphates is not thought to limit photosynthesis under normal growth conditions (McClain et al., 2023). It has also

been proposed that the magnitude of steady-state ΔΨ is smaller than generally accepted. This implies that the lumen acidification-induced mechanisms need additional forms of regulation. These may include, for example, the zeaxanthin-dependent allosteric regulation of qE and redox regulation of photosynthetic control at Cyt b_6f (Wilson et al., 2021).

1.5.6 Phosphorylation of thylakoid proteins

As the specific antenna systems of PSII and PSI can differ in size and light absorption properties, changing light conditions often lead to an uneven distribution of excitation energy and thus to an imbalance between the two photosystems. This functional imbalance can be restored by altering the distribution of excitation energy from the shared L-trimer antenna lake in a phosphorylation-dependent manner (Grieco et al., 2015). The LHCB1 and LHCB2 proteins in LHCII trimers are phosphorylated by the STN7 kinase, which is activated by binding of PQH_2 to the Q_O site of Cyt b_6f complex (Vener et al., 1997), and inhibited by reduced thioredoxins in the stroma (Rintamäki et al., 2000). Such dual regulation of STN7 links the excitation energy balancing between the two photosystems to the redox state of stromal metabolism. Based on redox regulation of the STN7 kinase, the formation of the phosphorylation-dependent PSI-LHCI-LHCII complex increases when the light intensity decreases from that under the growth light (Rintamäki et al., 1997), and under red light, which maximally activates the STN7 kinase due to the reduction of PQ pool. Conversely, the LCHII trimers are dephosphorylated, by TAP38 phosphatase (Shapiguzov et al., 2010), when light intensity increases over certain threshold due to Trx-dependent inhibition of STN7 and under far-red light, which preferentially excites PSI and keeps PQ pool mostly oxidised. Upon changing light conditions, the LHCB2 phosphorylation is considerably faster than LHCB1 phosphorylation (Leoni et al., 2013), and only LHCB2 phosphorylation is required to restore the functional balance between the photosystems (Cutolo et al., 2023).

The rebalancing of excitation energy is not only dependent on LHCII phosphorylation, but also involves the disassembly of larger PSII supercomplexes via the STN7 and STN8 kinase-dependent phosphorylation of PSII core proteins and the minor antenna LHCB4 (Tikkanen et al., 2006; Tikkanen et al., 2008; Dietzel et al., 2011). Phosphorylation of the PSII core proteins, D1, D2, CP43 and PSBH, by the STN8 kinase also controls the PSII repair cycle by promoting the disassembly of the supercomplexes, thereby allowing better access of damaged PSII to D1 proteases and for the contact with stroma-exposed membranes where the damaged D1 protein can be replaced by de novo synthesised D1 copy (Vainonen et al., 2005; Tikkanen et al., 2008; Nath et al., 2013). However, damaged D1 needs to be dephosphorylated

by PSII core phosphatase (PBCP) before it can be degraded (Rintamäki et al., 1995; Samol et al., 2012; Puthiyaveetil et al., 2014).

1.5.7 Thioredoxin-dependent redox regulation

Plant metabolism, especially in chloroplasts, is strongly redox-regulated by thioredoxins, which reduce disulfide bonds between cysteine residues in proteins (Buchanan, 2016; Geigenberger et al., 2017). The opening and formation of disulfide bridges alters the conformation of proteins, with consequences for their activity or ability to form complexes. Chloroplasts have several stromal thioredoxins, of which the major isoforms in leaves are Trx-f1, Trx-m1, Trx-m2, Trx-m4, Trx-x, Trx-y2 and Trx-z. These thioredoxins are mainly reduced by Fd-dependent thioredoxin reductase (FTR). However, Trx-f1 can also be reduced by chloroplastic NADPH-dependent thioredoxin reductase (NTRC) (Nikkanen et al., 2016), which also has a thioredoxin domain to reduce its targets directly with NADPH. Trx-f1 is the main regulator of CBB cycle enzymes and ATP synthase, whereas Trx-ms appears to regulate nitrogen metabolism and other high light-induced processes, such as inhibition of STN7-dependent LHCII phosphorylation (1.5.6) (Ancín et al., 2019; Ancín et al., 2021; González et al., 2021; Serrato et al., 2021). Trx-x and Trx-y2 are important electron donors for the antioxidant enzymes, PrxQ, MDHAR and methionine sulfoxide reductase (Okegawa et al., 2023), whereas NTRC is the main reductant of 2-CysPrx (Nikkanen and Rintamäki, 2019). Trx-z is the only plastid thioredoxin that has no known role in redox regulation, but is instead, it is a key structural component of the plastid-encoded RNA polymerase (Wimmelbacher and Börnke, 2014).

Thioredoxins also regulate alternative electron transfer pathways, in particular the malate valve and CET. The malate valve is activated by Trx-m1 and Trx-m2 (Thormählen et al., 2017), while Trx-m4 downregulates both CET pathways (Courteille et al., 2013; Okegawa and Motohashi, 2020; Ancín et al., 2022). In contrast, NTRC has been shown to activate NDH1-dependent CET (Nikkanen et al., 2018).

Thioredoxin-like proteins have been shown to mediate the oxidation of Trx target proteins, which is linked to the redox state of 2-CysPrx (Yokochi et al., 2021; Fukushi et al., 2024). These processes have also been suggested to affect the oxidative inactivation of stromal enzymes during the light-dark transition (Yokochi et al., 2021), and NTRC, as a major reductant in the junction between different thioredoxins, appears to be the most important regulator of CBB activity under fluctuating light intensities (Dziubek et al., 2023).

In addition to dynamic regulation of light reactions and stromal metabolism thioredoxins also affect the biogenesis and long-term regulation of PSII and Cyt b_6f (Wang et al., 2013; Chen et al., 2024).

1.5.8 Long-term regulation

Chloroplasts have several mechanisms to ensure that light reactions and stromal metabolism remain in balance under changing environmental conditions. As described above, exposing plants to higher light intensities than those during the growth period, activates the NPQ and photosynthetic control, thereby reducing the risk of ROS generation and photodamage (Bednarczyk et al., 2020). However, such a down-regulation of light reactions and the dissipation of excitation energy as heat would be detrimental to plant growth when the light intensity increases for longer time periods. To avoid this problem, plants have evolved acclimation strategies for the long-term regulation of photosynthesis. In the case of high light acclimation, plants increase the level of CBB cycle enzymes, thereby increasing the sink strength of stromal metabolism. Once the stromal sinks become stronger, plants can increase the amounts of ATP synthase and Cyt b_6f (Anderson et al., 1988; Yin and Johnson, 2000; Miller et al., 2017), which determines the maximum electron flux through the LET (Yamori et al., 2011). Proteomic analysis of high light acclimation shows that overall primary carbon metabolism is upregulated along with an increase in phenylpropanoid metabolism, and a similar trend is visible at metabolite levels (Dziubek et al., 2023). High light also upregulates nitrogen assimilation and thus the availability of organic nitrogen, and this occurs as early as the first day after the high light switch, which has been suggested to drive the upregulation of CBB cycle capacity (Baker et al., 2023), and may also explain why the *trx-m1m2* double mutant shows a weaker high light response (Dziubek et al., 2023). The increase in primary and secondary metabolism allows for an increase in the electron flow in light reactions, and the increase in resource production allows for improved growth.

Acclimation of light reactions and the CBB cycle to fluctuating light differs from high light acclimation. Rubisco up-regulation appears to follow the acclimation to the high-light periods, whereas Cyt b_6f expression responded positively to the length of high-light periods (Yin and Johnson, 2000). Fluctuating light also upregulates NDH1-dependent CET, which may be due to increased photorespiration during the high light periods (Niedermaier et al., 2020).

Arabidopsis plants grown under field conditions increased the levels of ATP synthase, Cyt b_6f and NDH1 even more than plants grown under controlled high light conditions (Flannery et al., 2021a; Flannery et al., 2021b). In addition, field experiments performed with different maize planting densities confirmed the importance of the length of the high light periods in acclimation (Wu et al., 2023),

similar to what has been inferred from acclimation to artificially fluctuating light conditions (Yin and Johnson, 2000).

High light acclimation also decreases the abundance of light-harvesting proteins and changes their composition, particularly the isoforms of LHCB4. In Arabidopsis and pea, the abundance of LHCB4.1 and LHCB4.2 decreased and LHCB4.3 increased in high light (Albanese et al., 2016; Flannery et al., 2021a). Not only did changes occur in light harvesting proteins, but the stoichiometry between photosystems also changed, with PSII remaining fairly stable but the amount of PSI decreasing (Flannery et al., 2021a). Again, these acclimation responses were stronger in field-grown Arabidopsis, with additional up-regulation of LHCA5 and LHCA6, which are required for the formation of the NDH1-PSI complex (Flannery et al., 2021b).

Low light acclimation responses are mostly the opposite of high light responses (Flannery et al., 2021a), but light is not the only factor that induces long-term acclimation responses. Lowering temperature also induces changes in the proteome, with some responses similar to high light acclimation. Exposure of plants to low temperature and moderate light leads to over-excitation because low temperature inhibits the activity of metabolic enzymes, causing an imbalance between metabolism and light reactions (Hüner et al., 2022). Increasing the sink strength by up-regulation the CBB cycle, as occurs in high light, is one of the mechanisms used by plants to restore the balance, but depending on the plant species, other strategies are also used. These include the upregulation of alternative electron transfer pathways, reduction of light-harvesting capacity by decreasing the amount of antenna proteins, activation of sustained quenching or synthesis of screening anthocyanins (subgroup of flavonoids) (Allen and Ort, 2001; Hüner et al., 2016; Hüner et al., 2022; Grebe et al., 2024).

2 Aims of the study

My thesis is focused on the regulation of photosynthesis in angiosperms, the model species Arabidopsis (*Arabidopsis thaliana*) and lettuce (*Lactuca sativa*), a non-model crop species. The main objectives of the experimental work were:

1. To understand the mechanisms that are critical for maintaining the functional balance between photosynthetic light reactions and stromal metabolism in chloroplasts under changing internal and external conditions (papers I, II, and III).
2. To understand the role of short- and long-term acclimation mechanisms following photoinhibition of either one of the two photosystems (papers I and II).
3. Elucidation of the diversity of mechanisms behind the quenching of excitation energy under combined high light and low temperature conditions in a non-model plant species lettuce (paper III).

3 Materials and Methods

3.1 Plant material and growth conditions

Wild-type (WT) Columbia ecotype Arabidopsis was grown in an 8 h photoperiod in constant moderate white light (paper I: 165 µmol photons m^{-2} s^{-1}, paper II: 120 µmol photons m^{-2} s^{-1}) with POWERSTAR HQI-T 400 W/D metal halide lamps (OSRAM GmbH, Munich, Germany) as the light source at 25°C and 60% relative humidity. The Arabidopsis plants used in the experiments were five to six-weeks-old.

Lettuce (*Lactuca sativa*) Hilde White Boston cultivar (paper III) was grown in a 16 h photoperiod in moderate white light (140 µmol photons m^{-2} s^{-1}) with POWERSTAR HQI-T 400W/D metal halide lamps (OSRAM GmbH) as the light source at 23°C. The lettuce plants used in the experiments were 4 weeks old.

3.2 Light treatments of plants

In paper I, whole Arabidopsis plants were treated with a specific fluctuating light regime to induce PSI photoinhibition (Tikkanen and Grebe, 2018). Plants were treated for 4 h and 8 h to induce moderate and severe PSI photoinhibition. Recovery plants were transferred to growth conditions for 24 h after the inhibition treatments. Control plants were taken directly from the growth conditions. After this control, PSI-inhibited and 24 h recovered plants were kept for 1 h in darkness, low light (35 µmol photons m^{-2} $s^{-}1$), growth light (165 µmol photons m^{-2} $s^{-}1$) and high light (635 µmol photons m^{-2} $s^{-}1$) before thylakoid isolation and leaf sampling.

In paper II, detached WT Arabidopsis leaves were collected on Petri plates with water (control) or 1 mg ml^{-1} lincomycin solution (treatment). The leaves were incubated on the Petri plates overnight after which the leaves were treated with high light (1000 µmol photons m^{-2} s^{-1}) for 0.5 or 1 h using a Heliospectra Dyna LED lamp to induce PSII photoinhibition. After the photoinhibition treatment, part of the leaves was treated with low light (50 µmol photons m^{-2} $s^{-}1$) or moderately high light (500 µmol photons m^{-2} s^{-1}) for 30 min with POWERSTAR HQI-T 400W/D metal halide lamps (OSRAM GmbH) as a light source before biophysical measurements and thylakoid isolation.

In paper III, lettuce plants were treated with high light (1500 µmol photons m^{-2} s^{-1}) for 4 h with Heliospectra Dyna LED lamps at low temperature (13°C) or at growth temperature (23°C). After the light treatment, one part of the plants was transferred to recover in the dark at growth temperature for 24 h and the other part was transferred to recover in growth conditions for 24 h. Control plants were taken directly from the growth conditions to the dark for 24 h.

3.3 Thylakoid isolations and chlorophyll determination

Arabidopsis leaf samples (papers I-II) for thylakoid isolation were collected in ice-cold isolation buffer (330 mM sorbitol, 5 mM $MgCl_2$, 50 mM Hepes-KOH pH 7.5, 10 mM NaF, 13.3 mM sodium ascorbate and 0.03% (w/v) BSA). Leaves were homogenised and filtered through Miracloth (Millipore). Chloroplasts were collected by centrifugation at 3950 g for 5 min at 4°C and ruptured osmotically in ice-cold shock buffer (5 mM $MgCl_2$, 50 mM Hepes-KOH pH 7.5, 10 mM NaF). The released thylakoid membranes were collected by centrifugation at 3950 g for 5 min at 4°C and suspended in storage buffer (100 mM sorbitol, 5 mM $MgCl_2$, 50 mM Hepes-KOH pH 7.5, 10 mM NaF). Lettuce leaf samples (paper III) were treated similarly, except those centrifugations were performed at a lower speed (1350 g) and thylakoids were washed twice with storage buffer, to avoid mitochondrial contamination. Thylakoid samples were stored at -80°C and, in the case of lettuce, thylakoids were aliquoted to several tubes to prevent repeated freeze-thaw cycles. Chlorophyll concentration was determined as described in (Porra et al., 1989).

3.4 Gel electrophoresis, protein staining and immunoblotting

3.4.1 Native gel electrophoresis

Isolated thylakoids were suspended in ice-cold 25BTH20G buffer (25 mM BisTris-HCl pH 7.0, 20% (v/v) glycerol, 0.25 mg/ml Pefabloc). Resuspended thylakoids were solubilised with an equal volume of 2% β-*D*-dodecyl maltoside (β-DM) (papers I-III), 2% digitonin (paper I) or 3% digitonin (paper III). β-DM samples were solubilised for 5 min on ice and digitonin samples were solubilised for 8 min at room temperature with gentle mixing. Insoluble material was removed by centrifugation at 16 000 g for 20 min at 4°C, and 1/10 volume of loading buffer (100 mM BisTris-HCl pH 7.0, 0.5 M aminocaproic acid, 30% (w/v) sucrose and 50 mg ml^{-1} Serva Blue G) (papers I and II) or 1/10 volume of 10% deoxycholate (paper III) was added to the supernatant. Solubilised thylakoidal protein complexes were separated with

3-12% (papers I-III) or 5-12% (paper III) acrylamide gradient gels according to (Järvi et al., 2011).

3.4.2 Denaturing gel electrophoresis and protein staining

Isolated thylakoids were solubilised with sample buffer (138 mM Tris-HCl pH 6.8, 6 M urea, 22.2% (v/v) glycerol, 4.3% (w/v) SDS, 10% (v/v) β-mercaptoethanol), and the insoluble material was removed by centrifugation. Solubilised proteins were separated on a SDS-PAGE gel containing 12% acrylamide and 6 M urea. Samples were loaded according to chlorophyll concentration.

In papers I and III, protein complexes in native gel electrophoresis strips were solubilised with (138 mM Tris-HCl pH 6.8, 6 M urea, 22.2% (v/v) glycerol, 4.3% (w/v) SDS, 5% (v/v) β-mercaptoethanol) for 30 min at room temperature, after which the solubilised proteins were separated on SDS-PAGE gel containing 12% acrylamide and 6 M urea.

In papers I and III, the separated proteins were fixed on gels (10% acetic acid, 50% methanol). The fixed gels were washed twice with water and the gels were incubated for 2 h with Pro-Q Diamond phosphoprotein stain (Invitrogen). Excess Pro-Q was destained (50 mM sodium acetate pH 4.0, 20% acetonitrile) and the gels were washed twice with water. Pro-Q-stained gels were imaged on a Perkin Elmer Geliance 1000 using the Cy3 filter. For paper I, the gels were washed with water after Pro-Q staining and the gels were incubated overnight with Sypro Ruby protein gel stain (Invitrogen). Gels were washed once (30% acetic acid, 7% methanol) and twice with water. Stained gels were imaged with Perkin Elmer Geliance 1000 with UV-filter.

3.4.3 Western blotting

Proteins separated by SDS-PAGE were electroblotted onto a PVDF membrane (Millipore) using a transfer buffer (20% methanol, 40 mM glycine, 50 mM Tris, 5 mM SDS). Membranes were blocked with 5% non-fat milk (Bio-Rad) in TBS (20 mM Tris-HCl pH 7.7, 150 mM NaCl), and the blocked membranes were incubated with primary antibodies overnight: In Paper I: PsaB (Agrisera), ATPF (Agrisera), PetA (Agrisera) and PsbA (Kettunen et al., 1996). In paper II: PsbA and P-Thr (New England Biolabs) and in paper III: P-Thr, diluted in 1% non-fat milk in TTBS (TBS with 0.05% Tween 20). The membranes were then washed with TTBS, and incubated for 1 h with infrared dye-labelled secondary antibody (IRDye® 800CW goat anti-rabbit IgG secondary antibody, Li-Cor) (papers I and III) or horseradish peroxidase-linked secondary antibody (Agrisera) (paper II) diluted in 1% non-fat milk in TTBS. The secondary antibody was detected using an Odyssey

CLx imager (Li-Cor) (papers I and III) or with an ECL detection kit (GE Healthcare) (paper II). In Paper I, signal quantification was performed with Image Studio (Li-COR) and the relative amounts of proteins were intrapolated from the linear regression of signals from control dilution series.

3.4.4 Protein redox labelling

Leaves frozen in liquid nitrogen were homogenised in 10% trichloroacetic acid and the precipitated proteins were pelleted by centrifugation. Precipitated proteins were washed twice with ice-cold buffered acetone (50 mM Tris-HCl pH 7.0, 80% acetone) and once with 100% acetone. The washed protein pellets were dried and resuspended in urea denaturing buffer (100 mM Tris-HCl pH 7.5, 8 M urea, 1 mM EDTA, 2% (w/v) SDS, Pierce™ protease inhibitor cocktail (Thermo Scientific)) with 50 mM N-ethylmaleimide (NEM). After 30 min incubation with NEM 1,4-dithiothreitol (DTT) was added to a final concentration of 100 mM to scavenge excess NEM and to reduce *in vivo* oxidised thiols. DTT was not added to the -DTT control samples. After overnight incubation at 4°C with DTT, the samples were filtered, and the proteins were precipitated with 10% trichloroacetic acid. The precipitated proteins were washed as before, and the washed proteins were resuspended in urea denaturing buffer containing 10 mM pegylated maleimide (MAL-PEG, 5 kDa). Samples were mixed for 2 h at 27°C and excess MAL-PEG was scavenged by adding DTT to a final concentration of 50 mM.

Redox labelling affects most commonly used protein content determination methods and to ensure equal loading in the western blots analysis the sample amounts were normalised to the content of Rubisco small subunit, which was determined with Sypro Ruby protein stained SDS-PAGE gels. Labelled protein samples were mixed with sample buffer (150 mM Tris-HCl pH 6.8, 6% SDS, 60% (v/v) glycerol) in a 2/1 ratio and the proteins were separated with SDS-PAGE gels containing 12% acrylamide and 6 M urea. The separated proteins were stained with Sypro Ruby protein stain and imaged as before (3.4.2). Sample loading for the determination of protein redox states was normalised to the amount of Rubisco small subunit in the first gel and the proteins were separated on an SDS-PAGE gel with a 5-15% acrylamide gradient and 6 M urea. The separated proteins were electroblotted onto PVDF membranes (Millipore). Membranes were blocked with 5% non-fat milk (Bio-Rad) in TBS, and the blocked membranes were incubated overnight with FBPase antibody (Sahrawy) diluted in 1% non-fat milk in TTBS. The membranes were then washed with TTBS and incubated for 1 h with horseradish peroxidase-linked secondary antibody (Amersham). The amount of bound secondary antibody was detected with an ECL detection kit (GE Healthcare) and the fluorescence was imaged with Perkin Elmer Geliance 1000.

3.5 Proteomics

In paper III, equal amounts of isolated thylakoids, based on Chl content, were solubilised by mixing the thylakoids with a buffer (0,1M Tris-NaOH pH 8) containing 6 M urea and 0.1% RapiGest (Waters). The concentrations of solubilised proteins were determined by the Bradford assay, and aliquots of solubilised proteins corresponding to 100 µg of protein were then subjected to reduction with dithiothreitol (DTT), and alkylation with iodoacetamide (IAA), followed by precipitation of the proteins in a cold acetone/ethanol mixture at -20°C overnight. The proteins were then digested with trypsin (1 µl 1 µg/µl, 1:100) in a buffer (5% acetonitrile (ACN), 0.05 M Tris-NaOH pH 8) for 4 h, after which a second batch of trypsin (1µ 1 µg/µl, 1:100) was added and the digestion was continued overnight. The peptide mixtures were desalted in parallel with Wet Sep-Pak 100 mg C18 96 (Waters) according to the manufacturer's protocol.

The peptide concentration of the desalted peptides was determined using a DeNovix DS-11+ spectrophotometer and equal amounts of peptides were injected for nLC-ESI-FAIMS-MS/MS analyses. Prior to injection, the samples were spiked with iRT synthetic peptides (Biognosys). The injected samples were first trapped on a pre-column and then separated on an analytical C18 column (75 µm x 15 cm, ReproSil-Pur 3 µm 120 Å C18-AQ, Dr. Maisch HPLC GmbH, Ammerbuch-Entringen, Germany) by a two-step, 110 min gradient from 5 to 26% solvent B over 70 min, followed by 26 to 49% B increase over 30 min. The mobile phase consisted of water with 0.1% formic acid (solvent A) or acetonitrile/water (80:20 (v/v)) with 0.1% formic acid (solvent B). The MS data were acquired automatically using Thermo Xcalibur 4.6 software (Thermo Fisher Scientific). FAIMS was operated at two compensation voltages (CV) values: -50 and -70 for both MS and MS/MS modes. The data-independent acquisition (DIA) method consisted of a survey scan of the mass range 395-1005 m/z with a maximum injection time of 50 ms and an automatic gain control (AGC) target set to 7e5 ions, followed by a series of tMS2 scans triggered by a set of variable isolation window for molecular ions. The isolation width of windows ranged from 15–110 m/z covering mass range of 395-1005 m/z for molecular ions (paper III, Supplemental table 1 contains the full list of isolation windows) with a maximum injection time of 52 ms and an AGC target of 1e6. All ions within the isolation windows were subjected to HCD fragmentation and the fragments were registered within 180-2000 m/z range. All precursors within the isolation windows were fragmented with a normalised collision energy of 28%. The spectra were registered at a resolution of 120 000 and 30 000 (at m/z 200) for full scan and fragment spectra, respectively.

Data analysis was performed using Spectronaut (version 16.1) software (Bruderer et al., 2015) (Biognosys, Schlieren, Switzerland). DIA data were searched against a customised FASTA file using the Pulsar directDIA™ algorithm. In paper

III the customized FASTA file was manually curated by combining the lettuce proteomes from UniProt and Swiss-Prot (paper III, Supplemental file 2). UniProt homologs of Swiss-Prot sequences were manually removed from the combined database based on BLAST searches (paper III, Supplemental files 3 and 4). Searches against the curated database (paper III, Supplemental file 5) were performed allowing a maximum of 2 missed trypsin cleavages, carbamidomethylation modification was set as static, while methionine oxidation, N-terminal acetylation, and lysine acetylation in addition to serine, threonine, and tyrosine phosphorylation were set as dynamic modifications. The FDR identification threshold (q-value) for peptides and proteins was set at 0.01. Data for target proteins and peptides (identified based on homology to Arabidopsis sequences (paper III, Supplemental files 6 and 7)) were extracted and analysed in Excel files. Protein and peptide abundances were normalised within samples, to the average of the detected PSI, ATP synthase, and Cyt b_6f subunits to avoid, as much as possible, the effect of contaminants from the isolations and differential attachment of stromal proteins to the thylakoids under changing experimental conditions (e.g. a switch to HL rapidly recruits ribosomes to the thylakoid membrane), similarly to previous studies on the plant thylakoid proteome (Flannery et al., 2021a; Flannery et al., 2021b).

For more detailed analysis of the PSII reaction centre, DIA data were searched against database containing only lettuce PsbA, PsbB, PsbC and PsbD sequences. Searches against the limited database were performed allowing semi-specific trypsin cleavages with a maximum of 2 missed cleavages. Carbamidomethylation modification was set as static, while methionine oxidation, N-terminal acetylation, lysine acetylation, serine, threonine, and tyrosine phosphorylation, tryptophan, tyrosine and histidine oxidation and dioxidation, and histidine conversion to aspartate and asparagine were set as dynamic modifications. The FDR identification threshold (q-value) for peptides and proteins was set at 0.01. Data for target peptides were extracted and analysed in Excel files. Peptide abundances were normalised within samples, to the average of the detected PSI, ATP synthase, and Cyt b_6f subunits from the previous analysis.

3.6 77 K chlorophyll fluorescence measurements

Isolated thylakoids were diluted with storage buffer to a chlorophyll concentration 10 µg ml^{-1}, and fluorescence spectra were measured with 480 nm excitation light in liquid nitrogen. Fluorescence was recorded using -Ocean Optics S2000 spectrophotometer. Spectra were normalised to the 685 nm peak or the ratio between 685 nm and 735 nm peaks was calculated to illustrate the distribution of excitation energy between PSII and PSI.

3.7 In-vivo functional measurements of photosynthesis

3.7.1 In-vivo chlorophyll fluorescence and near-infrared difference absorption measurements

In papers I and II, Dual KLAS-NIR was used to measure chlorophyll a fluorescence with pulse-modulated 540 nm measuring light, and P700, Fd and PC redox states were determined by deconvolution of pulse-modulated dual wavelength 785-840, 810-870, 870-970 and 795-970 nm signals. Deconvolution was performed using differential model plots measured from control plants according to (Klughammer and Schreiber, 2016). PSI quantum yield (Φ_I, Y(I)), donor side limitation (Φ_{ND}, Y(ND)) and acceptor side limitation (Φ_{NA}, Y(NA)) were calculated according to (Klughammer and Schreiber, 1994; Klughammer and Schreiber, 2008) using the average of control leaves maximal P700 oxidation (P_M) (paper I) or P_M of each individual leaf (paper II) measured with NIR MAX script (Klughammer and Schreiber, 2016). Fd results were not analysed further in paper I because the signal is partly derived from PSI iron-sulfur clusters (Klughammer and Schreiber, 2016), which are presumed to be damaged in the PSI photoinhibition treatment. While in paper II, relative Fd reduction was calculated analogously to Φ_{ND}. In paper I, maximal oxidation of P700 and PC (P_M* and PC_M*) were measured with a saturating pulse in the saturating light condition at the end part of the light curve (paper I, Table 2), where photosynthetic control is assumed to be able to keep them maximally oxidised. This is because the normal method of P_M determination in the dark with far-red pre-illumination followed by a saturating pulse is unable to fully oxidise P700 in severely PSI photoinhibited leaves due to the functional imbalance between the photosystems. In paper I, P_M* and PC_M* values were used to calculate the yields of functional PSI (marked with an asterisk): Φ_I*, Φ_{ND}* and Φ_{NA}* and the steady-state redox state of PC. In papers I and II, the steady-state oxidation of PC was calculated analogously to Φ_{ND}. quantum yield of PSII photochemistry (Φ_{II}) was calculated according to (Genty et al., 1989). Φ_{NPQ}, Φ_{NO} and qL_T were calculated according to (Kramer et al., 2004).

In paper III, chlorophyll a fluorescence was measured by FluorPen FP 110 using the saturating pulse method (Photon Systems Instruments, Drásov, Czech Republic) with default settings from control, treated and recovered plants immediately after the low temperature and high light treatments, without dark acclimation, and after 1 h and 24 h recovery in darkness or 24 h recovery in growth conditions. The quantum yield of PSII photochemistry (Y(II)) was estimated as previously. NPQ was calculated as ($F_M'^{ref}/F_M'$)-1 using the average of F_M' from control plants which had recovered for 24 h in darkness as the reference value ($F_M'^{ref}$). The fraction of open

and functional PSII reaction centres (qL_T) was calculated according to (Porcar-Castell, 2011).

3.7.2 Electrochromic shift measurements

In papers I and II, the electrochromic shift was recorded with Dual-PAM-100 equipped with a P515/535 module (Heinz Walz GmbH, Effeltrich, Germany). The electrochromic shift was determined by the difference between the 515 nm and 550 nm signals (Schreiber and Klughammer, 2008). Dark intervals were used to quantify thylakoid proton conductivity (g_{H+}) and proton motive force (pmf). g_{H+} was calculated as the inverse of the time constant of a first order exponential fit to the decay of the electrochromic shift (ECS) signal during the dark interval. (Kanazawa and Kramer, 2002) Pmf was calculated as the difference between the ECS in the light, before the dark interval, and the ECS dark baseline calculated from the first order exponential fit. In paper I, pmf was normalised to the chlorophyll content of measured leaves, whereas the data presented in paper II are not normalised as the leaf material was homogenous. The chlorophyll content of the leaves in paper I was determined by DMF extraction according to (Inskeep and Bloom, 1985)

3.7.3 Gas exchange measurements

In paper I, CO_2 assimilation was measured simultaneously with chlorophyll a fluorescence, P700, Fd and PC redox states using a GSF-3000 infrared gas analyser connected to a Dual-KLAS-NIR with 3010-Dual gas exchange cuvette (Heinz Walz GmbH, Effeltrich, Germany) The average of CO_2 assimilation was measured every 10 s during the light curve. The flow rate was set to 400 $\mu mol\ s^{-1}$, the cuvette temperature was kept constant at 25°C and the concentrations of CO_2 and H_2O were set to 400 and 18 000 ppm respectively. Assimilation was calculated according to (von Caemmerer and Farquhar, 1981).

4 Short overview of results

The experimental setups and detailed results of my research are described in papers I, II and III, and will not be repeated here. Instead, I have summarised below only the most important results from papers I-III, with some additional results (Figure 10). I consider these results to be particularly important for a general understanding of plant performance under abiotic stress conditions, which promote photoinhibition, and during subsequent recovery.

4.1 PSI is specifically damaged by customised fluctuating light treatment

In paper I, PSI inhibition was induced by a specific light treatment. The light treatment was designed to first accumulate electrons in the intersystem chain by illumination with red light, which excites PSII more efficiently than PSI. This was followed by a short high-light pulse, which rapidly consumes the accumulated electrons in the intersystem electron transfer chain (Tikkanen and Grebe, 2018). Such illumination cycles lead to periodic high acceptor-side limitation at PSI and exposes the reduced Fe_4S_4 clusters to damage by subsequent reaction with O_2 and formation of $O_2^{\bullet}$. Destruction of the Fe_4S_4 clusters was shown to prevent the oxidation of the P700 reaction centres, as evidenced by the decrease of P_M levels in PSI-inhibited plants compared to control plants (paper I, Figure 2a). The induced PSI inhibition appeared to have little effect on PSII function (paper I, Figure 2b). The designed fluctuating light treatment seems to be quite specific for the Fe_4S_4 clusters, since no clear decrease in the level of the PSI subunit PsaB was observed when compared to the control, despite a clear reduction in the P_M value (paper I, Figure 6a). However, we did not directly analyse the Fe_4S_4 clusters, which could confirm this interpretation.

4.2 PSII photoinhibition induced by high light is affected by the efficiency of PSII repair

PSII is inhibited by light, but the efficient repair cycle keeps PSII functional if the rate of damage is less than the capacity for repair. PSII was inhibited by high light,

either in the presence of lincomycin (paper II) or by simultaneous exposure to low temperature (paper III), both of which are known to inhibit PSII repair (Tyystjärvi and Aro, 1996; Murata et al., 2007). Consistent with the inhibition of the repair cycle, PSII photoinhibition decreased the PSII maximal quantum yield (F_V/F_M) and maximal fluorescence (F_M) more in lincomycin-treated leaves than in the just high light-treated and control leaves (paper II, Figures 2A-B). This was also seen in the increase in minimal fluorescence (F_0) in the high light treated leaves compared to the control, and the effect was more pronounced in the lincomycin treated leaves (paper II, Figure 2C). As expected, the PSII quantum yield was reduced more in low temperature and high light-treated plants than in high light treated plants and control plants (paper III, Figure 2). However, this could only be assessed after 24 h of dark recovery, when the relaxation of all NPQ mechanisms was complete (paper III, Figure 2B).

The proteomics data set generated in paper III, allowed me to look more closely at the changes in the PSII reaction centre after PSII photoinhibition. Treatment with low temperature and high light led to the accumulation of pre-D1 specific peptide (paper III, Figure 8A), which prevents PSII from assembling the OEC (Che et al., 2013). The amount of pre-D1 then decreased during the dark recovery, implying that the later stages of the D1 repair cycle can occur in darkness. This was also evident in the amount of mature D1 specific semi-tryptic peptide, which increased during the dark recovery of low temperature and high light treated plants (Figure 10A). These results also suggest that D1 processing is partially inhibited under stress conditions, and only resumes after the stress is over. At the same time, the fraction of open and functional PSII reaction centres (qL_T) increased during the dark recovery of low temperature and high light treated plants (paper III, Figure 8F).

I also detected an accumulation of the D1 DE-loop peptide, where histidine 252 is oxidised to aspartic acid, during the low temperature and high light treatment, and a decrease in the amount of modified peptide during the dark recovery (Figure 10B). There were no clear changes in the amount of unmodified peptide (data not shown), suggesting that only minor amount of D1 proteins have histidine 252 oxidised.

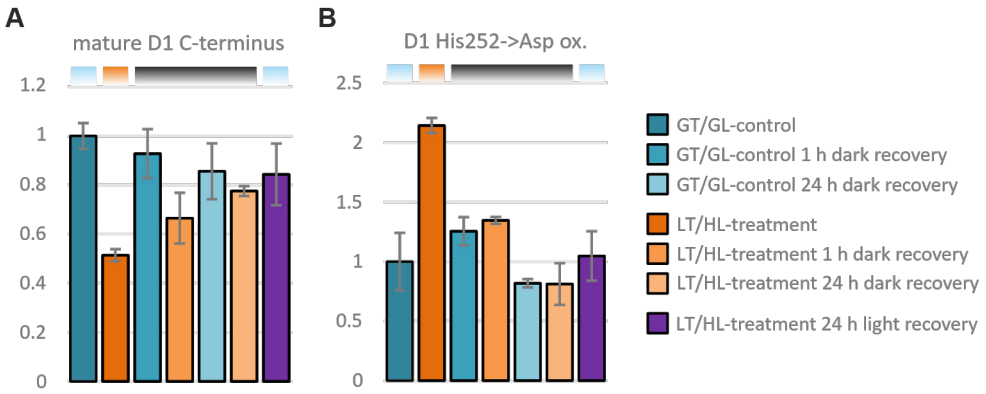

Figure 10. Effect of low temperature and high light treatment, and the subsequent recovery, on D1 maturation and oxidation in lettuce. **A)** mature D1 protein C-terminal peptide (NAHNFPLDLA) **B)** Oxidised D1 protein DE-loop peptide (FGQEEETYNIVAAH[His->Asp]GYFGR). Error bars show standard deviations among technical replicates (n = 3). Coloured bars above the graphs represent the temperature and light conditions from which the thylakoids used in the analyses were isolated: light blue for growth temperature and growth light (GT/GL), orange for low temperature and high light (LT/HL) and black for growth temperature and dark (GT/dark). More details in chapters 3.1, 3.3 and 3.5.

4.3 General consequences of PSII and PSI photoinhibition on light reactions

4.3.1 Quenching by damaged reaction centres decreases the light use efficacy and activation of NPQ

Photoinhibition of either photosystem reduces the light use efficiency because the damaged reaction centres still collect light but cannot use it for photochemistry. This was seen as an inability for net CO_2 assimilation under low light illumination and as lower net assimilation under growth and high light illumination in severely PSI photoinhibited plants compared to controls (paper I, Figure 2e), as well as in the yields of PSI and PSII as revealed by biophysical measurements (paper I, Figure 3b and paper II, Figure 6A). This led to a lower activation of qE in both PSI-inhibited and PSII-inhibited plants and leaves when compared to controls (paper I, Figure 3a and Paper II 6B), as the stromal metabolism remains unsaturated.

4.3.2 Photoinhibition-induced imbalance affects the apparent plastoquinone redox state revealed by fluorescence measurements

The effects of the photoinhibition of only one photosystem on the apparent redox state of the PQ pool were estimated by calculating the photochemical quenching of

fluorescence by open (oxidised PQ at the Q_B site) PSII reaction centres. In the case of PSI photoinhibition, qP was lower than in control plants, especially under low and growth light illumination, when the lower light-utilisation efficiency of photoinhibited PSI limits electron transfer (paper I, Supplemental Figure 5). Under high light illumination, the effects of PSI photoinhibition on the apparent redox state of the PQ pool were less pronounced, because the increased electron flow by functional PSI can compensate for the inhibited ones and the activation of the photosynthetic control has a greater contribution to the regulation of PQH_2 oxidation at Cyt b_6f (paper I, Supplemental Figure 5). On the other hand, photoinhibition of PSII had an oxidising effect on the apparent redox state (qL) of the PQ pool under both the low and high light illumination when compared to the control (paper II, figure 6C).

4.3.3 Plastocyanin redox state is sensitive to functional imbalances between photosystems

The redox state of intersystem electron carriers was also analysed by determining the redox state of PC and PSI RC (P700) using differential absorption spectroscopy. PC was shown to be less oxidised in PSI photoinhibited plants compared to control plants under growth and high light illumination (paper I, Figure 3d), and it also correlated with the lack of donor side limitation in PSI (Φ_{ND}) (paper I, Figure 3c). Notably, the oxidation state of PC was more sensitive than Φ_{ND} to the photosystem imbalance induced by PSI photoinhibition, as PC was more oxidised under growth light illumination when there were no detectable changes in Φ_{ND} when PSI-inhibited plants were compared with controls (paper I, Figures 3c-d). PSII photoinhibition had the opposite effect on PC oxidation, as PC was more oxidised in the control at low light intensity and the degree of oxidation was higher in more inhibited samples (paper II, Figure 7A). Also, in the case of PSII photoinhibition, the oxidation state of PC was more sensitive than Φ_{ND} to imbalances between photosystems, as increased oxidation in PC was detected before any changes in Φ_{ND} when PSII-inhibited plants were compared with control plants (paper II, Figures 7A-B).

4.3.4 PSI photoinhibition-induced changes on the acceptor side of PSI and the stromal redox regulation

Photoinhibition of both PSII and PSI also affects the PSI acceptor side limitation (Φ_{NA}), which is reflected in the changes in $\Phi_{ND,}$ in such a way that a decrease in Φ_{ND} increases Φ_{NA} and vice versa (paper I, Figure 3c and paper II, Figures 7A and 7B). This was visible in PSI photoinhibited plants when only the functional PSI centres

were determined (paper I, Figure 3c). These changes in Φ_{NA} were also reflected in the redox state of the CBB cycle enzyme FBPase (paper I, Figure 7d).

Photoinhibition of PSI also seems to affect the distribution of reducing power in stromal metabolism under growth light illumination (paper I, Figure 4), and the effect was even larger when changes in the distribution of excitation energy were considered (paper I, Supplemental figure 3).

4.3.5 Phosphorylation-dependent re-organization of the antenna system alters the light distribution between PSII and PSI after photoinhibition

PSI photoinhibition increased the phosphorylation of PSII core and LHCB1-2 proteins under all light conditions compared to control plants (paper I, figure 7b). LHCB1-2 phosphorylation increased the amount of PSI-LHCI-LHCII super-complex (paper I, Figure 7c), which was reflected in the higher relative PSI/PSII ratio obtained from 77K fluorescence measurements when compared to control plants (paper I, Figure 7a). PSII inhibition reduced the phosphorylation of LHCB1-2 proteins under low light illumination compared to control and the effect was even stronger in lincomycin-treated leaves (paper II, Figure 5). These changes also lowered the relative PSII/PSI ratio in 77K fluorescence compared to the control plants (paper II, figures 4A-B). The consequences from PSII photoinhibition were not as clear as those from PSI photoinhibition, suggesting that processes other than LHCB1-2 phosphorylation also affect the light distribution after PSII photoinhibition.

4.3.6 Long-term changes induced by PSI photoinhibition

PSI inhibition also altered the levels of key proteins involved in LET and its regulation. The levels of Cyt b_6f and ATP synthase were increased in PSI photoinhibited plants compared to the control (paper I, Figures 6c-e), which was also seen as lower Φ_{ND} and higher thylakoid proton conductance (g_{H+}) under high light illumination compared to control (paper II, Figures 3b and 5b).

4.4 Combined low temperature and high light stress leads to downregulation of PSII by several mechanisms in lettuce

Exposure of lettuce plants to low temperature and high light treatment induced high NPQ, of which only half can be clearly explained by canonical NPQ mechanisms (qE, qZ and qI) based on the relaxation kinetics (paper III, Figure 2B). Analysis of

the thylakoid proteome from low temperature and high light treated plants, in parallel with untreated control plants and plants recovered from the treatment in the dark and under growth conditions, revealed that zeaxanthin biosynthesis and Chl b degradation were increased during dark recovery (paper III, Figures 7D and 7G). These results were partially confirmed by pigment analysis for β-carotene and xanthophylls (paper III, Figure 9B and 9F-H). Proteomic analysis also revealed changes in the levels of the light-harvesting-like (LIL) proteins, early light induced protein (ELIP1.2) and stress enhanced protein (SEP2) (paper III, Figures 6A and 6D), which partly coincided with the formation and relaxation of the more persistent NPQ (paper III, Figure 2B). Low temperature and high light treatment also induced a strong phosphorylation of LHCB4 (paper III, Figure 8D), which seems to affect the stability of the PSII super-complexes (paper III, Figure 3C) and distribution of light from the antenna system (paper III, Figure 3F).

5 Discussion

In the previous section, I presented the main results of my experimental work. In this section, I will place them in a broader context and extend the interpretation of the results further from that in papers I, II and III. I also outline some new experiments that could be performed to test the hypotheses presented, new research directions and possible applications arising from my research.

5.1 Mechanisms of PSI photoinhibition depend on photoinhibition conditions

In paper I, I used a specific PSI photoinhibition treatment to study how photosynthesis acclimates to the functional imbalance of the photosystems. According to the P700 measurements, PSI function recovered faster (paper I, Figure 2a) than previously reported after the low temperature-induced PSI photoinhibition or high light induced PSI photoinhibition in Arabidopsis *pgr5* mutant (Kudoh and Sonoike, 2002; Zhang and Scheller, 2004; Lima-Melo et al., 2019). Additionally, I did not detect major changes in the amount of reaction centre protein PsaB (paper I, Figure 6a) which had been detected in above mentioned previous studies, indicating that there may be specific PSI photoinhibition mechanisms under different conditions. Chilling treatment, inactivating antioxidant enzymes (Asada, 1999), and high light treatment of *pgr5* mutant, unable to control electron transfer to PSI (Suorsa et al., 2012), are likely to cause continuous accumulation of $O_2^{\bullet}$ and H_2O_2 at PSI acceptor side, which can then damage proteins and cofactors. Our specific PSI photoinhibition protocol (paper I, Table 1), on the other hand, is likely to produce only short bursts of $O_2^{\bullet}$ and H_2O_2 production, allowing the antioxidant system to scavenge most of the ROS. However, these short bursts of ROS may be sufficient to damage the Fe_4S_4 clusters only on the stromal side of PSI, with minimal damage exerted to the PSI reaction centre proteins. Therefore, if only the Fe_4S_4 clusters on stromal side of PSI are damaged, they apparently can be repaired without the need for resynthesis of reaction centre proteins (Tiwari et al., 2024).

Another study, based on cucumber leaves treated either with high light at chilling temperature or with repetitive saturating flashes (6000 µmol photons m^{-2} $s^{-}1$), concluded that there are different PSI inhibition mechanisms operating during the

two different treatments (Shimakawa et al., 2024). The chilling treatment damaged the Fe_4S_4 clusters as has been reported previously, but the repetitive flash treatment was suggested to damage Chl_A and Chl_{0A} in the A branch of the reaction centre. Also, a differential susceptibility of PSI Fe_4S_4 clusters to photodamage (Tiwari et al., 2024) can be postulated as a reason for two different PSI photoinhibition mechanisms induced under different conditions. As I have not carried out detailed analysis on PSI function after our specific PSI photoinhibition treatment, it is unclear what the mechanism of inhibition is in our experimental setup. However, a similar treatment had effect on transcripts related to iron metabolism (Kılıç et al., 2023), suggesting that Fe_4S_4 clusters may be damaged and therefore the inhibited samples should be analysed, at least with EPR spectroscopy that can identify the functionality of all three PSI Fe_4S_4 clusters, two of them located on the stromal side of PSI and one deep inside the PSI complex ligated to the PsaA and PsaB reaction centre proteins.

5.2 PSI inhibition induces rapid responses resembling high light acclimation

The specific PSI photoinhibition treatment induced the accumulation of ATP synthase and Cyt b_6f (paper I, Figures 6c and 6d), which also occurs during high light acclimation of plants. However, the response in PSI photoinhibited plants was considerably faster than during high light acclimation, which usually takes days. The mechanisms behind the regulation of ATP synthase and Cyt b_6f amounts are not known (Schöttler and Tóth, 2014), but based on transcriptomic analysis after similar PSI photoinhibition treatment, the regulation is likely to occur, at least partly, at the transcriptional level and may be initiated by the iron released from damaged PSI Fe_4S_4 clusters (Kılıç et al., 2023). Transcriptomic analysis also revealed downregulation of light harvesting and upregulation of Cyt b_6f, NDH1, and enzymes of the violaxanthin cycle, CBB cycle and photorespiration, which are also hallmarks of high light acclimation. The upregulation of the CBB cycle is also partly visible in the CO_2 assimilation of the moderately recovered plants (paper I, Figure 2e), but as the standard deviation is quite high, this should be verified with more replicates. Due to a rapid high light response, the specific PSI photoinhibition treatment could be used as a model to study high light acclimation, and the specific PSI photoinhibition treatment could also be applied to harden indoor-grown plants before transferring them outdoors.

5.3 Acclimation to PSI photoinhibition alters the distribution of reducing power in stromal metabolism - who regulates the regulators?

Plants acclimated to PSI photoinhibition showed an increase in allocation of PSII-derived electrons to CO_2 fixation, especially under growth light, but also under high light, when the changes in the distribution of excitation energy between the two photosystems were taken into account (paper I, Figure 4 and Supplemental figure 3). We proposed that this was due reduced activity of the Trx-m1 and Trx-m2 regulated malate valve and reduced activity of nitrogen fixation. Unfortunately, I did not have access to a specific antibody against chloroplast MDH, that would have allowed me to compare its redox state in treated and control plants. However, the increase in STN7-dependent LHCII phosphorylation in PSI photoinhibited plants, compared to control plants (paper I, Figure 7a), suggests that Trx-ms are less active in inhibiting the STN7 kinase in PSI photoinhibited plants. A recent paper suggests that Trx-ms are regulated by CBSX2 protein, which contain cystathionine-b-synthase domain (Baudry et al., 2022), which may explain the observed changes in the distribution of reducing power in stromal metabolism. As the role of CBSX2 is controversial (Murai et al., 2021; Baudry et al., 2022), I will first briefly review the literature on CBSX proteins and then discuss how this relates to the changes observed in PSI photoinhibited plants.

Plants have two chloroplast-located CBSX proteins, CBSX1 and CBSX2, of which CBSX1 is the major isoform in heterotrophic tissues, whereas CBSX2 is the major isoform in leaves (Yoo et al., 2011). It has been suggested that CBSX2 forms an inhibitory complex with Trx-m1, Trx-m2 and Trx-m4 proteins (Baudry et al., 2022). In WT, the formation of the Trx-m-CBSX2 complex inhibits the activation of NADPH-MDH and therefore P700 oxidation is faster in the *cbsx1cbsx2* mutant during light to dark transition (Baudry et al., 2022), but the redox labelling of NADP-MDH showed no differences between WT and the *cbsx1cbsx2* mutant under the light conditions studied (Murai et al., 2021). The formation of the CBSX2-Trx-m complex is thought to be regulated by adenylate status, since the addition of ATP and ADP increases the activity of Trx-ms in the presence of CBSX2. This activation of Trx-ms has been proposed to downregulate CET via Trx-m4 (Baudry et al., 2022), but it could also activate the malate valve via Trx-m1 and Trx-m2. Given the different approaches of the CET and the malate valve in regulating the ATP/NADPH ratio, it would be logical that a high stromal ATP concentration would inactivate CET, which generates extra ATP at the expense of reductants, and at the same time activate malate valve, which consumes excess reductants that could then be used in other cellular compartments.

However, CBSX2 also interacts with NTRC and inhibits it in an AMP-dependent manner, and it also disturbs redox regulation in darkness (Li et al., 2023; Tran et al.,

2023). These results conflict with the previous interpretation of the role of CBSX2 in the regulation of alternative electron transfer pathways, as the inactivation of NTRC by low energy status would inhibit NDH1-dependent CET (Nikkanen et al., 2018). However, the misregulation of NTRC in the cbsx2 mutant would explain the reduction of ATP synthase, FBPase and SBPase in darkness since it is similar to the NTRC overexpression mutant (Nikkanen et al., 2016; Li et al., 2023).

The conflicting results with the CBSX2 protein could be explained by different in vitro reaction conditions, as the binding of adenylates can be affected by Mg^{2+} concentration and pH. Based on a structural study of the CBSX2-AMP complex, it has been suggested that ATP cannot bind to CBSX2 due to electrostatic repulsion (Jeong et al., 2013), but kinetic studies with CBS domain-regulated pyrophosphatases have shown that at least some CBS domains are cooperatively regulated by adenylates and Mg^{2+} (Salminen et al., 2014), which could mean that the electrostatic repulsion can be masked by Mg^{2+}. Considering that the activation of light reactions affects the adenylate status and Mg^{2+} concentration in the stroma, the regulation of the Trx-system by CBSX2 should be investigated at different adenylate and Mg^{2+} concentrations.

If Trx-m activity is indeed activated by ATP accumulation in the stroma, this may explain why the distribution of reducing power is altered in plants acclimated to PSI photoinhibition. PSI photoinhibited plants have lower pfm (ECS_t) than control plants under growth light illumination (paper I, Figure 5a), which would be expected to lead to lower ATP production, which would then keep Trx-ms inactive in complex with CBSX2. The changes in stromal metabolism after PSI photoinhibition would be interesting to investigate further using stromal-targeted Mg^{2+}, PO_4^{3-}, ATP and NADPH biosensors (Lindenburg et al., 2013; Mukherjee et al., 2015; Voon et al., 2018; Lim et al., 2020).

5.4 LHCII phosphorylation acts as a buffering system for light harvesting

Phosphorylation-dependent mechanisms have been shown to balance the excitation between photosystems under changing light qualities and intensities, in a process called state-transitions. However, our results with both the PSI and PSII photoinhibited plants imply that phosphorylation-dependent mechanisms are important also in balancing the rates of photosystems under conditions where the photoinhibition of either one of the photosystems disturbs the functional balance between the photosystems. PSII photoinhibition in lincomycin-treated leaves leads to complete dephosphorylation of LHCII (paper II, Figure 5), resembling the state under far-red illumination, which preferentially excites PSI and results in oxidation of the PQ pool. On the other hand, the hyperphosphorylation of both the LHCII and

PSII core proteins occurring after PSI photoinhibition (paper I, Figure 7b) has never been detected under different light quantities or qualities, but instead, such a phosphorylation state can be found in the *tap38* mutant under high light (Mekala et al., 2015). These results suggest that LCHII and PSII core protein phosphorylation-dependent regulation of light distribution likely acts as a buffering system that allows light reactions to get adjusted to changes in light use efficiency, apart from acclimation to changes in light intensity or quality. Since the current analyses were performed with WT plants, similar analyses with the kinase mutants would further test this hypothesis.

Changes in the distribution of excitation energy between the two photosystems were more pronounced in low temperature and high light treated lettuce (paper III, Figure 3F), than in PSI photoinhibited Arabidopsis (paper I, Figure 7a). Apart from the different plant species and light treatments, the extent of the changes in energy distribution to photosystems is likely to be influenced by the inhibition of the PSII repair cycle, as observed in lincomycin and high light treated Arabidopsis (paper II, Figure 4D), together with phosphorylation of the minor antenna protein LHCB4 (paper III, Figures 3A and 8D), or by LHCB4 phosphorylation alone. In further studies, it would be fascinating to investigate whether the greater flexibility in excitation energy distribution allows lettuce to acclimate to PSI photoinhibition better than Arabidopsis

5.5 Evolution and role of LHCB4 phosphorylation

The detection of major LHCB4 phosphorylation in lettuce (paper III, Figures 3A and 8D) was surprising, as this modification was previously reported only in grasses among land plants (Chen et al., 2013). The functional considerations of LHCB4 phosphorylation in downregulation of PSII light harvesting, by dissociation of M-LHCII from PSII supercomplexes, were discussed in detail in paper III, but here I will focus more on the evolution of LHCB4 protein phosphorylation.

LHCB4 is evolutionarily the oldest of the external light-harvesting antenna proteins (Koziol et al., 2007), and crucial for linking the M-LHCII complex to the PSII core. It is therefore surprising how much variation there is in LHCB4s between land plant orders, as the isoform composition changes from one to three (Grebe et al., 2019). *Eurosids* and *Caryophyllales* are the only angiosperm orders with three isoforms, LHCB4.1, LHCB4.2 and LHCB4.3, the latter also called LHCB8 (Klimmek et al., 2006; Grebe et al., 2019). Most angiosperms have only LHCB4.1 and LHCB4.2, whereas most gymnosperms, with the exception of *Cycadales,* have only LHCB8 (LHCB4.3) (Grebe et al., 2019). In Arabidopsis and pea (*Pisum sativum*), LHCB4.3 (LHCB8) is expressed only under excess light, which leads to a decrease in PSII antenna size, since the PSII supercomplexes with LHCB4.3

(LHCB8) completely lacks M-LHCII and LHCB6 (Albanese et al., 2019), as do the PSII supercomplexes of spruce (*Picea abies*), which have only LHCB8 (Opatíková et al., 2023). In contrast, lettuce and grasses studied so far do not possess LHCB4.3 (LHCB8), but they have more pronounced phosphorylation of LHCB4 (paper III, Figures 3A and 8D) (Chen et al., 2013; Betterle et al., 2017). It is therefore conceivable that the phosphorylation of LHCB4 (lettuce and grasses) under excess illumination has the same function as the accumulation of LHCB4.3 (LHCB8) (Arabidopsis and pea) to reduce the PSII antenna size. However, LHCB4 phosphorylation is a more dynamic process due to its rapid reversibility (paper III, Figures 3A and 8D), which may make it more advantageous under rapidly changing environmental conditions.

Differences in LHCB4 phosphorylation dynamics between species are difficult to explain because of their very similar LHCB4 sequences. Only one threonine residue close to the phosphosite in Arabidopsis is replaced by phenylalanine in lettuce (paper III, Figure 8), and similar substitutions have occurred in grasses (Chen et al., 2013), which might affect the recognition of the phosphorylation site by the STN8 kinase. The N-terminal extension of rice STN8 has been speculated to affect substrate recognition (Betterle et al., 2015), but such a clear difference is missing when comparing Arabidopsis and lettuce STN8 kinases. To my knowledge, the major LHCB4 phosphorylation under excess illumination has been shown to occur in the green alga *Chlamydomonas reinhardtii* (Chlamydomonas) (Turkina et al., 2004), and apart from the lettuce in our study, only in grasses among the land plants. It is therefore difficult to assess the main reason for the loss of LHCB4 phosphorylation in other lineages, or whether the LHCB4 phosphorylation has evolved independently in the lineages studied so far. However, lettuce and grasses have the same phosphosites, whereas Chlamydomonas phosphosites are different (Chen et al., 2013), which would support the independent evolution of LHCB4 phosphorylation in these lineages.

Expression of lettuce LHCB4 in the Arabidopsis *lhcb4* mutant (de Bianchi et al., 2011) could be used to test whether changes in LHCB4 phosphorylation are due to a change in an amino acid. Furthermore, the generated mutant could also be used to study the functional role of major LHCB4 phosphorylation.

5.6 Role of SEP2 in photoprotection under low temperature and high light stress

In paper III, we showed that lettuce has high non-photochemical quenching during combined low temperature and high light stress, and that it persists even after 1 h dark recovery (paper III, Figure 2B). Based on the biochemical and proteomic analyses, we proposed that LHCB4 phosphorylation together with SEP2

accumulation may be behind the formation and relaxation of the sustained quenching (paper III, Figures 2B, 6D and 8D).

The SEP2 protein has also been suggested to play a role in Chl catabolism as the Arabidopsis overexpression mutant has a pale green phenotype and has a reduced amount of Chl compared to the wild type (Ren et al., 2023). However, SEP2 overexpression also leads to upregulation of ELIP1 and ELIP2 and to downregulation of protochlorophyllide oxidoreductase A (PORA) transcription (Ren et al., 2023), suggesting that upregulation of ELIPs inhibits Chl biosynthesis (Tzvetkova-Chevolleau et al., 2007), explaining the phenotype. In the paper III we proposed that LHCB4 and SEP2 compete for the binding site at CP47, which would also explain why the SEP2 overexpression mutant plants and plants in which SEP2 has been silenced do not exhibit fluorescence phenotypes under stable growth conditions (Ren et al., 2023), since the PSII super-complexes are intact under stable conditions and SEP2 is unable to bind to the PSII core.

The proposed role of SEP2 in sustained quenching and its importance in acclimation to excess excitation stress should be verified by determining the localisation and interaction partners of the SEP2 protein, spectroscopic studies of putative SEP2-PSII complexes and characterisation of lettuce SEP2 deletion mutants as well as LHCB4 phosphosite mutants.

5.7 Reaction centre quenching is likely to be induced by the accumulation of pre-D1 and oxidative modification of the D1 protein

In the reanalysis of the proteomics data (Chapters 3.5 and 4.2) generated from thylakoids isolated from low temperature and high light treated lettuce (paper III), I detected the accumulation of pre-D1 protein during the treatment and a gradual increase in the amount of mature D1 protein during dark recovery (paper III, Figure 8A and thesis, Figure 10A). In addition to changes in D1 processing, I also detected an oxidative modification of the D1 protein (Figure 10B). In this chapter, I will explore how these changes at the protein level could explain why the fraction of open and functional PSII reaction centres (qL_T) increased during dark recovery (paper III, Figure 8F), where D1 translation is not expected to occur and how these changes could promote NPQ.

One mechanism of PSII reaction centre quenching is based on recombination reactions between $P680^{+\bullet}$ and $Q_A^{-\bullet}$, or in some cases $Q_B^{-\bullet}$, which prevent the accumulation of $P680^{+\bullet}$, thus reducing the probability of direct oxidative damage to the reaction centre proteins or cofactors (Sane et al., 2003; Ivanov et al., 2008). Recombination can be direct from $Q_A^{-\bullet}$ to $P680^{+\bullet}$ or indirect via $Phe^{-\bullet}$ to $P680^{+\bullet}$. The

direct reaction is considered as safe recombination route as it does not carry a risk of $^1O_2$ formation as the indirect route (Johnson et al., 1995).

The inhibited processing of pre-D1 disrupts the correct binding of CP43 to the reaction centre and the proper formation of OEC, but the Arabidopsis *ctpa* mutant is still able to accumulate some non-functional PSII-LHCII supercomplexes (Shi et al., 2021). Accumulation of pre-D1 and the chemical removal of the manganese clusters have been shown to increase the midpoint potential (E_m) of $Q_A/Q_A^{-\bullet}$ (Johnson et al., 1995). However, more recent reports suggest that this is due to altered binding of extrinsic lumenal subunits and changes in the binding of CP43, rather than the absence of the manganese cluster (Roose et al., 2010; Kato and Noguchi, 2021), and that the increase in on E_m of $Q_A/Q_A^{-\bullet}$ during chemical removal of the manganese cluster is due to the concomitant removal of bicarbonate from the ferrous iron (Brinkert et al., 2016; Sugo and Ishikita, 2022). However, regardless of the mechanism, increase in the E_m of $Q_A/Q_A^{-\bullet}$ slows down forward electron transfer and promotes the direct recombination route, protecting the donor side from oxidative damage, while at the same time minimising ^{3}Chl formation and $^1O_2$ production (Johnson et al., 1995; Sane et al., 2003). Increase in the E_m of $Q_A/Q_A^{-\bullet}$ could also upregulate direct quenching by increasing the lifetime of $Q_A^{-\bullet}$ (Farooq et al., 2018).

My results (paper III, Figure 8A and thesis, Figure 10) suggest that D1 processing is partially inhibited under low temperature and high light stress, and that D1 processing resumes after the stress is over. Such regulation of the PSII repair cycle would allow D1 to be resynthesised under conditions where ATP is available for D1 degradation and translation, while protecting the new D1 from photodamage. This would allow the rapid restoration of PSII functionality even under low light illumination, where the availability of ATP may be limited. Furthermore, this type of regulation of D1 processing means that the later steps of PSII repair can take place also in the dark. Cleavage of the C-terminus allows the correct binding of CP43, which would lower the E_m of $Q_A/Q_A^{-\bullet}$. This allows forward electron transfer and reduces reaction centre quenching, thereby explaining the recovery in Y(II) (paper III, Figure 2A) and qL_T (paper III, Figure 8F), and the changes observed in the fluorescence of PSII monomers in the clear native gels (paper III, Figure 3C). However, the manganese cluster would not form in the dark because it requires photoactivation.

His252 is important for the protonation of Q_B and mutations in this site affect the E_m of $Q_B/Q_B^{-\bullet}$ (Kobayashi et al., 2022). Moreover, His252 resides adjacent to the DE loop, which is cleaved during the PSII repair cycle. His252 oxidation has been studied previously and it was proposed to lead to the formation of an oxidative adduct between D1 and cytochrome b_{559} during high light illumination of solubilised thylakoids (Lupínková et al., 2002). Formation of such an adduct is oxygen dependent, prevented by chemical modification of histidine and reduced in the

presence of the singlet oxygen scavenger histidine and the triplet quencher propyl gallate (Lupínková et al., 2002; Widengren et al., 2007). Adduct formation also coincides with a slight electrophoretic shift in D1 migration on SDS-PAGE, suggesting that the protein is modified. Mutation of His252 to Ala, Glu, Gln, Gly, Leu, Lys or Tyr impairs the reduction of Q_B by interfering with the coupled protonation step (Lupínková et al., 2002; Kobayashi et al., 2022; Forsman et al., 2024; Sheridan et al., 2024). This is especially true for Leu and Tyr mutants, as these mutations are likely to completely prevent the formation of the hydrogen bond network for Ser264 to protonate Q_B. The susceptibility of D1 to degradation is also affected by mutations in this site. The His252Leu mutation does not affect D1 degradation (Lupínková et al., 2002), but the Ala, Gln and Tyr mutants have higher D1 turnover (Forsman et al., 2024), and D1 fragmentation has been detected in the Leu mutant even under growth conditions (Lupínková and Komenda, 2004). The Gln mutant also appears to protect PSII from photoinhibition and it has lower ROS production under high light illumination (Sheridan et al., 2024).

The detected oxidation of His252 to aspartic acid (Figure 10B) could induce reaction centre quenching by increasing $S_2Q_B^{-\bullet}$ recombination, similar to the proposed destabilisation of $Q_B^{-\bullet}$ by deprotonated His252 when stromal pH is high (Kobayashi et al., 2022). The probably small amount of reaction centres with oxidised His252 could therefore play a minor role in the formation and relaxation of the sustained quenching in low temperature and high light treated lettuce, but it could also lead to $^1O_2$ generation, unless the E_m of $Q_A/Q_A^{-\bullet}$ is also altered in the same reaction centres. Oxidation of His252 could also affect the recognition of D1 by DEG protease and lead to degradation of damaged D1 during dark recovery when low temperature does not limit enzyme activity. In conclusion, this type of oxidative modification may also be responsible for the higher E_m of $Q_B/Q_B^{-\bullet}$ detected in cold acclimated plants (Sane et al., 2003).

These hypotheses presented above, on the role of pre-D1 accumulation and His252 oxidation in acclimation to low temperature and high light stress, could be tested with spectroscopic and functional measurements using isolated thylakoids. $Q_A^{-\bullet}$ oxidation kinetics with flash fluorescence measurements would provide more information on the rates of forward electron transfer and recombination reactions, while information on thermoluminescence yield and temperature of the bands would complement these measurements (Sane et al., 2003). In addition, oxygen evolution measurements with 2,6-dichloro-1,4-benzoquinone (DCBQ), which accepts electrons from Q_A, and 2,6-dimethoxy-1,4-benzoquinone (DMBQ), which accepts electrons from Q_B, would also allow the analysis of the rate of electron transfer from Q_A to Q_B. The same measurements with thylakoids pre-treated with low illumination in the presence of $MnCl_2$, $CaCl_2$ and 2,6-dichlorophenolindophenol (DCIP), as an artificial electron acceptor, could be used to study PSII photoactivation (Johnson et

al., 1995). Localisation of pre-D1 with 2D immunoblots would also help to identify which complexes should be analysed further. In addition to these further studies, the results of the MS analysis should also be verified with synthetic peptides.

The detection of histidine oxidation to aspartic acid also opens new directions for mechanistic studies of PSII photoinhibition. Histidine is the most reactive amino acid with $^1O_2$ (Remucal and Mcneill, 2011; Miyahara et al., 2020), but for some reason, this modification has not been analysed in studies of PSII oxidation using MS-based methods (Kale et al., 2017; Weisz et al., 2017; Kumar et al., 2021). Moreover, MS-based studies of light-induced oxidation of PSII, including ours, have used trypsin to digest the proteins. This means that the hydrophobic core of the reaction centre is not analysed because there are no cleavage sites in the transmembrane region and the resulting peptides are likely to be too long and hydrophobic for analysis. Therefore, oxidative modifications in the transmembrane helices of the PSII reaction centre may have eluded detection due to methodological problems. Further studies on chymotryptic peptides, cleaved at the sites of aromatic amino acids, could reveal if or how D1 protein is altered during photoinhibition.

6 Conclusions

Photosynthesis is a complex and fascinating research subject, and the regulation of photosynthesis is even more so. In my PhD thesis, I sought to understand how photoinhibition alters the function and regulation of the photosynthetic machinery, from changes in specific amino acids to the overall organisation of photosynthetic supercomplexes and stromal redox regulatory networks. I have been able to elucidate many regulatory aspects of PSII and PSI photoinhibition, and their interaction with a number of regulatory mechanisms involved in protecting the photosynthetic apparatus under changing environmental conditions and in allowing plants to acclimate to photoinhibition (papers I, II and III). As is often the case with this type of exploratory research, my work was not able to fully answer the original research questions, but it did lead to the formulation of several hypotheses that would be interesting to explore further through more specific experiments, some of which were outlined in the discussion.

Acknowledgemets

This PhD thesis is based on work that was carried out in the Photosynthesis group at the Molecular Plant Biology unit at the department of Life Technologies, University of Turku. The financial support from the University of Turku Graduate School and Jane and Aatos Erkko foundation are gratefully acknowledged.

First, I would like to thank Professor Roman Sobotka and Professor Anjana Jajoo for reviewing my thesis, and most of all Professor Giles Johnson for accepting to be my opponent.

I would like to express my deepest gratitude to my supervisors Eva-Mari, Eevi, Mikko and Dorota who have pushed, guided, challenged, steered and supported me during these years. It has been a long journey, but not a fruitless one, since I have learned a lot from you. I also had an additional unofficial supervisor in Vipu, who thought me to master most of the biochemical methods used in my work, while at the same time giving additional mental support. I would also like to thank Julia for introducing proteomics for me. Working on the PSII inhibition paper with Sanna and Henna was hands down the nicest project during my PhD studies, we formed a great team together, thank you for that. Also, thank you to other past and present members of Photosynthesis group for help and ideas, especially Steffen from introducing me to biophysichs and Andrea for always bringing the new exciting papers to discuss in the group meetings.

Molecular Plant Biology unit has always been a place where help is given when it is asked, thank you for everyone working in the unit. My work would have not been possible without Mika, Eve, Anniina, Tapsa and Laura K keeping the labs running and helping in technical problems. You and the reinforcements from biochemistry side have also been great coffee company, which has made bad days more bearable and good days even better. Thank you for Aiste and Marjaana for all the help and support since the beginning. Lauri N helped me to get started with redox labelling and ECS, while scientific discussion with Minna and Tuomas helped me a lot while trying to make some sense of what happens in lettuce. Thank you for Laura L and Michal for the great company in the Venice trip and after it. Tommi, strictly speaking you are not part of the unit, but nevertheless thanks for the indiscriminate ranting company during our luch breaks, it has been a great way to

blow off steam. Finally, Sema thanks for being the best office mate one could hope for.

So many more people have helped and supported me during my studies before I stared my PhD. Jorma for being the best tutor ever and finally being one of the supervisors of my master's thesis with Jussi. Juha-Pekka thank you for introducing me to the wonderful chemistry of plants that finally led me to plant biochemistry. Paula, Taina, Esa and Saija thanks for the well needed encouragement when I was still a chemistry student.

All of this would not have been possible without my wonderful friends outside the unit who have kept me relatively sane during these years. I would have not started my PhD studies without the help of Milla and Markus. On top of that you have alse been great gym buddies and listened my worries with compassion. The first years of my PhD studies were the best thanks to the Arcane Union of Pure and Applied Food Woting, yeah in the end our system was quite crazy, but I think it suited all of us. Asmo, Jorma, Milla, Pasi, Tähtiville, Eskoville, Markus, Tatu and Milla V our lunch breaks were often the highlight of the day, especially during the pandemic. I will try to start the harvest festivals again next year so that we can catch up atleast once a year. Boardgaming with Saku, Tatu, Osku, Pasi and Jorma has always been a nice way to unwind, thank you for putting up with my slow thinking. Raili, Maria and Marjukka thanks for our fun padel games, it was mostly core training due to all the laughter but hopefully we can make it a more regular thing some day. Also rest of the Kermistit have been extremely important to me during my time at the uni, it's a shame we don't see so often anymore. Venla, Maria, Timo, Perttu, Emilia and Jorma thanks for the great company during most mandatory holidays and the interim get-togethers. Thank you Teemu for all the nature trips, it was an invaluable way to get my mind off things when I was fighting with this book. Luckily, I have also some friends left from my hometown. Otto, we have been friends since kids, and it is nice that it continues to be so. Maija and Jannnika, we have been friends since high school, thank you for still not giving up on trying to civilise me.

Lopuksi vielä suurin kiitos perheelleni. Olette opettaneet minulle mikä on tärkeää ja oikein. Olen aina voinut luottaa tukeenne ja siihen että olen hyvä näin.

Turku, November 2024

List of References

Albanese P, Manfredi M, Marengo E, Saracco G, Pagliano C (2019) Structural and functional differentiation of the light-harvesting protein Lhcb4 during land plant diversification. Physiol Plant **166**: 336–350

Albanese P, Manfredi M, Meneghesso A, Marengo E, Saracco G, Barber J, Morosinotto T, Pagliano C (2016) Dynamic reorganization of photosystem II supercomplexes in response to variations in light intensities. Biochim Biophys Acta Bioenerg **1857**: 1651–1660

Allen DJ, Ort DR (2001) Impacts of chilling temperatures on photosynthesis in warm-climate plants. Trends Plant Sci **6**: 36–42

Allen JF (2015) Why chloroplasts and mitochondria retain their own genomes and genetic systems: Colocation for redox regulation of gene expression. Proc Natl Acad Sci U S A **112**: 10231–10238

Amstutz CL, Fristedt R, Schultink A, Merchant SS, Niyogi KK, Malnoë A (2020) An atypical short-chain dehydrogenase–reductase functions in the relaxation of photoprotective qH in Arabidopsis. Nat Plants **6**: 154–166

Ancín M, Fernandez-Irigoyen J, Santamaria E, Larraya L, Fernández-San Millán A, Veramendi J, Farran I (2022) New In Vivo Approach to Broaden the Thioredoxin Family Interactome in Chloroplasts. Antioxidants. doi: 10.3390/antiox11101979

Ancín M, Larraya L, Florez-Sarasa I, Bénard C, Fernández-San Millán A, Veramendi J, Gibon Y, Fernie AR, Aranjuelo I, Farran I (2021) Overexpression of thioredoxin m in chloroplasts alters carbon and nitrogen partitioning in tobacco. J Exp Bot **72**: 4949–4964

Ancín M, Millan AFS, Larraya L, Morales F, Veramendi J, Aranjuelo I, Farran I (2019) Overexpression of thioredoxin m in tobacco chloroplasts inhibits the protein kinase STN7 and alters photosynthetic performance. J Exp Bot **70**: 731–733

Anderson J, Chow W, Goodchild D (1988) Thylakoid Membrane Organisation in Sun/Shade Acclimation. Functional Plant Biology **15**: 11

Arrivault S, Obata T, Szecówka M, Mengin V, Guenther M, Hoehne M, Fernie AR, Stitt M (2017) Metabolite pools and carbon flow during C4 photosynthesis in maize: 13CO 2 labeling kinetics and cell type fractionation. J Exp Bot **68**: 283–298

Asada K (2006) Production and scavenging of reactive oxygen species in chloroplasts and their functions. Plant Physiol **141**: 391–396

Asada K (1999) THE WATER-WATER CYCLE IN CHLOROPLASTS: Scavenging of Active Oxygens and Dissipation of Excess Photons. Annu Rev Plant Physiol Plant Mol Biol **50**: 601–639

Athanasiou K, Dyson BC, Webster RE, Johnson GN (2010) Dynamic acclimation of photosynthesis increases plant fitness in changing environments. Plant Physiol **152**: 366–373

Awad J, Stotz HU, Fekete A, Krischke M, Engert C, Havaux M, Berger S, Mueller MJ (2015) 2-Cysteine Peroxiredoxins and Thylakoid Ascorbate Peroxidase Create a Water-Water Cycle That Is Essential to Protect the Photosynthetic Apparatus under High Light Stress Conditions. Plant Physiol **167**: 1592–1603

Baker CR, Cocuron JC, Alonso AP, Niyogi KK (2023) Time-resolved systems analysis of the induction of high photosynthetic capacity in Arabidopsis during acclimation to high light. New Phytol **240**: 2335–2352

Balcke GU, Bennewitz S, Bergau N, Athmer B, Henning A, Majovsky P, Jiménez-Gómez JM, Hoehenwarter W, Tissier A (2017) Multi-omics of tomato glandular trichomes reveals distinct features of central carbon metabolism supporting high productivity of specialized metabolites. Plant Cell **29**: 960–983

Bathellier C, Yu L-J, Farquhar GD, Coote ML, Lorimer GH, Tcherkez G (2020) Ribulose 1,5-bisphosphate carboxylase/oxygenase activates O2 by electron transfer. Proc Natl Acad Sci U S A **117**: 24234–24242

Baudry K, Barbut F, Domenichini S, Guillaumot D, Thy MP, Vanacker H, Majeran W, Krieger-Liszkay A, Issakidis-Bourguet E, Lurin C (2022) Adenylates regulate Arabidopsis plastidial thioredoxin activities through the binding of a CBS domain protein. Plant Physiol 1–17

Bednarczyk D, Aviv-Sharon E, Savidor A, Levin Y, Charuvi D (2020) Influence of short-term exposure to high light on photosynthesis and proteins involved in photo-protective processes in tomato leaves. Environ Exp Bot **179**: 104198

Belgio E, Kapitonova E, Chmeliov J, Duffy CDP, Ungerer P, Valkunas L, Ruban A V. (2014) Economic photoprotection in photosystem II that retains a complete light-harvesting system with slow energy traps. Nat Commun **5**: 1–8

Betterle N, Ballottari M, Baginsky S, Bassi R (2015) High light-dependent phosphorylation of photosystem II inner antenna CP29 in monocots is STN7 independent and enhances nonphotochemical quenching. Plant Physiol **167**: 457–471

Betterle N, Poudyal RS, Rosa A, Wu G, Bassi R, Lee CH (2017) The STN8 kinase-PBCP phosphatase system is responsible for high-light-induced reversible phosphorylation of the PSII inner antenna subunit CP29 in rice. Plant Journal **89**: 681–691

de Bianchi S, Betterle N, Kouril R, Cazzaniga S, Boekema E, Bassi R, Dall'Osto L (2011) Arabidopsis mutants deleted in the light-harvesting protein Lhcb4 have a disrupted photosystem II macrostructure and are defective in photoprotection. Plant Cell **23**: 2659–2679

von Bismarck T, Korkmaz K, Ruß J, Skurk K, Kaiser E, Correa Galvis V, Cruz JA, Strand DD, Köhl K, Eirich J, et al (2023) Light acclimation interacts with thylakoid ion transport to govern the dynamics of photosynthesis in Arabidopsis. New Phytologist **237**: 160–176

Brinkert K, De Causmaecker S, Krieger-Liszkay A, Fantuzzi A, Rutherford AW (2016) Bicarbonate-induced redox tuning in Photosystem II for regulation and protection. Proceedings of the National Academy of Sciences **113**: 12144–12149

Brooks MD, Sylak-Glassman EJ, Fleming GR, Niyogi KK (2013) A thioredoxin-like/ -propeller protein maintains the efficiency of light harvesting in Arabidopsis. Proceedings of the National Academy of Sciences **110**: E2733–E2740

Bru P, Steen CJ, Park S, Amstutz CL, Sylak-Glassman EJ, Lam L, Fekete A, Mueller MJ, Longoni F, Fleming GR, et al (2022) The major trimeric antenna complexes serve as a site for qH-energy dissipation in plants. Journal of Biological Chemistry. doi: 10.1016/j.jbc.2022.102519

Bruderer R, Bernhardt OM, Gandhi T, Miladinović SM, Cheng LY, Messner S, Ehrenberger T, Zanotelli V, Butscheid Y, Escher C, et al (2015) Extending the limits of quantitative proteome profiling with data-independent acquisition and application to acetaminophen-treated three-dimensional liver microtissues. Molecular and Cellular Proteomics **14**: 1400–1410

Buchanan BB (2016) The Path to Thioredoxin and Redox Regulation in Chloroplasts. Annu Rev Plant Biol **67**: 1–24

Burgess AJ, Durand M, Gibbs JA, Retkute R, Robson TM, Murchie EH (2021) The effect of canopy architecture on the patterning of "windflecks" within a wheat canopy. Plant Cell Environ **44**: 3524–3537

von Caemmerer S, Farquhar GD (1981) Some relationships between the biochemistry of photosynthesis and the gas exchange of leaves. Planta **153**: 376–387

Caffarri S, Tibiletti T, Jennings RC, Santabarbara S (2014) A comparison between plant photosystem I and photosystem II architecture and functioning. Curr Protein Pept Sci **15**: 296–331

Cao P, Pan X, Su X, Liu Z, Li M (2020) Assembly of eukaryotic photosystem II with diverse light-harvesting antennas. Curr Opin Struct Biol **63**: 49–57

Caspy I, Borovikova-Sheinker A, Klaiman D, Shkolnisky Y, Nelson N (2020) The structure of a triple complex of plant photosystem I with ferredoxin and plastocyanin. Nat Plants **6**: 1300–1305

Che Y, Fu A, Hou X, McDonald K, Buchanan BB, Huang W, Luan S (2013) C-terminal processing of reaction center protein D1 is essential for the function and assembly of photosystem II in Arabidopsis. Proc Natl Acad Sci U S A **110**: 16247–16252

Chen Q, Xiao Y, Wu Z, Ming Y, Xiao W, Wang H Bin, Jin HL (2024) m-Type thioredoxin regulates cytochrome b_6f complex of photosynthesis. Plant Physiol **194**: 1294–1298

Chen YE, Zhao ZY, Zhang HY, Zeng XY, Yuan S (2013) Significance of CP29 reversible phosphorylation in thylakoids of higher plants under environmental stresses. J Exp Bot **64**: 1167–1178

Courteille A, Vesa S, Sanz-Barrio R, Cazalé AC, Becuwe-Linka N, Farran I, Havaux M, Rey P, Rumeau D (2013) Thioredoxin m4 controls photosynthetic alternative electron pathways in Arabidopsis. Plant Physiol **161**: 508–520

Croce R, van Amerongen H (2020) Light harvesting in oxygenic photosynthesis: Structural biology meets spectroscopy. Science (1979). doi: 10.1126/science.aay2058

Croce R, Van Amerongen H (2013) Light-harvesting in photosystem i. Photosynth Res **116**: 153–166

Cutolo EA, Caferri R, Guardini Z, Dall'Osto L, Bassi R (2023) Analysis of state 1-state 2 transitions by genome editing and complementation reveals a quenching component independent from the formation of PSI-LHCI-LHCII supercomplex in Arabidopsis thaliana. Biol Direct **18**: 49

Dall'Osto L, Cazzaniga S, Bressan M, Paleeèk D, Židek K, Niyogi KK, Fleming GR, Zigmantas D, Bassi R (2017) Two mechanisms for dissipation of excess light in monomeric and trimeric light-harvesting complexes. Nat Plants. doi: 10.1038/nplants.2017.33

Daloso D de M, Morais EG, Oliveira e Silva KF, Williams TCR (2023) Cell-type-specific metabolism in plants. Plant Journal **114**: 1093–1114

Davis GA, Kanazawa A, Schöttler MA, Kohzuma K, Froehlich JE, Rutherford AW, Satoh-Cruz M, Minhas D, Tietz S, Dhingra A, et al (2016) Limitations to photosynthesis by proton motive force-induced photosystem II photodamage. Elife **5**: 23–27

Degen GE, Johnson MP (2024) Photosynthetic control at the cytochrome b_6f complex. Plant Cell. doi: 10.1093/plcell/koae133

Dethloff F, Orf I, Kopka J (2017) Rapid in situ 13C tracing of sucrose utilization in Arabidopsis sink and source leaves. Plant Methods. doi: 10.1186/s13007-017-0239-6

Dietz K-J (2016) Thiol-Based Peroxidases and Ascorbate Peroxidases: Why Plants Rely on Multiple Peroxidase Systems in the Photosynthesizing Chloroplast? Mol Cells **39**: 20–5

Dietzel L, Bräutigam K, Steiner S, Schüffler K, Lepetit B, Grimm B, Schöttler MA, Pfannschmidta T (2011) Photosystem II supercomplex remodeling serves as an entry mechanism for state transitions in Arabidopsis. Plant Cell **23**: 2964–2977

Dziubek D, Poeker L, Siemiątkowska B, Graf A, Marino G, Alseekh S, Arrivault S, Fernie AR, Armbruster U, Geigenberger P (2023) NTRC and thioredoxins m 1/ m 2 underpin the light acclimation of plants on proteome and metabolome levels. Plant Physiol 1–24

Engelken J, Brinkmann H, Adamska I (2010) Taxonomic distribution and origins of the extended LHC (light-harvesting complex) antenna protein superfamily. BMC Evol Biol **10**: 233

Erling Tjus S, Lindberg Møller B, Vibe Scheller H (1999) Photoinhibition of Photosystem I damages both reaction centre proteins PSI-A and PSI-B and acceptor-side located small Photosystem I polypeptides.

Farmer EE, Mueller MJ (2013) ROS-Mediated Lipid Peroxidation and RES-Activated Signaling. Annu Rev Plant Biol **64**: 429–450

Farooq S, Chmeliov J, Wientjes E, Koehorst R, Bader A, Valkunas L, Trinkunas G, Van Amerongen H (2018) Dynamic feedback of the photosystem II reaction centre on photoprotection in plants. Nat Plants **4**: 225–231

Fernández-Marín B, Gulías J, Figueroa CM, Iñiguez C, Clemente-Moreno MJ, Nunes-Nesi A, Fernie AR, Cavieres LA, Bravo LA, García-Plazaola JI, et al (2020) How do vascular plants perform photosynthesis in extreme environments? An integrative ecophysiological and biochemical story. The Plant Journal 979–1000

Flannery SE, Hepworth C, Wood WHJ, Pastorelli F, Hunter CN, Dickman MJ, Jackson PJ, Johnson MP (2021a) Developmental acclimation of the thylakoid proteome to light intensity in Arabidopsis. Plant Journal **105**: 223–244

Flannery SE, Pastorelli F, Wood WHJ, Hunter CN, Dickman MJ, Jackson PJ, Johnson MP (2021b) Comparative proteomics of thylakoids from Arabidopsis grown in laboratory and field conditions. Plant Direct **5**: 1–18

Florez-Sarasa I, Ribas-Carbo M, Del-Saz NF, Schwahn K, Nikoloski Z, Fernie AR, Flexas J (2016) Unravelling the in vivo regulation and metabolic role of the alternative oxidase pathway in C3 species under photoinhibitory conditions. New Phytol **212**: 66–79

Forsman JA, Sheridan KJ, Singh H, Brown TJ, Vass I, Summerfield TC, Eaton-Rye JJ (2024) The Psb27 Assembly Factor and Histidine-252 of the D1 Protein Modify Energy Transfer to Photosystem II in Synechocystis sp. PCC 6803. Physiol Plant. doi: 10.1111/ppl.14154

Foyer CH, Kunert K (2024) The ascorbate–glutathione cycle coming of age. J Exp Bot. doi: 10.1093/jxb/erae023

Fristedt R, Carlberg I, Zygadlo A, Piippo M, Nurmi M, Aro EM, Scheller HV, Vener A V. (2009) Intrinsically unstructured phosphoprotein TSP9 regulates light harvesting in Arabidopsis thaliana. Biochemistry **48**: 499–509

Fukushi Y, Yokochi Y, Hisabori T, Yoshida K (2024) Overexpression of thioredoxin-like protein ACHT2 leads to negative feedback control of photosynthesis in Arabidopsis thaliana. J Plant Res. doi: 10.1007/s10265-024-01519-2

Geigenberger P, Thormählen I, Daloso DM, Fernie AR (2017) The Unprecedented Versatility of the Plant Thioredoxin System. Trends Plant Sci **22**: 249–262

Genty B, Briantais JM, Baker NR (1989) The relationship between the quantum yield of photosynthetic electron transport and quenching of chlorophyll fluorescence. Biochim Biophys Acta Gen Subj **990**: 87–92

Giannakis K, Arrowsmith SJ, Richards L, Gasparini S, Chustecki JM, Røyrvik EC, Johnston IG (2022) Evolutionary inference across eukaryotes identifies universal features shaping organelle gene retention. Cell Syst **13**: 874-884.e5

González MC, Cejudo FJ, Sahrawy M, Serrato AJ (2021) Current knowledge on mechanisms preventing photosynthesis redox imbalance in plants. Antioxidants. doi: 10.3390/antiox10111789

Grebe S, Porcar-Castell A, Riikonen A, Paakkarinen V, Aro E-M (2024) Accounting for photosystem I photoinhibition sheds new light on seasonal acclimation strategies of boreal conifers. J Exp Bot. doi: 10.1093/jxb/erae145

Grebe S, Trotta A, Bajwa AA, Suorsa M, Gollan PJ, Jansson S, Tikkanen M, Aro EM (2019) The unique photosynthetic apparatus of pinaceae: Analysis of photosynthetic complexes in Picea abies. J Exp Bot **70**: 3211–3225

Grieco M, Suorsa M, Jajoo A, Tikkanen M, Aro EM (2015) Light-harvesting II antenna trimers connect energetically the entire photosynthetic machinery - Including both photosystems II and I. Biochim Biophys Acta Bioenerg **1847**: 607–619

Haferkamp I, Schmitz-Esser S (2012) The plant mitochondrial carrier family: Functional and evolutionary aspects. Front Plant Sci. doi: 10.3389/fpls.2012.00002

Hagino T, Kato T, Kasuya G, Kobayashi K, Kusakizako T, Hamamoto S, Sobajima T, Fujiwara Y, Yamashita K, Kawasaki H, et al (2022) Cryo-EM structures of thylakoid-located voltage-dependent chloride channel VCCN1. Nat Commun **13**: 2505

Hakala M, Tuominen I, Keränen M, Tyystjärvi T, Tyystjärvi E (2005) Evidence for the role of the oxygen-evolving manganese complex in photoinhibition of Photosystem II. Biochim Biophys Acta Bioenerg **1706**: 68–80

Hakala-Yatkin M, Mntysaari M, Mattila H, Tyystjärvi E (2010) Contributions of visible and Ultraviolet parts of sunlight to photoinhibition. Plant Cell Physiol **51**: 1745–1753

Havaux M, Davaud A (1994) Photoinhibition of photosynthesis in chilled potato leaves is not correlated with a loss of Photosystem-II activity : Preferential inactivation of Photosystem I. Photosynth Res **40**: 75–92

Hayase T, Shimada Y, Mitomi T, Nagao R, Noguchi T (2023) Triplet Delocalization over the Reaction Center Chlorophylls in Photosystem II. Journal of Physical Chemistry B **127**: 1758–1770

Heineke D, Riens B, Grosse H, Hoferichter P, Peter U, Flügge UI, Heldt HW (1991) Redox Transfer across the Inner Chloroplast Envelope Membrane. Plant Physiol **95**: 1131–7

Hendron RW, Kelly S (2020) Subdivision of Light Signaling Networks Contributes to Partitioning of C4 Photosynthesis. Plant Physiol **182**: 1297–1309

Herdean A, Teardo E, Nilsson AK, Pfeil BE, Johansson ON, Ünnep R, Nagy G, Zsiros O, Dana S, Solymosi K, et al (2016) A voltage-dependent chloride channel fine-tunes photosynthesis in plants. Nat Commun. doi: 10.1038/ncomms11654

Höhner R, Day PM, Zimmermann SE, Lopez LS, Krämer M, Giavalisco P, Galvis VC, Armbruster U, Schöttler MA, Jahns P, et al (2021) Stromal NADH supplied by PHOSPHOGLYCERATE DEHYDROGENASE3 is crucial for photosynthetic performance. Plant Physiol **186**: 142–167

Holzwarth AR, Miloslavina Y, Nilkens M, Jahns P (2009) Identification of two quenching sites active in the regulation of photosynthetic light-harvesting studied by time-resolved fluorescence. Chem Phys Lett **483**: 262–267

Hüner NPA, Dahal K, Bode R, Kurepin L V., Ivanov AG (2016) Photosynthetic acclimation, vernalization, crop productivity and "the grand design of photosynthesis". J Plant Physiol **203**: 29–43

Hüner NPA, Smith DR, Cvetkovska M, Zhang X, Ivanov AG, Szyszka-Mroz B, Kalra I, Morgan-Kiss R (2022) Photosynthetic adaptation to polar life: Energy balance, photoprotection and genetic redundancy. J Plant Physiol **268**: 153557

Igamberdiev AU, Bykova N V (2022) Mitochondria in photosynthetic cells: Coordinating redox control and energy balance. Plant Physiol. doi: 10.1093/plphys/kiac541

Ilik P, Pavlovic A, Kouril R, Alboresi A, Morosinotto T, Allahverdiyeva Y, Aro EM, Yamamoto H, Shikanai T (2017) Alternative electron transport mediated by flavodiiron proteins is operational in organisms from cyanobacteria up to gymnosperms. New Phytologist **214**: 967–972

Inskeep WP, Bloom PR (1985) Extinction Coefficients of Chlorophyll a and b in N,N-Dimethylformamide and 80% Acetone. Plant Physiol **77**: 483–485

Ivanov AG, Sane P V., Hurry V, Öquist G, Huner NPA (2008) Photosystem II reaction centre quenching: Mechanisms and physiological role. Photosynth Res **98**: 565–574

Järvi S, Suorsa M, Aro EM (2015) Photosystem II repair in plant chloroplasts - Regulation, assisting proteins and shared components with photosystem II biogenesis. Biochim Biophys Acta Bioenerg **1847**: 900–909

Järvi S, Suorsa M, Paakkarinen V, Aro E-M (2011) Optimized native gel systems for separation of thylakoid protein complexes: novel super- and mega-complexes. Biochemical Journal **439**: 207–214

Jeong BC, Park SH, Yoo KS, Shin JS, Song HK (2013) Change in single cystathionine β-synthase domain-containing protein from a bent to flat conformation upon adenosine monophosphate binding. J Struct Biol **183**: 40–46

Johnson GN (2003) Thiol regulation of the thylakoid electron transport chain - A missing link in the regulation of photosynthesis? Biochemistry **42**: 3040–3044

Johnson GN, Rutherford AW, Krieger A (1995) A change in the midpoint potential of the quinone QA in Photosystem II associated with photoactivation of oxygen evolution. Biochimica et Biophysica Acta (BBA) - Bioenergetics **1229**: 202–207

Joliot P, Johnson GN (2011) Regulation of cyclic and linear electron flow in higher Plants. Proc Natl Acad Sci U S A **108**: 13317–13322

Juan CA, Pérez de la Lastra JM, Plou FJ, Pérez-Lebeña E (2021) The Chemistry of Reactive Oxygen Species (ROS) Revisited: Outlining Their Role in Biological Macromolecules (DNA, Lipids and Proteins) and Induced Pathologies. Int J Mol Sci **22**: 4642

Kale R, Hebert AE, Frankel LK, Sallans L, Bricker TM, Pospíšil P (2017) Amino acid oxidation of the D1 and D2 proteins by oxygen radicals during photoinhibition of Photosystem II. Proc Natl Acad Sci U S A **114**: 2988–2993

Kanazawa A, Kramer DM (2002) In vivo modulation of nonphotochemical exciton quenching (NPQ) by regulation of the chloroplast ATP synthase. Proc Natl Acad Sci U S A **99**: 12789–12794

Kanazawa A, Ostendorf E, Kohzuma K, Hoh D, Strand DD, Sato-Cruz M, Savage L, Cruz JA, Fisher N, Froehlich JE, et al (2017) Chloroplast ATP Synthase Modulation of the Thylakoid Proton Motive Force: Implications for Photosystem I and Photosystem II Photoprotection. Front Plant Sci **8**: 1–12

Karim MF, Johnson GN (2021) Acclimation of Photosynthesis to Changes in the Environment Results in Decreases of Oxidative Stress in Arabidopsis thaliana. Front Plant Sci **12**: 683986

Kato Y, Noguchi T (2021) Effects of Stromal and Lumenal Side Perturbations on the Redox Potential of the Primary Quinone Electron Acceptor QA in Photosystem II. Biochemistry **60**: 3697–3706

Kettunen R, Tyystjärvi E, Aro EM (1996) Degradation pattern of photosystem II reaction center protein D1 in intact leaves: The major photoinhibition-induced cleavage site in D1 polypeptide is located amino terminally of the DE loop. Plant Physiol **111**: 1183–1190

Khorobrykh S, Havurinne V, Mattila H, Tyystjärvi E (2020) Oxygen and ROS in Photosynthesis. Plants (Basel). doi: 10.3390/plants9010091

Kinoshita H, Nagasaki J, Yoshikawa N, Yamamoto A, Takito S, Kawasaki M, Sugiyama T, Miyake H, Weber APM, Taniguchi M (2011) The chloroplastic 2-oxoglutarate/malate transporter has dual function as the malate valve and in carbon/nitrogen metabolism. Plant Journal **65**: 15–26

Kılıç M, Käpylä V, Gollan PJ, Aro EM, Rintamäki E (2023) PSI Photoinhibition and Changing CO2 Levels Initiate Retrograde Signals to Modify Nuclear Gene Expression. Antioxidants. doi: 10.3390/antiox12111902

Klimmek F, Sjödin A, Noutsos C, Leister D, Jansson S (2006) Abundantly and rarely expressed Lhc protein genes exhibit distinct regulation patterns in plants. Plant Physiol **140**: 793–804

Klughammer C, Schreiber U (1994) An Improved Method, Using Saturating Light-Pulses, for the Determination of Photosystem-I Quantum Yield Via P700+-Absorbency Changes at 830 Nm. Planta **192**: 261–268

Klughammer C, Schreiber U (2016) Deconvolution of ferredoxin, plastocyanin, and P700 transmittance changes in intact leaves with a new type of kinetic LED array spectrophotometer. Photosynth Res **128**: 195–214

Klughammer C, Schreiber U (2008) Saturation Pulse method for assessment of energy conversion in PS I. PAM Application Notes 11–14

Kobayashi T, Shimada Y, Nagao R, Noguchi T (2022) pH-Dependent Regulation of Electron Flow in Photosystem II by a Histidine Residue at the Stromal Surface. Biochemistry **61**: 1351–1362

Kobayashi Y, Inoue Y, Furuya F, Shibata K, Heber U (1979) Regulation of adenylate levels in intact spinach chloroplasts. Planta **147**: 69–75

Komenda J, Sobotka R (2016) Cyanobacterial high-light-inducible proteins - Protectors of chlorophyll-protein synthesis and assembly. Biochim Biophys Acta Bioenerg **1857**: 288–295

Koziol AG, Borza T, Ishida KI, Keeling P, Lee RW, Durnford DG (2007) Tracing the evolution of the light-harvesting antenna in chlorophyll a/b-containing organisms. Plant Physiol **143**: 1802–1816

Kramarenko GG, Hummel SG, Martin SM, Buettner GR (2006) Ascorbate reacts with singlet oxygen to produce hydrogen peroxide. Photochem Photobiol **82**: 1634–1637

Kramer DM, Johnson G, Kiirats O, Edwards GE (2004) New Fluorescence Parameters for the Determination of QA Redox State and Excitation Energy Fluxes. Biol Chem 209–218

Kress E, Jahns P (2017) The Dynamics of Energy Dissipation and Xanthophyll Conversion in Arabidopsis Indicate an Indirect Photoprotective Role of Zeaxanthin in Slowly Inducible and Relaxing Components of Non-photochemical Quenching of Excitation Energy. Front Plant Sci **8**: 2094

Kudoh H, Sonoike K (2002) Irreversible damage to photosystem I by chilling in the light: Cause of the degradation of chlorophyll after returning to normal growth temperature. Planta **215**: 541–548

Kumar A, Prasad A, Sedlářová M, Kale R, Frankel LK, Sallans L, Bricker TM, Pospíšil P (2021) Tocopherol controls D1 amino acid oxidation by oxygen radicals in Photosystem II. Proc Natl Acad Sci U S A. doi: 10.1073/pnas.2019246118

Kunz HH, Armbruster U, Mühlbauer S, de Vries J, Davis GA (2024) Chloroplast ion homeostasis – what do we know and where should we go? New Phytologist. doi: 10.1111/nph.19661

Laihonen L, Rantala M, Ranasinghe U, Tyystjärvi E, Mulo P (2024) Transcriptomic and proteomic analyses of distinct Arabidopsis organs reveal high PSI-NDH complex accumulation in stems. Physiol Plant. doi: 10.1111/ppl.14227

Lee CP, Elsässer M, Fuchs P, Fenske R, Schwarzländer M, Millar AH (2021) The versatility of plant organic acid metabolism in leaves is underpinned by mitochondrial malate-citrate exchange. Plant Cell **33**: 3700–3720

Lee JW, Lee SH, Han JW, Kim GH (2020) Early Light-Inducible Protein (ELIP) Can Enhance Resistance to Cold-Induced Photooxidative Stress in Chlamydomonas reinhardtii. Front Physiol. doi: 10.3389/fphys.2020.01083

Leonardelli M, Tissot N, Podolec R, Ares-Orpel F, Glauser G, Ulm R, Demarsy E (2024) Photoreceptor-induced sinapate synthesis contributes to photoprotection in Arabidopsis. Plant Physiol. doi: 10.1093/plphys/kiae352

Leoni C, Pietrzykowska M, Kiss AZ, Suorsa M, Ceci LR, Aro EM, Jansson S (2013) Very rapid phosphorylation kinetics suggest a unique role for Lhcb2 during state transitions in Arabidopsis. Plant Journal **76**: 236–246

Levin G, Yasmin M, Liveanu V, Burstein C, Hanna R, Kleifeld O, Simanowitz MC, Meir A, Tadmor Y, Hirschberg J, et al (2023) A desert *Chlorella* sp. that thrives at extreme high-light intensities using a unique photoinhibition protection mechanism. The Plant Journal. doi: 10.1111/tpj.16241

Li Y, Zhang L, Shen Y, Peng L, Gao F (2023) CBSX2 is required for the efficient oxidation of chloroplast redox-regulated enzymes in darkness. Plant Direct. doi: 10.1002/pld3.542

Lim SL, Voon CP, Guan X, Yang Y, Gardeström P, Lim BL (2020) In planta study of photosynthesis and photorespiration using NADPH and NADH/NAD+ fluorescent protein sensors. Nat Commun. doi: 10.1038/s41467-020-17056-0

Lima-Melo Y, Gollan PJ, Tikkanen M, Silveira JAG, Aro EM (2019) Consequences of photosystem I damage and repair on photosynthesis and carbon use in Arabidopsis thaliana. Plant Journal 1061–1072

Lindenburg LH, Vinkenborg JL, Oortwijn J, Aper SJA, Merkx M (2013) MagFRET: The first genetically encoded fluorescent Mg2+ sensor. PLoS One. doi: 10.1371/journal.pone.0082009

Lupínková L, Komenda J (2004) Oxidative Modifications of the Photosystem II D1 Protein by Reactive Oxygen Species: From Isolated Protein to Cyanobacterial Cells. Photochem Photobiol **79**: 152–162

Lupínková L, Metz JG, Diner BA, Vass I, Komenda J (2002) Histidine residue 252 of the Photosystem II D1 polypeptide is involved in a light-induced cross-linking of the polypeptide with the alpha subunit of cytochrome b-559: study of a site-directed mutant of Synechocystis PCC 6803. Biochim Biophys Acta **1554**: 192–201

Malnoë A, Schultink A, Shahrasbi S, Rumeau D, Havaux M, Niyogi KK (2017) The Plastid Lipocalin LCNP is Required for Sustained Photoprotective Energy Dissipation in Arabidopsis. Plant Cell **30**: tpc.00536.2017

Mano J, Kanameda S, Kuramitsu R, Matsuura N, Yamauchi Y (2019) Detoxification of reactive carbonyl species by glutathione transferase tau isozymes. Front Plant Sci. doi: 10.3389/fpls.2019.00487

Maruta T, Tanaka Y, Yamamoto K, Ishida T, Hamada A, Ishikawa T (2024) Evolutionary insights into strategy shifts for the safe and effective accumulation of ascorbate in plants. J Exp Bot. doi: 10.1093/jxb/erae062

Mattila H, Mishra S, Tyystjärvi T, Tyystjärvi E (2023) Singlet oxygen production by photosystem II is caused by misses of the oxygen evolving complex. New Phytologist **237**: 113–125

Mazor Y, Borovikova A, Nelson N (2015) The structure of plant photosystem I super-complex at 2.8 Å resolution. Elife **4**: e07433

McClain AM, Cruz JA, Kramer DM, Sharkey TD (2023) The time course of acclimation to the stress of triose phosphate use limitation. Plant Cell Environ **46**: 64–75

McClain AM, Sharkey TD (2019) Triose phosphate utilization and beyond: from photosynthesis to end product synthesis. J Exp Bot **70**: 1755–1766

Meierhoff K, Westhoff P (1993) Differential biogenesis of photosystem II in mesophyll and bundle-sheath cells of monocotyledonous NADP-malic enzyme-type C4 plants: the non-stoichiometric abundance of the subunits of photosystem II in the bundle-sheath chloroplasts and the translational activity of the plastome-encoded genes. Planta **191**: 23–33

Mekala NR, Suorsa M, Rantala M, Aro E-M, Tikkanen M (2015) Plants Actively Avoid State Transitions upon Changes in Light Intensity: Role of Light-Harvesting Complex II Protein Dephosphorylation in High Light. Plant Physiol **168**: 721–34

Messant M, Hani U, Lai T-L, Wilson A, Shimakawa G, Krieger-Liszkay A (2024) Plastid terminal oxidase (PTOX) protects photosystem I and not photosystem II against photoinhibition in Arabidopsis thaliana and Marchantia polymorpha. Plant Journal **117**: 669–678

Miller MAE, O'Cualain R, Selley J, Knight D, Karim MF, Hubbard SJ, Johnson GN (2017) Dynamic acclimation to high light in arabidopsis thaliana involves widespread reengineering of the leaf proteome. Front Plant Sci **8**: 1–15

Miyahara Y, Shintani K, Hayashihara-Kakuhou K, Zukawa T, Morita Y, Nakazawa T, Yoshida T, Ohkubo T, Uchiyama S (2020) Effect of UVC Irradiation on the Oxidation of Histidine in Monoclonal Antibodies. Sci Rep. doi: 10.1038/s41598-020-63078-5

Møller IM, Rasmusson AG, Van Aken O (2021) Plant mitochondria – past, present and future. The Plant Journal 1–48

Mueller MJ, Berger S (2009) Reactive electrophilic oxylipins: Pattern recognition and signalling. Phytochemistry **70**: 1511–1521

Mukherjee P, Banerjee S, Wheeler A, Ratliff LA, Irigoyen S, Garcia LR, Lockless SW, Versaw WK (2015) Live imaging of inorganic phosphate in plants with cellular and subcellular resolution. Plant Physiol **167**: 628–638

Munné-Bosch S (2005) The role of α-tocopherol in plant stress tolerance. J Plant Physiol **162**: 743–748

Murai R, Okegawa Y, Sato N, Motohashi K (2021) Evaluation of CBSX Proteins as Regulators of the Chloroplast Thioredoxin System. Front Plant Sci. doi: 10.3389/fpls.2021.530376

Murata N, Takahashi S, Nishiyama Y, Allakhverdiev SI (2007) Photoinhibition of photosystem II under environmental stress. Biochim Biophys Acta **1767**: 414–21

Nath K, Poudyal RS, Eom JS, Park YS, Zulfugarov IS, Mishra SR, Tovuu A, Ryoo N, Yoon HS, Nam HG, et al (2013) Loss-of-function of OsSTN8 suppresses the photosystem II core protein phosphorylation and interferes with the photosystem II repair mechanism in rice (Oryza sativa). Plant Journal **76**: 675–686

Nawrocki WJ, Bailleul B, Picot D, Cardol P, Rappaport F, Wollman FA, Joliot P (2019) The mechanism of cyclic electron flow. Biochim Biophys Acta Bioenerg. doi: 10.1016/j.bbabio.2018.12.005

Nawrocki WJ, Liu X, Raber B, Hu C, De Vitry C, Bennett DIG, Croce R (2021) Molecular origins of induction and loss of photoinhibition-related energy dissipation qI. Sci Adv **7**: 1–14

Montané MH, Kloppstech K (2000) The family of light-harvesting-related proteins (LHCs, ELIPs, HLIPs): was the harvesting of light their primary function? Gene **258**: 1–8

Neilson JAD, Durnford DG (2010) Structural and functional diversification of the light-harvesting complexes in photosynthetic eukaryotes. Photosynth Res **106**: 57–71

Nicol L, Croce R (2021) The PsbS protein and low pH are necessary and sufficient to induce quenching in the light-harvesting complex of plants LHCII. Sci Rep **11**: 1–8

Niedermaier S, Schneider T, Bahl MO, Matsubara S, Huesgen PF (2020) Photoprotective Acclimation of the Arabidopsis thaliana Leaf Proteome to Fluctuating Light. Front Genet **11**: 1–15

Nikkanen L, Rintamäki E (2019) Chloroplast thioredoxin systems dynamically regulate photosynthesis in plants. Biochemical Journal **476**: 1159–1172

Nikkanen L, Toivola J, Rintamäki E (2016) Crosstalk between chloroplast thioredoxin systems in regulation of photosynthesis. Plant Cell Environ **39**: 1691–1705

Nikkanen L, Toivola J, Trotta A, Diaz MG, Tikkanen M, Aro EM, Rintamäki E (2018) Regulation of cyclic electron flow by chloroplast NADPH-dependent thioredoxin system. Plant Direct. doi: 10.1002/pld3.93

Oguchi R, Terashima I, Chow WS (2009) The involvement of dual mechanisms of photoinactivation of photosystem II in capsicum annuum L. plants. Plant Cell Physiol **50**: 1815–1825

Okegawa Y, Motohashi K (2020) M-type thioredoxins regulate the PGR5/PGRL1-dependent pathway by forming a disulfide-linked complex with PGRL1. Plant Cell **32**: 3866–3883

Okegawa Y, Sato N, Nakakura R, Murai R, Sakamoto W, Motohashi K (2023) x - and y -type thioredoxins maintain redox homeostasis on photosystem I acceptor side under fluctuating light. Plant Physiol. doi: 10.1093/plphys/kiad466

Oliver T, Kim TD, Trinugroho JP, Cordón-Preciado V, Wijayatilake N, Bhatia A, Rutherford AW, Cardona T (2023) The Evolution and Evolvability of Photosystem II. Annu Rev Plant Biol 2023 **74**: 225–257

Opatíková M, Semchonok DA, Kopečný D, Ilík P, Pospíšil P, Ilíková I, Roudnický P, Zeljković SĆ, Tarkowski P, Kyrilis FL, et al (2023) Cryo-EM structure of a plant photosystem II supercomplex with light-harvesting protein Lhcb8 and α-tocopherol. Nat Plants **9**: 1359–1369

Pan X, Ma J, Su X, Cao P, Chang W, Liu Z, Zhang X, Li M (2018) Structure of the maize photosystem I supercomplex with light-harvesting complexes I and II. Science (1979) **360**: 1109–1113

Petersen J, Förster K, Turina P, Gräber P (2012) Comparison of the H+/ATP ratios of the H+-ATP synthases from yeast and from chloroplast. Proc Natl Acad Sci U S A **109**: 11150–11155

Porcar-Castell A (2011) A high-resolution portrait of the annual dynamics of photochemical and non-photochemical quenching in needles of Pinus sylvestris. Physiol Plant **143**: 139–153

Porra RJ, Thompson WA, Kriedemann PE (1989) Determination of accurate extinction coefficients and simultaneous equations for assaying chlorophylls a and b extracted with four different solvents: verification of the concentration of chlorophyll standards by atomic absorption spectroscopy. BBA - Bioenergetics **975**: 384–394

Psencik J, Hey D, Grimm B, Lokstein H (2020) Photoprotection of photosynthetic pigments in plant one-helix protein 1/2 heterodimers. Journal of Physical Chemistry Letters 9387–9392

Puthiyaveetil S, Woodiwiss T, Knoerdel R, Zia A, Wood M, Hoehner R, Kirchhoff H (2014) Significance of the photosystem II Core phosphatase PBCP for plant viability and protein repair in thylakoid membranes. Plant Cell Physiol **55**: 1245–1254

Rantala M, Rantala S, Aro EM (2020) Composition, phosphorylation and dynamic organization of photosynthetic protein complexes in plant thylakoid membrane. Photochemical and Photobiological Sciences **19**: 604–619

Remucal CK, Mcneill K (2011) Photosensitized Amino Acid Degradation in the Presence of Riboflavin and Its Derivatives. Environ Sci Technol **45**: 5230–5237

Ren L, Ma H, Chao D, Zhang H, Qiao K, Feng S, Zhou A (2023) Sep2, a light-harvesting complex-like protein, is involved in light stress response by binding to free chlorophylls. Environ Exp Bot 105429

Reyes-Prieto A, Moustafa A (2012) Plastid-localized amino acid biosynthetic pathways of Plantae are predominantly composed of non-cyanobacterial enzymes. Sci Rep. doi: 10.1038/srep00955

Richardson KH, Wright JJ, Šimėnas M, Thiemann J, Esteves AM, McGuire G, Myers WK, Morton JJL, Hippler M, Nowaczyk MM, et al (2021) Functional basis of electron transport within photosynthetic complex I. Nat Commun. doi: 10.1038/s41467-021-25527-1

Rintamäki E, Kettunen R, Tyystjärvi E, Aro E -M (1995) Light-dependent phosphorylation of D1 reaction centre protein of photosystem II: hypothesis for the functional role in vivo. Physiol Plant **93**: 191–195

Rintamäki E, Martinsuo P, Pursiheimo S, Aro EM (2000) Cooperative regulation of light-harvesting complex II phosphorylation via the plastoquinol and ferredoxin-thioredoxin system in chloroplasts. Proc Natl Acad Sci U S A **97**: 11644–11649

Rintamäki E, Salonent M, Suoranta UM, Carlberg I, Andersson B, Aro EM (1997) Phosphorylation of light-harvesting complex II and photosystem II core proteins shows different irradiance-dependent regulation in vivo. Application of phosphothreonine antibodies to analysis of thylakoid phosphoproteins. Journal of Biological Chemistry **272**: 30476–30482

Roose JL, Frankel LK, Bricker TM (2010) Documentation of significant electron transport defects on the reducing side of photosystem II upon removal of the PsbP and PsbQ extrinsic proteins. Biochemistry **49**: 36–41

Ruban A V., Saccon F (2022) Chlorophyll a de-excitation pathways in the LHCII antenna. Journal of Chemical Physics. doi: 10.1063/5.0073825

Saccon F, Giovagnetti V, Shukla MK, Ruban A V. (2020) Rapid regulation of photosynthetic light harvesting in the absence of minor antenna and reaction centre complexes. J Exp Bot **71**: 3626–3637

Saito K, Rutherford AW, Ishikita H (2013) Mechanism of proton-coupled quinone reduction in Photosystem II. Proc Natl Acad Sci U S A **110**: 954–959

Salminen A, Anashkin VA, Lahti M, Tuominen HK, Lahti R, Baykov AA (2014) Cystathionine β-synthase (CBS) domains confer multiple forms of Mg2+-dependent cooperativity to family II pyrophosphatases. Journal of Biological Chemistry **289**: 22865–22876

Samol I, Shapiguzov A, Ingelsson B, Fucile G, Crèvecoeur M, Vener A V., Rochaix JD, Goldschmidt-Clermont M (2012) Identification of a photosystem II phosphatase involved in light acclimation in Arabidopsis. Plant Cell **24**: 2596–2609

Sane PV, Ivanov AG, Hurry V, Huner NPA, Öquist G (2003) Changes in the redox potential of primary and secondary electron-accepting quinones in photosystem II confer increased resistance to photoinhibition in low-temperature-acclimated arabidopsis. Plant Physiol **132**: 2144–2151

Sarewicz M, Pintscher S, Pietras R, Borek A, Bujnowicz Ł, Hanke G, Cramer WA, Finazzi G, Osyczka A (2021) Catalytic Reactions and Energy Conservation in the Cytochrome bc1 and b_6f Complexes of Energy-Transducing Membranes. Chem Rev. doi: 10.1021/acs.chemrev.0c00712

Sarewicz M, Szwalec M, Pintscher S, Indyka P, Rawski M, Pietras R, Mielecki B, Koziej Ł, Jaciuk M, Glatt S, et al (2023) High-resolution cryo-EM structures of plant cytochrome b_6f at work. Sci Adv **9**: eadd9688

Scheller, Henrik V, Haldrup A (2005) Photoinhibition of photosystem I. Planta **221**: 5–8

Schiphorst C, Achterberg L, Go R, Koehorst R, Bassi R, Amerongen H Van, Osto LD, Wientjes E (2021) The role of light-harvesting complex I in excitation energy transfer from LHCII to photosystem I in Arabidopsis. Plant Physiol 1–12

Schöttler MA, Tóth SZ (2014) Photosynthetic complex stoichiometry dynamics in higher plants: environmental acclimation and photosynthetic flux control. Front Plant Sci **5**: 1–15

Schreiber U, Klughammer C (2008) New accessory for the DUAL-PAM-100. The P515/535 module and examples of its application. PAM Application Notes **10**: 1–10

Selinski J, Scheibe R (2018) Malate valves: Old shuttles with new perspectives. Plant Biol **21**: 21–30

Serrato AJ, Rojas-González JA, Torres-Romero D, Vargas P, Mérida Á, Sahrawy M (2021) Thioredoxins m are major players in the multifaceted light-adaptive response in Arabidopsis thaliana. The Plant Journal 1–14

Shameer S, Ratcliffe RG, Sweetlove LJ (2019) Leaf energy balance requires mitochondrial respiration and export of chloroplast NADPH in the light. Plant Physiol **180**: pp.00624.2019

Shapiguzov A, Ingelsson B, Samol I, Andres C, Kessler F, Rochaix JD, Vener A V., Goldschmidt-Clermont M (2010) The PPH1 phosphatase is specifically involved in LHCII dephosphorylation and state transitions in Arabidopsis. Proc Natl Acad Sci U S A **107**: 4782–4787

Sharma RK, Dhillon J, Kumar P, Bheemanahalli R, Li X, Cox MS, Reddy KN (2023) Climate trends and maize production nexus in Mississippi: empirical evidence from ARDL modelling. Sci Rep. doi: 10.1038/s41598-023-43528-6

Shen L, Tang K, Wang W, Wang C, Wu H, Mao Z, An S, Chang S, Kuang T, Shen JR, et al (2022) Architecture of the chloroplast PSI–NDH supercomplex in Hordeum vulgare. Nature **601**: 649–654

Sheridan KJ, Eaton-Rye JJ, Summerfield TC (2024) Mutagenesis of Ile184 in the cd-loop of the photosystem II D1 protein modifies acceptor-side function via spontaneous mutation of D1-His252 in Synechocystis sp. PCC 6803. Biochem Biophys Res Commun. doi: 10.1016/j.bbrc.2024.149595

Shi Y, Che Y, Wang Y, Luan S, Hou X (2021) Loss of mature D1 leads to compromised CP43 assembly in Arabidopsis thaliana. BMC Plant Biol. doi: 10.1186/s12870-021-02888-9

Shikanai T (2023) Molecular Genetic Dissection of the Regulatory Network of Proton Motive Force in Chloroplasts. Plant Cell Physiol. doi: 10.1093/pcp/pcad157

Shimakawa G, Müller P, Miyake C, Krieger-Liszkay A, Sétif P (2024) Photo-oxidative damage of photosystem I by repetitive flashes and chilling stress in cucumber leaves. Biochim Biophys Acta Bioenerg. doi: 10.1016/j.bbabio.2024.149490

Sierra J, Escobar-Tovar L, Leon P (2023) Plastids: diving into their diversity, their functions, and their role in plant development. J Exp Bot **74**: 2508–2526

Sirohiwal A, Pantazis DA (2021) Electrostatic profiling of photosynthetic pigments: implications for directed spectral tuning. Phys Chem Chem Phys **23**: 24677

Sirohiwal A, Pantazis DA (2023) Reaction Center Excitation in Photosystem II: From Multiscale Modeling to Functional Principles. Acc Chem Res **56**: 2921–2932

Smith K, Strand DD, Kramer DM, Walker BJ (2023) The role of photorespiration in preventing feedback regulation via ATP synthase in Nicotiana tabacum. Plant Cell Environ 1–13

Son M, Pinnola A, Gordon SC, Bassi R, Schlau-Cohen GS (2020a) Observation of dissipative chlorophyll-to-carotenoid energy transfer in light-harvesting complex II in membrane nanodiscs. Nat Commun **11**: 1295

Son M, Pinnola A, Schlau-Cohen GS (2020b) Zeaxanthin independence of photophysics in light-harvesting complex II in a membrane environment. Biochim Biophys Acta Bioenerg. doi: 10.1016/j.bbabio.2019.148115

Sonoike K (2007) Photoinhibition and Protection of Photosystem I. Photosystem I 657–668

Sonoike K, Terashima I, Iwaki M, Itoh S (1995) Destruction of photosystem I iron-sulfur centers in leaves of Cucumis sativus L. by weak illumination at chilling temperatures. FEBS Lett **362**: 235–238

Strand DD, Fisher N, Kramer DM (2017) The higher plant plastid NAD(P)H dehydrogenase-like complex (NDH) is a high efficiency proton pump that increases ATP production by cyclic electron flow. Journal of Biological Chemistry **292**: 11850–11860

Su X, Ma J, Wei X, Cao P, Zhu D, Chang W, Liu Z, Zhang X, Li M (2017) Structure and assembly mechanism of plant C2S2M2-type PSII-LHCII supercomplex. Science **357**: 815–820

Sugo Y, Ishikita H (2022) Proton-mediated photoprotection mechanism in photosystem II. Front Plant Sci. doi: 10.3389/fpls.2022.934736

Suorsa M, Järvi S, Grieco M, Nurmi M, Pietrzykowska M, Rantala M, Kangasjärvi S, Paakkarinen V, Tikkanen M, Jansson S, et al (2012) PROTON GRADIENT REGULATION5 is essential for proper acclimation of Arabidopsis photosystem I to naturally and artificially fluctuating light conditions. Plant Cell **24**: 2934–2948

Sweetlove LJ, Beard KFM, Nunes-Nesi A, Fernie AR, Ratcliffe RG (2010) Not just a circle: Flux modes in the plant TCA cycle. Trends Plant Sci **15**: 462–470

Takahashi H, Kopriva S, Giordano M, Saito K, Hell R (2011) Sulfur assimilation in photosynthetic organisms: Molecular functions and regulations of transporters and assimilatory enzymes. Annu Rev Plant Biol **62**: 157–184

Takegawa Y, Nakamura M, Nakamura S, Noguchi T, Sellés J, Rutherford AW, Boussac A, Sugiura M (2019) New insights on Chl D1 function in Photosystem II from site-directed mutants of D1/T179 in Thermosynechococcus elongatus. Biochim Biophys Acta Bioenerg **1860**: 297–309

Takizawa K, Kanazawa A, Kramer DM (2008) Depletion of stromal Pi induces high "energy-dependent" antenna exciton quenching (qE) by decreasing proton conductivity at CF O-CF1 ATP synthase. Plant Cell Environ **31**: 235–243

Terashima I, Funayama S, Sonoike K (1994) The site of photoinhibition in leaves of Cucumis sativus L. at low temperatures is photosystem I, not photosystem II. Planta **193**: 300–306

Thormählen I, Zupok A, Rescher J, Leger J, Weissenberger S, Groysman J, Orwat A, Chatel-Innocenti G, Issakidis-Bourguet E, Armbruster U, et al (2017) Thioredoxins Play a Crucial Role in Dynamic Acclimation of Photosynthesis in Fluctuating Light. Mol Plant **10**: 168–182

Tikkanen M, Grebe S (2018) Switching off photoprotection of photosystem I – a novel tool for gradual PSI photoinhibition. Physiol Plant **162**: 156–161

Tikkanen M, Nurmi M, Kangasjärvi S, Aro EM (2008) Core protein phosphorylation facilitates the repair of photodamaged photosystem II at high light. Biochim Biophys Acta Bioenerg **1777**: 1432–1437

Tikkanen M, Piippo M, Suorsa M, Sirpiö S, Mulo P, Vainonen JP, Vener A, Allahverdiyeva Y, Aro E-M (2006) State transitions revisited - A buffering system for dynamic low light acclimation of Arabidopsis. Plant Mol Biol **62**: 779–793

Timm S, Florian A, Fernie AR, Bauwe H (2016) The regulatory interplay between photorespiration and photosynthesis. J Exp Bot **67**: 2923–2929

Tiwari A, Mamedov F, Fitzpatrick D, Gunell S, Tikkanen M, Aro E-M (2024) Differential FeS cluster photodamage plays a critical role in regulating excess electron flow through photosystem I. Nat Plants. doi: 10.1038/s41477-024-01780-2

Tiwari A, Mamedov F, Grieco M, Suorsa M, Jajoo A, Styring S, Tikkanen M, Aro E-M (2016) Photodamage of iron–sulphur clusters in photosystem I induces non-photochemical energy dissipation. Nat Plants 16035

Tjus SE, Møller BL, Scheller H V (1998) Photosystem I is an early target of photoinhibition in barley illuminated at chilling temperatures. Plant Physiol **116**: 755–64

Toleco MR, Naake T, Zhang Y, Heazlewood JL, Fernie AR (2020) Plant mitochondrial carriers: Molecular gatekeepers that help to regulate plant central carbon metabolism. Plants. doi: 10.3390/plants9010117

Tran CM, Mihara S, Yoshida K, Hisabori T (2023) Cystathionine-β-synthase X proteins negatively regulate NADPH-thioredoxin reductase C activity. Biochem Biophys Res Commun **653**: 47–52

Turkina M V., Villarejo A, Vener A V. (2004) The transit peptide of CP29 thylakoid protein in Chlamydomonas reinhardtii is not removed but undergoes acetylation and phosphorylation. FEBS Lett **564**: 104–108

Tyystjärvi E, Aro EM (1996) The rate constant of photoinhibition, measured in lincomycin-treated leaves, is directly proportional to light intensity. Proc Natl Acad Sci U S A **93**: 2213–8

Tzvetkova-Chevolleau T, Franck F, Alawady AE, Dall'Osto L, Carrière F, Bassi R, Grimm B, Nussaume L, Havaux M (2007) The light stress-induced protein ELIP2 is a regulator of chlorophyll synthesis in Arabidopsis thaliana. Plant Journal **50**: 795–809

Uflewski M, Mielke S, Galvis VC, von Bismarck T, Chen X, Tietz E, Ruß J, Luzarowski M, Sokolowska E, Skirycz A, et al (2021) Functional characterization of proton antiport regulation in the thylakoid membrane. Plant Physiol **187**: 2209–2229

Uflewski M, Rindfleisch T, Korkmaz K, Tietz E, Mielke S, Correa Galvis V, Dünschede B, Luzarowski M, Skirycz A, Schwarzländer M, et al (2024) The thylakoid proton antiporter KEA3 regulates photosynthesis in response to the chloroplast energy status. Nat Commun **15**: 2792

Ustynyuk LY, Tikhonov AN (2018) The cytochrome b_6f complex: DFT modeling of the first step of plastoquinol oxidation by the iron-sulfur protein. J Organomet Chem **867**: 290–299

Vainonen JP, Hansson M, Vener A V. (2005) STN8 protein kinase in Arabidopsis thaliana is specific in phosphorylation of photosystem II core proteins. Journal of Biological Chemistry **280**: 33679–33686

Vass I (2012) Molecular mechanisms of photodamage in the Photosystem II complex. Biochim Biophys Acta Bioenerg **1817**: 209–217

Vener A V, van Kan PJ, Rich PR, Ohad I, Andersson B (1997) Plastoquinol at the quinol oxidation site of reduced cytochrome bf mediates signal transduction between light and protein phosphorylation: thylakoid protein kinase deactivation by a single-turnover flash. Proc Natl Acad Sci U S A **94**: 1585–90

Vera-Vives AM, Novel P, Zheng K, Tan S-L, Schwarzländer M, Alboresi A, Morosinotto T (2024) Mitochondrial respiration is essential for photosynthesis-dependent ATP supply of the plant cytosol. New Phytol. doi: 10.1111/nph.19989

Voon CP, Guan X, Sun Y, Sahu A, Chan MN, Gardeström P, Wagner S, Fuchs P, Nietzel T, Versaw WK, et al (2018) ATP compartmentation in plastids and cytosol of Arabidopsis thaliana revealed by fluorescent protein sensing. Proc Natl Acad Sci U S A **115**: E10778–E10787

Walker B, Schmiege SC, Sharkey TD (2024) Re-evaluating the energy balance of the many routes of carbon flow through and from photorespiration. Plant Cell Environ. doi: 10.1111/pce.14949

Wang P, Grimm B (2021) Connecting Chlorophyll Metabolism with Accumulation of the Photosynthetic Apparatus. Trends Plant Sci **26**: 484–495

Wang P, Liu J, Liu B, Feng D, Da Q, Wang P, Shu S, Su J, Zhang Y, Wang J, et al (2013) Evidence for a role of chloroplastic m-type thioredoxins in the biogenesis of photosystem II in arabidopsis. Plant Physiol **163**: 1710–1728

Weisz DA, Gross ML, Pakrasi HB (2017) Reactive oxygen species leave a damage trail that reveals water channels in Photosystem II. Sci Adv **3**: eaao3013

Widengren J, Chmyrov A, Eggeling C, Löfdahl PÅ, Seidel CAM (2007) Strategies to improve photostabilities in ultrasensitive fluorescence spectroscopy. Journal of Physical Chemistry A **111**: 429–440

Wilson S, Johnson MP, Ruban A V. (2021) Proton motive force in plant photosynthesis dominated by ΔpH in both low and high light. Plant Physiol **187**: 263–275

Wimmelbacher M, Börnke F (2014) Redox activity of thioredoxin z and fructokinase-like protein 1 is dispensable for autotrophic growth of Arabidopsis thaliana. J Exp Bot **65**: 2405–2413

Wu HY, Qiao MY, Zhang YJ, Kang WJ, Ma QH, Gao HY, Zhang WF, Jiang CD (2023) Photosynthetic mechanism of maize yield under fluctuating light environments in the field. Plant Physiol **191**: 957–973

Yadav KNS, Semchonok DA, Nosek L, Kouřil R, Fucile G, Boekema EJ, Eichacker LA (2017) Supercomplexes of plant photosystem I with cytochrome b_6f, light-harvesting complex II and NDH. Biochim Biophys Acta Bioenerg **1858**: 12–20

Yamori W, Shikanai T (2016) Physiological Functions of Cyclic Electron Transport Around Photosystem I in Sustaining Photosynthesis and Plant Growth. Annu Rev Plant Biol **67**: 81–106

Yamori W, Takahashi S, Makino A, Price GD, Badger MR, von Caemmerer S (2011) The roles of ATP synthase and the cytochrome b6/f complexes in limiting chloroplast electron transport and determining photosynthetic capacity. Plant Physiol **155**: 956–962

Yin ZH, Johnson GN (2000) Photosynthetic acclimation of higher plants to growth in fluctuating light environments. Photosynth Res **63**: 97–107

Yokochi Y, Fukushi Y, Wakabayashi KI, Yoshida K, Hisabori T (2021) Oxidative regulation of chloroplast enzymes by thioredoxin and thioredoxin-like proteins in Arabidopsis thaliana. Proc Natl Acad Sci U S A **118**: 1–8

Yokono M, Takabayashi A, Akimoto S, Tanaka A (2015) A megacomplex composed of both photosystem reaction centres in higher plants. Nat Commun. doi: 10.1038/ncomms7675

Yokono M, Takabayashi A, Kishimoto J, Fujita T, Iwai M, Murakami A, Akimoto S, Tanaka A (2019) The PSI–PSII megacomplex in green plants. Plant Cell Physiol **60**: 1098–1108

Yoo KS, Ok SH, Jeong BC, Jung KW, Cui MH, Hyoung S, Lee MR, Song HK, Shin JS (2011) Single cystathionine β-synthase domain-containing proteins modulate development by regulating the thioredoxin system in Arabidopsis. Plant Cell **23**: 3577–3594

Zhang P, Allahverdiyeva Y, Eisenhut M, Aro EM (2009) Flavodiiron proteins in oxygenic photosynthetic organisms: Photoprotection of photosystem II by FIv2 and FIv4 in Synechocystis sp. PCC 6803. PLoS One. doi: 10.1371/journal.pone.0005331

Zhang S, Scheller HV (2004) Photoinhibition of photosystem I at chilling temperature and subsequent recovery in Arabidopsis thaliana. Plant Cell Physiol **45**: 1595–1602

Zhang Z, Jia Y, Gao H, Zhang L, Li H, Meng Q (2011) Characterization of PSI recovery after chilling-induced photoinhibition in cucumber (Cucumis sativus L.) leaves. Planta **234**: 883–889

Zheng Y, Cabassa-Hourton C, Planchais S, Lebreton S, Savouré A (2021) The proline cycle as an eukaryotic redox valve. J Exp Bot **72**: 6856–6866

Zhou X, Wang Q, Yang T (2020) Decreases in days with sudden day-to-day temperature change in the warming world. Glob Planet Change. doi: 10.1016/j.gloplacha.2020.103239

TURUN
YLIOPISTO
UNIVERSITY
OF TURKU

Painosalama, Turku, Finland 2024

ISBN 978-951-29-9992-7 (PRINT)
ISBN 978-951-29-9993-4 (PDF)
ISSN 0082-7002 (Print)
ISSN 2343-3175 (Online)